SEMMELWEIS EGYETEM

DOKTORI ISKOLA

Ph.D. értekezések

2936.

GYÜRE ZSOLT TAMÁS

A humán molekuláris genetika és a géndiagnosztika alapjai
című program

Programvezető: Dr. Szalai Csaba, egyetemi tanár

Témavezető: Dr. Szüts Dávid, tudományos tanácsadó

INVESTIGATING THE ROLE OF DNA DAMAGE TOLERANCE IN MUTAGENESIS USING WHOLE-GENOME SEQUENCING

PhD thesis

Zsolt Tamás Gyüre

Molecular Medicine Doctoral School

Semmelweis University

Supervisor: Dávid Szüts, DSc

Official reviewers: Arányi Tamás, MD, PhD
Burkovics Péter, PhD

Head of the Complex Examination Committee: Geiszt Miklós, DSc

Members of the Complex Examination Committee: Unk Ildikó, PhD
Szalai Bence, MD, PhD

Budapest
2023

Table of contents

List of Abbreviations

6-4PP	6-4 photoproducts
8-oxoG	8-hydroxyguanine
9-1-1	Rad9-Rad1-Hus1 complex
ADP	adenosine diphosphate
AEP	archaeo-eukaryotic primase
AID	activation-induced deaminase
APOBEC3	apolipoprotein B mRNA editing enzyme 3
ASCAT	allele-specific copy number analysis of tumors
BAF	B allele frequency
BER	base excision repair
BLM	Bloom syndrome protein
BP-G	benzo[a]pyrene-guanine
BRCA1	breast cancer gene 1
BRCA2	breast cancer gene 2
CCL	chronic lymphoid leukemia
CMG	Cdc45-MCM-GINS complex
CNA	copy number alteration
COSMIC	Catalogue Of Somatic Mutations In Cancer
CPD	cyclobutene pyrimidine dimer
CRISPR	Clustered Regularly Interspaced Short Palindromic Repeats
CSR	class switch recombination
CTD	C-terminal domain
DDR	DNA damage response
DDT	DNA damage tolerance
DDX11	ATP-dependent DNA helicase DDX11
DLBCL	diffuse large B cell lymphoma

DMEM	Dulbecco's Modified Eagle Medium
DNA	Deoxyribonucleic acid
DNA2	DNA Replication Helicase/Nuclease 2
DSB	double strand break
DSBR	double-strand break repair
DUB	deubiquitinating enzyme
EXO1	Exonuclease 1
FBS	fetal bovine serum
FDA	Food and Drug Administration
FEN-1	flap structure-specific endonuclease 1
FR	fork reversal
GATK	genome analysis toolkit
GFP	green fluoresence protein
H_2O_2	hydrogen peroxide
HEK293T	Human embryonic kidney 293 cell line
HLTF	Helicase-like transcription factor
HMEC	human mammary epithelial cell line
HNSC	head and neck squamous carcinoma
HR	homologous recombination
HRD	homologous recombination deficient
ICL	intrastrand crosslink
ID	insertion or deletion
IgV	immunoglobulin variable gene
ISG	interferon-stimulated gene
LOF	loss-of-function
MEF	mouse embryonic fibroblasts
MMR	mismatch repair
MMS	methyl-methanosulfonate

MRE11	Double-strand break repair protein MRE11
MUTYH	mutY DNA glycosylase
NER	nucleotide excision repair
NHEJ	nonhomologous end joining
NMF	non-negative matrix factorization
OGG1	8-Oxoguanine glycosylase
PAF15	PCNA Associated Factor 15
PARP1	poly(ADP-ribose) polymerase 1
PBD	phosphate buffered saline
PCA	principal component analysis
PCNA	proliferating cell nuclear antigen
PIF1	ATP-dependent DNA helicase PIF1
PIP	PCNA-interaction protein motifs
PPI	protein-protein interaction
PRIMPOL	primase and DNA directed Polymerase
PRR	postreplicative repair
RAD	radiation-sensitive
RECQ1	ATP-dependent DNA helicase Q1
REV1	DNA repair protein REV1
REV3L	Protein reversionless 3-like
RMI1	RecQ-mediated genome instability protein 1
RMI2	RecQ-mediated genome instability protein 2
RNA	Ribonucleic acid
ROS	reactive oxygen species
RPA	replication protein A
RPE-1	retina pigment epithelium 1 cell line
SBS	single nucleotide substitution
SCJ	sister chromatid junction

Sgs1	slow growth suppressor 1
SHM	somatic hypermutation
SHPRH	SNF2 Histone Linker PHD RING Helicase
SIZ1	SAP and Miz domain 1
SMARCAL1	SWI/SNF-related matrix-associated actin-dependent regulator of chromatin subfamily A-like protein 1
SPARTAN	SprT-Like N-Terminal Domain
ssDNA	single strand DNA
SUMO	small ubiquitin-related modifier
SWI/SNF	SWItch/Sucrose Non-Fermentable
TERT	Telomerase Reverse Transcriptase
TLS	translesion synthesis
TMEJ	DNA polymerase theta (θ)-mediated end joining
TNBC	triple negative breast cancer
TOP1	topoisomerase 1
TOP3A	DNA topoisomerase 3-alpha
TSw	template-switch
UBM	ubiquitin-binding motif
UBP	ubiquitin-binding protein
UBZ	ubiquitin-binding zinc finger
USP	Ubiquitin carboxyl-terminal hydrolase
UV	ultraviolet
VCP	valosin-containing protein
WGS	whole-genome sequencing
WRN	WRN RecQ Like Helicase
XP-V	xeroderma pigmentosum variant
XPD	xeroderma pigmentosum group D
XRCC2	X-ray repair cross-complementing protein 2

XRCC3	X-ray repair cross-complementing protein 3
ZnF	zinc finger
ZRANB3	Zinc finger Ran-binding domain-containing protein 3

1 Introduction

1.1 Stalled replication fork, genomic instability and DNA Damage Tolerance

Replication of genome is one of the most fundamental phenomena for every living organism. It requires accurate copying millions or billions of nucleotides in coordination with the cell cycle. Improper or incomplete replication can lead to DNA double-strand breaks (DSB), rearrangement and missegregation of chromosomes. This excessive changes of genetic information is called genome instability, an important hallmark of cancer (1, 2).

The replication machinery, named the replisome, is continuously challenged by intrinsic and extrinsic mutagenic agents. In mammalian cells, tens of thousands genomic lesions arise per day, either from endogenous sources, like oxidation of bases by cellular metabolism byproducts reactive oxygen species (ROS), or mutagenic environmental agents, like UV- and ionizing radiation. (3, 4). In normal cells, damaged DNA triggers coordinated activation of DNA damage checkpoints and variety of repair pathways, two processes known together as DNA damage response (DDR) (5). Despite diverse repair mechanisms, some lesions manage to escape repair before the replication machinery reaches the damaged site and it is encountered by replicative polymerases (6).

Accurate replication requires high-fidelity DNA polymerases. Due to their nucleotide selectivity and 3'→5' proofreading activity, error rates of replicative polymerases Polδ and Polε are estimated to be around 10^{-7} (1 error in 10 million nucleotides polymerized) (7). Damaged DNA impedes the progression of the replication fork as replicative polymerases are unable to process damaged templates, causing transient slowing or stalling of the replication machinery (8) (Fig. 1A). This is called replication stress and is a primary source of genome instability (9, 10). Besides DNA-lesions, repetitive genomic sequences, depletion of the nucleotide pool, transcribing RNA-polymerases, covalently bound DNA-protein complexes and unusual DNA-structures, like G-quadruplexes, can also form obstacles for the replication machinery. Furthermore, alteration in replication timing or progression caused by oncogene activation can also lead to replication stress (9, 11, 12).

Prolonged stalling of the replisome is potentially dangerous as it leads to collapse of the replication fork, generating DSB-s, which can lead to chromosomal rearrangements and genomic instability (13, 14). To avoid this, a variety of DNA damage tolerance (DDT) pathways have evolved.

1.2 DNA Damage Tolerance pathways

First of all, it is important to point out that DDT pathways are involved in protection of stalled replication fork and continuity of replication without repairing DNA damage (8). For the sake of simplicity, the primary cause of replication fork stalling is the incompatibility of the template (damaged DNA) and the reader (replicative polymerases). To resolve this discrepancy, there are two possible strategies: replacing either the template or the reader.

Replacing the template can be a homology-mediated process or restarting the replication downstream the lesion. These pathways are called template-switch (TSw) (Fig. 1I) and replication repriming (Fig. 1F), respectively (15, 16). A third pathway, called fork reversion (FR), is based on the complementarity of freshly synthetized DNA strands to protect replication fork from collapse (16) (Fig. 1C).

In contrast to high-fidelity replicative polymerases, which are unable to process damaged template, there are several DNA polymerases with orders of magnitudes lower in fidelity specialized to bypass lesion or extend mismatched primer. This process called translesion synthesis (TLS) and the polymerases involved are called TLS-polymerases (Fig 1B,H) (17). In contrast to the recombination-based pathways which are considered error-free, TLS is a potentially error-prone pathway as low fidelity polymerases can bypass lesions in expense of increased the risk of the introduction of mutations (16).

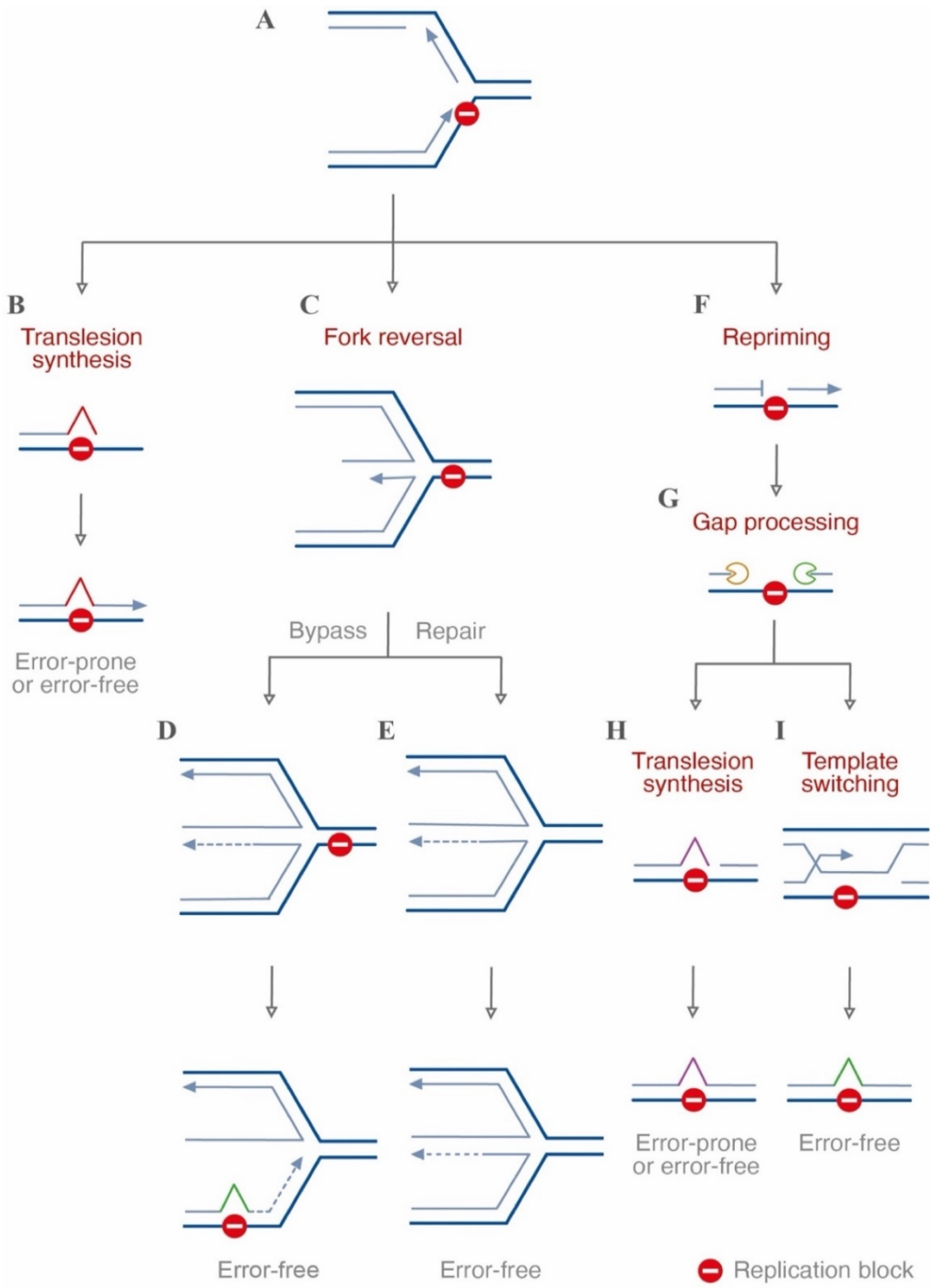

Figure 1 *Pathways of DNA damage tolerance. (A) Replication fork encounters DNA lesion and stalls. Replicative TLS (B) and repriming (F) maintain the progression of replication fork. In contrast, fork reversal (C) stabilizes stalled fork forming four-way junction. One model of fork reversal proposes that newly synthetized complementary strand provides template for DNA synthesis and replication continue behind lesion upon remodelling (D). Other hypothesis suggests that fork reversal provides time for DNA repair to remove lesion (E). Repriming results in accumulation of ssDNA gaps behind the replication fork. These gaps are pre-processed by exonucleases (G) followed by filling by either postreplicative TLS (H) or template-switch (I).*

1.2.1 (Re)priming replication

Most DNA polymerases, including replicative polymerases δ and ε, are unable to perform *de novo* DNA-synthesis, thus requires a pre-existing primer to extend and initiate synthesis of the new strand. In eukaryotes, the primase/Polα complex, part of the replisome, is responsible for the synthesis of short RNA-DNA primers elongated further by Polδ and ε (18, 19). Due to the geometry of replication, namely that DNA-synthesis happens simultaneously in both strands, in the same direction (5'→3'), though the two DNA-templates have opposite polarities, replication is performed semi-discontinuously. This means that synthesis of the new strand is continuous in one strand (leading strand, replicated by Polε) and happens in small units in the other one (lagging strand, replicated by Polδ). These small units are called Okazaki fragments (20). This means that (assuming unperturbed synthesis) priming happens once in the leading strand, but continuously in the lagging strand as well, as every distinct Okazaki-fragment requires its own primer (20).

Previous studies showed that UV-treatment promotes the accumulation of single strand DNA (ssDNA) gaps in bacteria, budding yeast and mammalian cells (21-24). Formation of gaps in lagging strand can be explained by Okazaki-fragment synthesis. Conversely, existence of leading strand gaps suggests that the replisome is capable of reinitiating DNA-synthesis in the leading strand as well, in response to DNA damage (25, 26). In budding yeast, primase/Polα is able to reprime replication downstream DNA-lesions (22), but primase activity in vertebrates was discovered only 10 years ago by Mourón and colleagues (15). This protein is the Primase and DNA- directed Polymerase (encoded by human gene CDCC111) or PRIMPOL.

PRIMPOL was the first identified member of the archaeo-eukaryotic primase (AEP) superfamily (27) and conserved in plants, vertebrates and lower-eukaryotes, but lacking from *C. elegans*, *Drosophila* and budding yeast (27, 28). In addition to AEP-domain (characteristic domain of the whole superfamily) responsible for primase and polymerase activity, PRIMPOL carries a Replication Protein A (RPA) binding domain, and a zinc finger (ZnF) domain (29). The latter one stabilizes the interaction between PRIMPOL and ssDNA (30).

PRIMPOL is a surprisingly versatile polymerase. It acts both as DNA- and RNA polymerase (31), and, in contrast to other DNA-polymerases, it is capable of *de novo* DNA-synthesis (32). Furthermore, it shows unprecedented capacity to tolerate 8-oxoG lesions (32), which is the most common oxidative damage of DNA (33). Besides 8-oxoG lesions, PRIMPOL is able to synthetize through UV-induced DNA-lesions such as cyclobutene pyrimidine dimers (CPDs) and 6-4 photoproducts (6-4PP) (15, 28, 32) and tolerates distortions in both template and primer strands (31). This flexibility is associated with very limited processivity, incorporating only a couple (usually up to four) of nucleotides on an undamaged template (29), and remarkably low fidelity with 10^{-4} error-rate (34). Interestingly, PRIMPOL shows unique mutation patterns, mostly dominated by indels (34) which might be attributed to PRIMPOL "pseudo-TLS" activity, namely PRIMPOL is able to loop out template DNA and realigns its primer terminus to a location downstream the lesion. This can occur at DNA regions with short, direct nucleotide repeats (15, 31, 35). It's important to highlight that TLS, "pseudo-TLS" and RNA-polymerase activity have been observed only *in vitro* so far, in contrast to its ability to reinitiate replication (26, 36-38).

Repriming of replication can rescue stalled replication fork, but results in discontinuities in the freshly synthetized DNA-strand. These gaps are filled in a later time point of the cell cycle, uncoupling DDT and the replication fork (25, 39), and, because of this, these pathways are parts of the postreplication repair, or PRR for short (Fig. 1F-I).

1.2.2 Translesion synthesis (TLS)

In contrast to replicative polymerases, TLS-polymerases can synthetize through even "unreadable" genomic sites. Major TLS-polymerases belongs to the Y-family of DNA-polymerases (REV1, Polι, Polκ and Polη) except for Polζ, which is a member of the B-family together with the replicative polymerases. Although members of the X- and A-family polymerases can exhibit TLS-activity as well, however this activity is either weak or not their primary function (40) (Table 1.) therefore I will be focusing on the five major TLS-polymerases mentioned above.

Table 1 List of human DNA polymerases, based on Loeb and Monnat (41)

Polymerase	Gene	Family	Primary function
α (alpha)	POLA	B	Replication initiation
ε (epsilon)	POLE1	B	Leading strand replication
δ (delta)	POLD1	B	Lagging strand replication
γ (gamma)	POLG1	A	Mitochondrial DNA replication
REV1	REV1	Y	TLS
ζ (zeta)	REV3L	B	TLS
η (eta)	POLH	Y	TLS
κ (kappa)	POLK	Y	TLS
ι (iota)	POLI	Y	TLS
PRIMPOL	PRIMPOL	AEP	Replication repriming
β (beta)	POLB1	X	BER
λ (lambda)	POLL	X	BER, NHEJ
μ (mu)	POLM	x	NHEJ
θ (theta)	POLQ	A	TMEJ (42)
ν (nu)	POLN	A	Unknown, suggested role in ICL repair, HR (43, 44)

The abundance of the TLS-polymerases has an important function: although TLS is usually considered as the "error-prone" DDT-pathway, every TLS-polymerase has its "preferred" lesion(s) which it can bypass more or less accurately. These lesions referred to as "cognate-lesion" of the polymerase (40). For example, Polη performs efficient and error-free bypass of UV-induced lesion CPDs and cisPT-GG (intra-strand lesion formed by the chemotherapy drug cisplatin), while carries out error-prone TLS of benzo[a]pyrene-guanine (BP-G, major tobacco-smoke induced lesion) (6, 45, 46). Similarly, Polι and Polκ are proved to be error-free against 8-oxoG and BP-G lesions, respectively (45, 47), while REV1 shows strong specificity for both template guanin (and exocylic guanin adducts) and only incorporates the nucleotide dCTP (48-50). Interestingly, upon dCTP-incorporation, REV1 uses its own arginine-residue as template rather than the DNA, which is unique mechanism among DNA-polymerases (51). Importantly, polymerase-cognate lesion pairs are not exclusive, certain lesion can be cognate-lesion for multiple TLS-polymerases: 8-oxoG can be bypassed in error-free manner by both Polι and Polη (47, 52). These results suggest that these polymerases have been evolved to cope with frequent (like 8-oxoG) or evolutionarily important (like UV-photoproducts) lesions. Given the wide variety of lesions, it must be assumed, that, besides specialized TLS-pathways, a general TLS-system is required as well to bypass

more “exotic” lesions. In their study, Shachar and colleagues investigated role of Polη, Polκ and Polζ in bypass over six diverse, site-specific lesions. Their results suggest the existence of a slow and more mutagenic TLS-pathway compared to the fast and more accurate bypass with cognate lesion-polymerase pairs (45).

Bypassing of a single lesion is assumed to require a sequential act of several TLS-polymerases (Fig. 2): the first polymerase inserts a nucleotide opposite to the lesion followed by switch to a polymerase able to efficiently extend the mispaired primer after the lesion (53). Early works suggest that the B-family polymerase Polζ acts as universal extender polymerase for Polη, Polκ and Polι (45, 54). Polζ can efficiently extend from nucleotide inserted opposite to AP-sites in yeast and cisplatin-induced lesions *in vitro* (55, 56). Furthermore, REV3, the catalytic subunit of Polζ is essential for post-replicative repair of UV-damaged sites in mouse embryonic fibroblasts (MEFs) (57), in contrast to its inability to bypass UV-induced lesions (54). Nevertheless, disruption of *Rev3l* gene causes embryonic lethality in mice (58-60). Besides Polζ, Polκ and Polη have also been proven to be able to act as extensor polymerases *in vitro* (61-63) with the restriction that Polη can only extend primers without mismatches. Interestingly, Polη can perform one-step TLS in CPD lesions (45).

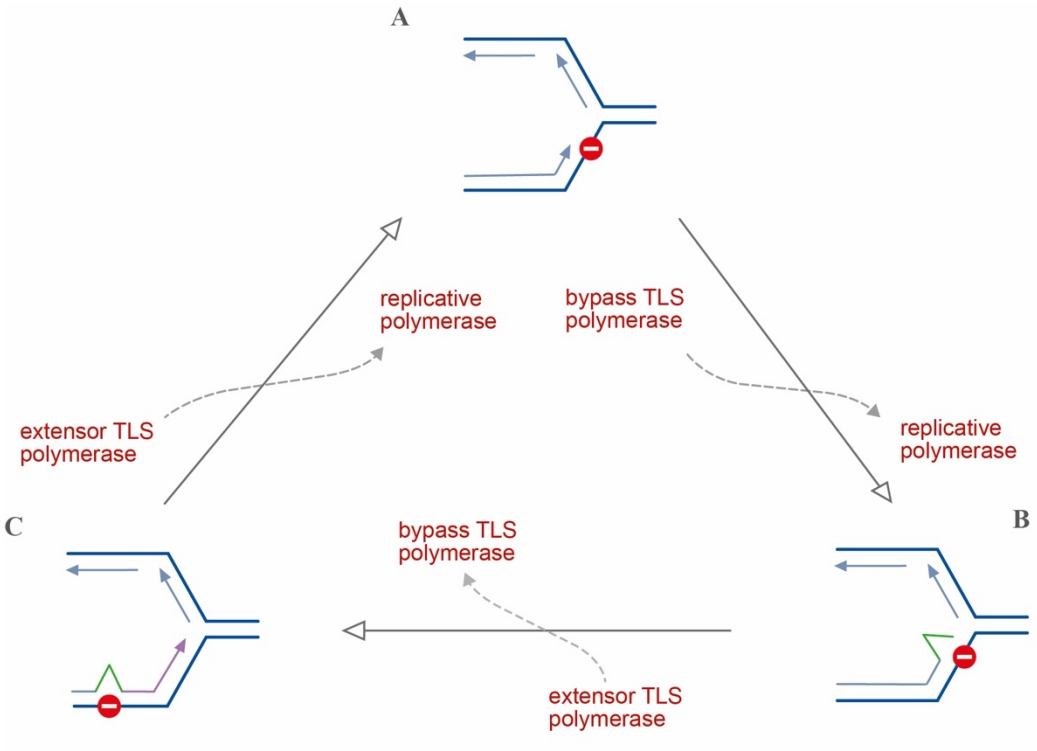

Figure 2 *Sequential steps of translesion synthesis. Stalled replicative polymerase (A) are replaced to TLS polymerase able to bypass DNS lesion (B), followed by switch to the extensor TLS polymerase which extends mispaired primer (C). Exchanging extensor TLS polymerase to replicative polymerase completes the cycle.*

1.2.3 Recombination-mediated DDT

1.2.3.1 Template-switch (TSw)

Post-replicative ssDNA gaps arising from repriming of replication can be filled by the homology-based mechanism TSw (16). Replication gaps filled via recombination was first observed in Escherichia coli (64), and seemed to be missing from mammalian cells (23), which lead to a first model of information exchange between sister chromatids, proposing that recombination events take place at the stalled replication fork (65). Subsequent works connected sister chromatid junctions (SCJ - cruciform, X-shaped DNA-structure, intermediate product of homologous recombination) with PRR, proving the role of homologous recombination in gap filling (22, 66). This finding has been further reinforced by genetic screens in budding yeasts (67, 68).

Due to the lack of mutations, investigating error-free TSw is difficult with conventional genetic methods. One widely used methods is to deploy special plasmids carrying DNA lesions with mismatching opposite bases, such as CC dimer placed opposite of 6-4 photoproduct (TT) (69). Disadvantage of this method is that synthesis of lesion containing oligonucleotides is difficult and the effect of chromatin context cannot be investigated. Branzei and colleagues utilized 2D gel electrophoreses to directly visualize SCJ-s in yeast, making possible quantitative analysis of TSw in different genetical background (70). Furthermore, the adaptive immune system of higher eukaryotes provides a natural genetic assay, called immunoglobulin variable gene (*IgV*) diversification (discussed in details latter) to investigate TSw (71, 72).

The most recent model of TSw has been established by Karras and colleagues using genome-wide genetic screens in thermosensitive *pol32*-mutant (inducible model for replication stress (68)) budding yeast strain (67). According to this model, ssDNA gaps, which accumulate behind replication fork in response to replication stress, are further 5`→3` expanded by exonuclease Exo1. Expansion of gaps facilitates topological DNA transaction, mediated by Rad51 and other recombination factors, forming SCJ-s.

Recombination intermediate structures are eventually resolved by Sgs1-Top3-Rmi1 complex (BLM-TOP3-RMI1/RMI2 complex in humans). According to more recent results, gaps are expanded in not only 5`→3` but 3`→5` direction as well by the action of Pif1 helicase and a yet unknown nuclease (73). Independently of Karras et al, Piberger and colleagues proposed a very similar model in human cells (26) with the addition that gaps are extended in 3`→5` direction by MRE11 complex (Fig. 1G). Resected 3' end is subsequently unwound by XPD family helicase DDX11 which facilitates the formation of SCJ-s (74) (Fig. 1I).

Involvement of "classical" (DSB-induced) recombination factors in TSw had been pending for decades. Answers came from systematic analysis of IgV gene conversion (i.e., TSw) events in HR-mutant DT40 cells. Independent results suggest that absence of BRCA1, BRCA2 and RAD54, as well as RAD51 paralogs RAD51B, RAD51C, RAD51D, XRCC2 and XRCC3 decreases frequency of gene conversion events (75-77). Furthermore, in contrast to being dispensable in DSB repair (74), ablation of DDX11 causes similar developmental abnormalities that had been described in Brca2 and Palb2 mutant mice (78-80), suggesting that HR-factors play role in TSw.

1.2.3.2 Replication fork reversal (FR)

The third way of preventing collapse of stalled replisome fork is the fork reversal. This can be divided in to two main steps:

Step 1) coordinated (re)annealing of two freshly synthetized strands which leads to a four-way junction structure, the so-called "chicken leg" (Fig. 1C) and

Step 2) remodeling fork to continue replication (81).

Stabilization of a stalled fork provides opportunity to the excision repair pathways to fix the causative DNA lesion or for second incoming fork to complete replication (Fig. 1E). Alternatively, the newly synthesized strand of sister chromatid serves as temporary alternative template for stalled strand, thus the lesions are bypassed upon subsequent restart of the fork (82) (Fig. 1D-E).

Several enzymes have been proven to exhibit *in vivo* fork reversal (step 1) activity, including SWI/SNF family member ZRANB3, SMARCAL1 and HLTF (36, 82-86) together with recombination factor RAD51 (87). Formation of a "fourth" branch,

consisting of annealed daughter strands results in free DNA ends, structurally similar to the results of DNA double strand breaks. To protect the exposed DNA ends from exonucleases, RAD51 is loaded by BRCA1 and BRCA2. In absence of the formation of stable RAD51 filaments, reversed replication forks are resected by sequential degradation steps involving MRE11, EXO1 and DNA2 (85, 88-90). Same studies draw the conclusion that BRCA1 and BRCA2 are not involved in fork reversal itself, they just protect the already reversed fork.

To continue replication, a reversed fork must be remodeled back to the classical three-way structure (step 2). RECQ1 helicase was the first known enzyme with the ability to remodel a reversed fork (87, 91). RECQ1 binding inhibits an alternative restart pathway involving WRN helicase which is able to remodel reversed fork followed by nucleotide degradation of regressed strand by DNA2 (92).

1.3 Regulation of DDT

The very fundamental event of replication stalling is when the replicative polymerase encounters the obstruction. Synthesis of new strand slows down or even stops. As DNA lesions and hard-to-replicate genomic sites usually do not interfere with replicative CMG-helicase, stall of polymerases causes uncoupling of replication and parental-strand unwinding (93). Resulting region of single-strand DNA is rapidly coated by replication protein A (RPA). These RPA-covered ssDNA filaments recruit RAD18/RAD6 complex, RAD17 and PRIMPOL (34, 94-97). Paradoxically, RPA-coated ssDNA stimulates activation of RAD18 and RAD17, but inhibits primase activity of PRIMPOL *in vitro* (98), though other results suggest that the inhibitory effect prevails only if RPA-covered ssDNA filament is short, and presence of longer (several kb) gaps, however, enhances both polymerase and primase activity of PRIMPOL (99). A possible explanation is that, after repriming, restricted activity of highly mutagenic PRIMPOL is favorable for cells. This theory is supported by the aforementioned low processivity of PRIMPOL (29). The fork remodeler enzyme SMARCAL1 also carries an RPA-binding domain, which is required for its replication function (84). In contrast, HLTF, a key protein of FR, carries no RPA-binding motif but an ancient ssDNA 3’ end recognition motif HIRAN domain (100) which may restrict its activity to stalled replication fork and prevents accession to ssDNA gaps.

Activated ubiquitin-ligase (E3) RAD18 and its cognate ubiquitin-conjugating enzyme (E2) RAD6 monoubiquitinates Proliferating Cell Nuclear Antigen (PCNA) on a highly conserved lysine, K164, which mechanism is conserved from yeast to humans (101). PCNA is a homotrimer which forms a sliding clamp around DNA and provides a docking platform for factors involved in metabolism of DNA via PCNA-Interaction Protein (PIP) motifs, carried by numerous replication and DNA repair proteins (102, 103). As a processivity cofactor for DNA polymerases, PCNA is involved in replication, nucleotide excision repair (NER), mismatch repair (MMR), base excision repair (BER) and double-strand break repair (DSBR) (103-107). Furthermore, PCNA interacts with Okazaki-fragment maturation factors flap structure-specific endonuclease 1 (FEN-1) and DNA ligase I (108, 109). PCNA monoubiquitination is the key initiation step of TLS, recruiting TLS-polymerases via protein-protein interaction (PPI) through ubiquitin-binding motifs (UBMs) of REV1 and Polι, and ubiquitin-binding zinc finger (UBZ) domains of Polκ and Polη (110, 111). In contrast to all TLS-polymerases, PRIMPOL carries neither PCNA- nor monoubiquitinated PCNA binding domains (29, 34), which may be associated with its the low processivity. Observations in budding yeast suggest that ubiquitination enables TLS polymerases to outcompete Polδ (and maybe Polε) (112, 113). However, monoubiquitination of PCNA is not essential for TLS in mammalian cells or the chicken cell line DT40 (71, 114, 115), probably due to alternative recruitment of TLS-polymerases by REV1 (114). REV1 carries multiple protein-protein interaction domains, thus providing the ability to organize the sequential steps of TLS. Besides carrying an UBM domain, its N-terminal BRCT domain binds unmodified and monoubiquitinated PCNA, while C-terminal domain (CTD) interacts with PIP-domains of TLS-polymerases (116-118). The variety of PPI motif carried by REV1 (REV1-bridge) and the ability of homo-trimeric PCNA to be monoubiquitinated in each subunit (PCNA-toolbelt model) provide the structural basis of the assembly of multi-protein complex, called mutasome, which accomplishes the sequential steps of lesion bypass (119-122). Furthermore, *in vivo* evidence shows that interaction with REV1 is essential for the function of Polκ (123). Existence of partly independent alternative pathways for regulation of TLS (PCNA-Ub and REV1) raises the question whether these mechanisms are temporally or spatially separated. Indeed, REV1 seems to coordinate TLS at the replication fork ("on-the-fly") while PCNA-monoubiquitination is responsible for filling

postreplicative gaps in DT40 (124, 125). Conversely, in mammals, the REV1-REV3L complex is involved in PRR (25, 57) and seems not to be required for maintenance of fork progression (36, 126).

While monoubiquitination of PCNA triggers TLS, deubiquitination by deubiquitinating enzymes (DUBs) terminates it, preventing excessive usage of a potentially error-prone mechanism (127). Several DUBs, including USP1-UAF1 complex, USP7 and USP10 are known to deubiquitinate PCNA, though USP7 seems to regulate DNA-repair-coupled, but not replication-coupled PCNA-ubiquitination (127-129). In case of USP10, deubiquitination is regulated by another post-translation modification of PCNA called ISGylation. EFP is an E3 ligase for ISG15 (a ubiquitin-like protein) and recognizes monoubiquitinated PCNA via its PIP domain. Upon PCNA-binding EFP ISGylates PCNA at two different residues. ISGylated PCNA recruits USP10 for deubiquitination of PCNA and, in turn, for release of TLS-polymerases. Finally, ISG15-s are removed by UBP43, allowing the reload of replicative polymerases (129). Similar mechanism for regulation of USP1 is unknown, probably because USP1 is inactivated upon exposure to genotoxic agents like UV and H_2O_2 (127, 130), suggesting that USP1 is responsible for the prevention of unnecessary activation of TLS, rather than termination.

Deubiquitination-independent regulation of access of TLS-polymerases to PCNA also exists, explaining the observations that PCNA monoubiquitination remains elevated long after the elimination of TLS foci (131) or in the absence of ISGylation of PCNA in HEK293T cell line (129). SPARTAN acts as a DNA damage-targeting adaptor for p97 (or valosin-containing protein - VCP) segregase, recruiting it to stalled replication fork, and facilitating the replacement of TLS-polymerases (132, 133). Conversely, other studies demonstrated that SPARTAN recruits Polη (134, 135) and facilitates TLS during IgV diversification (see later) in DT40 cells (136). Nevertheless, PCNA Associated Factor 15 (PAF15) also modulates PCNA-TLS-polymerases interaction by physically masking binding sites of PCNA. Upon fork stalling, double monoubiquitinated PAF15 is deubiquitinated, thus releasing PCNA, making it accessible for modification and TLS polymerases (137-139). Defect in any of these mechanisms causes increased spontaneous or induced mutagenesis, supporting theory that tight regulation of lesion bypass minimizes the usage of error-prone TLS-pathway (127, 133, 139).

The K164 residue of PCNA can also be subject of SUMOylation (modification with small ubiquitin-related modifier - SUMO) (101, 140). In budding yeast, the Rad18-Rad5-dependent TSw pathway requires Siz1-mediated SUMOylation of PCNA (70). Similarly, PCNA-SUMO promotes TSw in human TK6 and chicken DT40 cells lines, but without the association of RAD18 (141). Interestingly, besides facilitating recombination mediated TSw, SUMOylated PCNA proved to prevent unintended recombination at the stalled replication fork (70, 140, 142), distinguishing recombination-based DDT at, and behind the replication fork.

Furthermore, the ubiquitin of monoubiquitinated PCNA can be extended to K63-linked polyubiquitin chain by Ubc13/Rad5 E2/E3 enzymes, promoting TSw in budding yeast (69, 70, 101). Based on budding yeast results, there has long been a widely accepted model of DDT-activation: monoubiquitination promotes error-prone TLS and polyubiquitination activates error-free TSw. More recently, this model is challenged by the result that PCNA polyubiquitination promotes TLS in fission yeast and DT40 (141, 143) and not required for TSw in DT40 (115). In mammals, yeast Rad5 has two orthologs, HLTF and SHPRH, both contributing to PCNA polyubiquitination (144), but in a lesion-specific manner, as HLTF acts in response to UV-exposure, while SHPRH is activated upon methyl-methanosulfonate (MMS) derived DNA damage (145). PCNA polyubiquitination happens in the absence of HLTF and SHPRH, implying the existence of at least one additional PCNA-Ub specific E3 enzyme (146). Furthermore, 30-40% of TSw events seem to be RAD52-dependent and PCNA polyubiquitination-independent in yeast, suggesting existence of two alternative recombination based pathways (69). Besides possessing ubiquitin-ligase activity, HLTF takes part in remodeling of stalled replication fork via its DNA translocase domain, together with ZRANB3 and SMARCAL1 translocases (147). Interestingly, the three enzymes show decreasing dependence on PCNA modification: it is essential for HLTF, important, but not essential for ZRANB3, while SMARCAL1 seems to act PCNA ubiquitination-independently (148). This, taken together with the observation of distinct substrate preferences, suggests that the three enzymes act on different types of stalled fork structures (100).

PCNA is not the sole DNA-clamp involved in DDT. The 9-1-1 trimeric complex (Rad9-Rad1-Hus1) plays a central role in checkpoint activation (149-151), but it is involved in TSw as well, and the latter function seems to be independent from check-

point activation (67). Loading 9-1-1 to 5` ends of post-replicative gaps by its clamp-loader RAD17 (Rad24 in yeast) stimulates 5`→3` resection of gaps by recruiting EXO1, while PCNA facilitates 3`→5` resection via PIF1 (budding yeast) and MRE11 (mammals) (26, 67). Furthermore, 9-1-1 member RAD1 and its yeast orthologue (which is confusingly called Rad17) interacts with recombination factor RAD51 (152, 153), possibly facilitating the initiation of recombination. Furthermore, 9-1-1 subunit RAD9 and clamp-loader RAD17 are essential for Ig gene conversion, but not for DSB induced by fork-collapse or SceI endonuclease (71, 154).

Up to this point, I focused on protein-protein interactions driven by mainly post-translational modifications of PCNA as key regulators of DDT pathways. This type of regulation is indeed important, but not the sole way to hold the DDT pathways under control:

Abundance of Polη and REV1 is regulated via proteasomal degradation in cell cycle- and DNA damage-specific manner, which has been observed in eukaryotes from yeasts (both fission and budding yeast) to humans (155-160). Furthermore, yeast REV1 oscillates not only in protein but in mRNA levels throughout the cell cycle (155). Similarly, upregulation of Polκ interferes replication and slows down the replication fork (161), suggesting that Polκ expression is also under tight regulation. Finally, low processivity is a shared characteristic of Y-family polymerases REV1 (48, 162), Polι (163), Polκ (164), Polη (52) and PRIMPOL (29) *in vitro,* likely preventing excessive usage of error-prone polymerases in the absence of activation signals discussed above.

1.4 Crosstalk between DDT-pathways

Up to this point, I have discussed DDT pathways as more or less independent, distinct mechanisms which share only a low number of regulator proteins like PCNA. In contrast, discoveries from the past few years revealed that certain key proteins are involved in multiple pathways making DDT an interconnected network of molecular mechanisms that responds to replication stress.

First, there are mutually exclusive mechanisms: stalled forks can be rescued by either fork reversal, repriming or TLS. Observations in human cell lines revealed that overexpression of PRIMPOL suppresses fork reversal (37), while, in absence of HLTF, cells rely on either PRIMPOL or REV1 to maintain unrestrained replication (36).

Interestingly, HLTF seems to simultaneously recruit REV1 to stalled replication fork by an unknown mechanism, and restrict its access to the DNA by binding the free 3`-OH end (36). These results support the model of Zellweger and colleagues according to which FR is the default response of eukaryotes to replication stress (87), in contrast to dominance of PRR (TLS and TSw) in yeasts (165). Bai and colleagues propose an evolutionary point of view model, suggesting that multicellular organisms prioritize fidelity of replication to avoid accumulation of potentially harmful mutations and tumorous transformation of cell in protection of the whole organism (36).

BRCA1 is involved in protection of reversed replication forks (84) and TSw (25, 77, 166), promotes ubiquitination of PCNA via either interacting with RAD18 (167) or direct ubiquitination (168), thus plays a role in all DDT pathways. Furthermore, in absence of BRCA1, the resulting instability of replication fork activates repriming as a compensatory mechanism and the resulting ssDNA gaps are filled by REV1/Polζ-mediated TLS, maintaining the viability of cells at the expense of enhanced mutagenesis (37, 38). Conversely, the PCNA deubiquitinase enzyme USP1 is in synthetic lethal interaction with BRCA1. This phenotype can be rescued by inhibition of REV1 or Polκ, suggesting that persistent recruitment of TLS polymerases to replication further destabilize replication fork (169). These two, apparently conflicting, observations highlight the distinct usage of replication-related and postreplicative TLS.

Moreover, results of Tirman and colleagues shows that the REV1/Polζ TLS-complex is involved in not only TLS-mediated PRR gap filling but in TSw as well, proposing a closer interaction between the previously considered distinct pathways of TLS and TSw (25).

1.5 Medical importance of DDT pathways

1.5.1 Beyond Replication stress: key role of DDT in IgV diversification

Diversification of immunoglobulin variable (IgV) genes plays a central role in the adaptive immune response. The astounding repertoire of antibodies is generated by three, seemingly distinct processes: somatic hypermutation (SHM), gene conversion from homologous pseudogenes, not present in humans (GC) and class switch recombination (CSR) (124) but all three are initiated by regulated deamination of genomic cytidines by Activation-Induced Deaminase (AID) (170-172). Deamination of cytidines yields

genomic uracil residues which are subsequently excised by uracil DNA glycosylase UNG (173, 174) and resulting replication-stalling abasic sites trigger either TLS (SHM) or template switch (GC). While TLS introduces new point mutations, TSw utilizes pseudo V (ψV) donors as template (124, 170).

Dependence of SHM on TLS regulators varies between species: Defect of PCNA ubiquitination strongly decreases the frequency of new mutations in DT40 (175), but has only mild effect on mice and rather changes pattern of new mutations, decreasing A to T mutations via its inability to recruit Polη (176, 177). Similarly, absence of REV1 does not decrease overall mutation numbers in IgV locus, but completely abolishes C to G transversion and decreases C to G transversion in mice (178). Interestingly, during SHM, REV1 acts as an actual TLS-polymerase instead of a regulator (179), while knockout of Polκ has no effect on SHM in mice (180).

As mentioned before, TSw factor RAD17 and 9-1-1 complex member RAD9 are essential for GC and their absence increases frequency of SHM (71), similarly to deficiency of BRCA1, BRCA2, RAD51 or its paralogs in DT40 cells (75-77). Interestingly, DDX11, SPARTAN and Polη stimulate both SHM and GC (74, 136, 181), while absence of RAD54 decreases GC without influencing frequency of SHM (182).

Although involvement of DDT factors in human immunodeficiencies are yet unknown, abnormal activity of AID and subsequent processing of resulting abasic sites may be implicated in development of chronic lymphoid leukemia (CCL) (183).

1.5.2 DDT and cancer, therapeutic perspective

Tolerance of DNA damage is a double-edged sword. Bypass of DNA lesions by the corresponding cognate TLS polymerase decreases mutagenesis (40), while repriming and fork reversal protect stalled replisome, preventing DSB-s, thus suppressing genomic rearrangements (37, 82) and altered balance of DDT pathways can contribute to tumorous transformation. For example, in the absence of Polη, the cognate polymerase of UV-induced CPD, lesion bypass is performed by more mutagenic polymerases, which contributes to carcinogenesis in XP-V patients and associated with elevated risk of melanoma (184, 185). Similarly, polymorphisms of REV1 and Polι are associated with increased risk of squamous cell carcinoma and adenocarcinoma, respectively (186) and loss of REV3L enhances spontaneous tumorigenesis in mice (187). Furthermore,

expression of microRNA miR-205-5p, negative regulator of both BRCA1 and RAD17, is elevated in tumoral and peritumoral head and neck squamous carcinoma (HNSC) tissues, leading to increased chromosomal instability (188). Last but not least, disturbance of expression or activity of HLTF is observed in colon cancer (189), acute myeloid leukemia (190), thyroid cancer (191) and head and neck cancer (192), while loss-of-function (LOF) mutation of ZRANB3 is associated with endometrial cancer (193).

On the other hand, DDT pathways can protect cancer cells from elevated replication stress originating from rapid replication or oncogene activation and may contribute to the adaptation to cancer therapies (37, 194-196). Indeed, increased expression of TLS polymerases or RAD18 correlates with poorer prognoses of certain types of cancer (197-202). Given their role in the survival and chemoresistance of tumorous cells, DDT pathways have become attractive targets for cancer therapies lately, mainly focusing on TLS (203).Targeting Polη or Polι with small-molecule inhibitors improves chemosensitivity (204, 205). Alternatively, inhibition of homology-based DDT pathways by targeting UBC13 with small molecular inhibitor NSC697923 has shown promising results in neuroblastoma, melanoma and diffuse large B cell lymphoma (DLBCL) cells (206-208).

Inhibition of poly(ADP-ribose) polymerase 1 (PARP1) is widely used in the treatment of HR-deficient cancers (especially those harboring BRCA1/2 mutation) (209-211). Although the underlying molecular mechanism of sensitivity has yet to be unraveled (212), several studies suggest its role in instability of replication fork (85, 88, 90, 213) and the accumulation of ssDNA gaps in (38, 90). This, taken together with the fact that PARP inhibitors trap PARP1 on DNA forming blockage for replication fork (214), suggests an attractive model that impaired DDT pathways are responsible for PARPi sensitivity of HR-deficient cells (215). Unfortunately, efficiency of PARP-inhibitors is hampered due to subsequent development of resistance (216). Besides restoration of HR, resistance to PAPR-inhibition can be acquired by either stabilization of replication forks (217) or activation of repriming and subsequent gap-filling processes (25, 37, 38), making DDT pathways attractive targets in treatment of PARPi-resistant HR-deficient cancers.

1.6 Mutagenic signatures

Somatic mutations are results of a DNA damaging or modifying effect (either exogenous or endogenous) and the subsequently activated repair process (or its absence), are forming a mutagenic process together. Mutagenic processes show DNA-context specificity, generating characteristic patterns of mutations including base substitutions, insertions and deletions (indels for short) and large-scale alteration of genome like rearrangements and copy number variations (218, 219). These patterns are called mutational signatures (218). Cells, regardless of being a cell line, healthy cell or cancer cell from a tumorous tissue, keep being exposed to mutagenic effects since the fertilization of the egg, resulting in unique mutational landscape which is shaped by combinations of superimposed signatures (218). Mutational signatures belonging to distinct mutational processes can be deciphered from DNA-sequencing data of cancer samples with unsupervised learning methods like non-negative matrix factorization (NMF) or hierarchical Dirichlet process (220, 221). These "basic" signatures are accessible from online databases like COSMIC (222) or Signal (223), but the exact contents are continuously updated due to the growth of the underlying databases. Based on the types of mutations, signatures have been categorized as single nucleotide substitution (SBS) signatures, doublet base substitution (DBS) signatures, indel (ID) signatures, rearrangement signatures (RS) and copy number (CN) signatures (224). The most recent version of COSMIC database consists of 67 SBS signatures (of which 49 were considered to be of biological origin), 11 DBS signatures, 18 ID signatures and 21 CN signatures, some of known aetiologies (but many of unknown) (225). For example, SBS31 and SBS35 are attributed to platinum chemotherapy; SBS4, DBS2 and ID3 are associated with tobacco smoking while SBS3 and ID6 have been attributed to defect of HR repair (225).

Properly performed mutational signature analysis of cancer genomes provides insight into tissue-specific mutagenic processes that can contribute to the development of cancer (218), as well as to the formation of metastases (226, 227). Cell lines defective in certain repair pathways or exposed to mutagenic agents are often used to validate or elucidate molecular mechanisms behind signatures (228).

1.7 Cisplatin, a DNA lesion-forming agent

Cis-diamminedichloroplatinum(II), best known as cisplatin, is an FDA-approved cytotoxic platinum agent widely employed in the treatment of various types of tumors including bladder, lung, ovarian, testicular cancer and wide array of paediatric tumors (229-233). The main molecular mechanism by which cisplatin exerts its anticancer role is the formation of DNA adducts followed by activation of DDR and apoptosis (234). The majority of cisplatin-derived lesions are crosslinked GA or GG dinucleotides of the same strand (235) interfering with replication. Preventing PCNA-monoubiquitination sensitizes cancer cells to cisplatin in cell-based assay (236), similarly to inhibition of RAD18 and REV1 which, in combination with cisplatin treatment, increase accumulation of genotoxic ssDNA gaps in BRCA1/2-deficent cells (38). Likewise, elevated expression of Polη and RAD18 contribute to cisplatin resistance in ovarian and glioblastoma cells, respectively (237, 238), as well as absence of REV1 or REV3L re-sensitizes cisplatin-resistant cancer cells (239, 240). These results highlight the role of TLS polymerases in the development of chemoresistance to cisplatin (Fig. 3), making them attractive therapeutic targets.

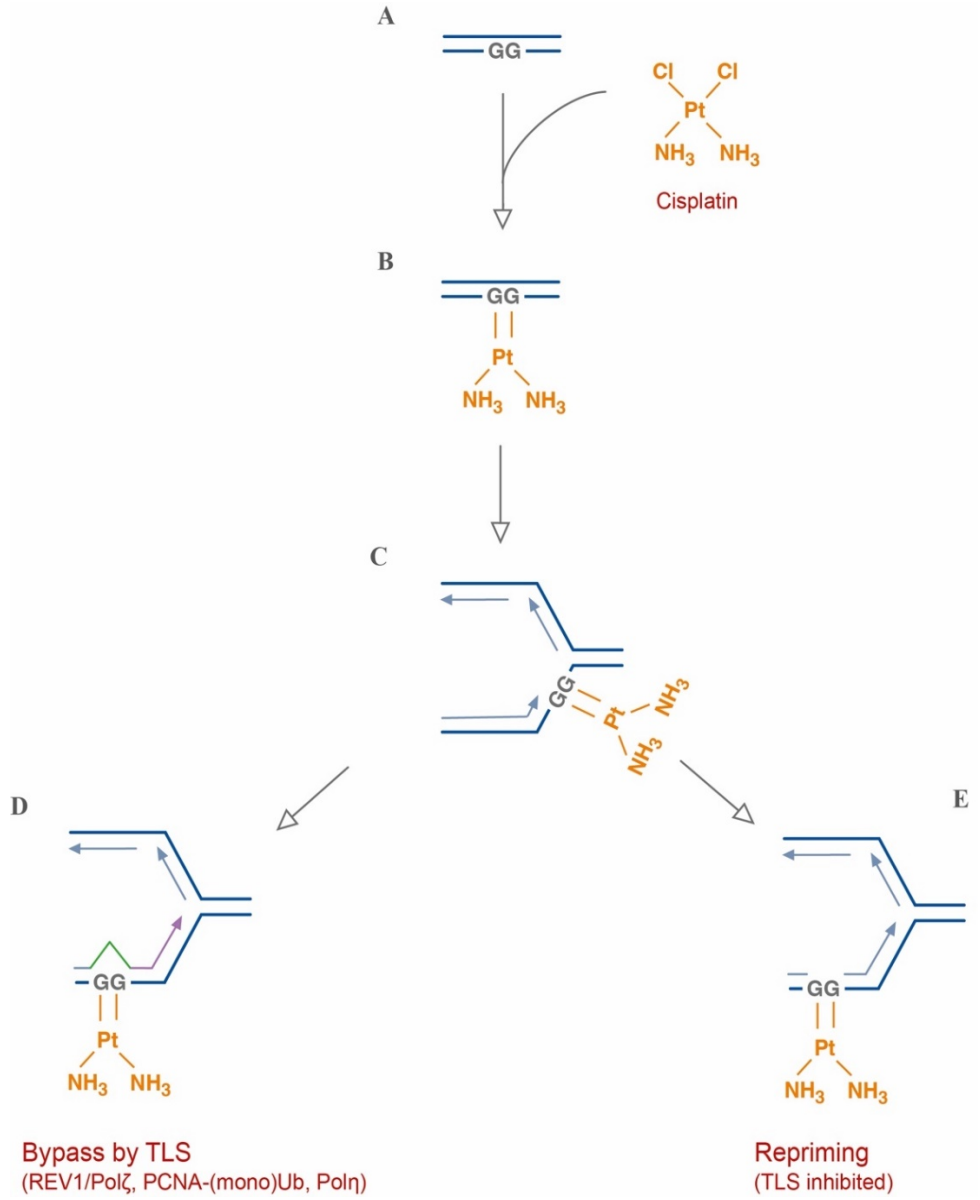

Figure 3 *Formation of cisplatin-induced DNA lesions and inference with replication. The major cisplatin-derived DNA adduct is the crosslinked adjacent guanine bases, denoted as cis-Pt-GG. (A-B) Unrepaired cis-Pt-GG-s form obstructions for replication fork (C). Stalled replication can be rescued by translesion bypass through PCNA-(mono)ubiquitination, by Polη or REV1/Polζ (D). In the absence of TLS, accumulation of ssDNA gaps suggests the usage of repriming (E).*

2 Objectives

Aims of my PhD research were the following:

1. Establishment of a collection of mutant cell lines in hTERT RPE-1 *TP53*$^{-/-}$ carrying mutations in key regulators of all DNA damage tolerance pathways: translesion synthesis, template switch, replication repriming and fork reversal.
2. Determination of mutagenic signatures arising from the action of low-fidelity DNA polymerases and evaluation of their contribution to the spontaneous mutagenesis in DDT mutant RPE-1 cell lines and cultured human cell lines of tumor origin, utilizing whole genome sequencing data and the unsupervised learning technique non-negative matrix factorization. Evaluation of the role of that DDT pathways plays in the large-scale integrity of genome.
3. To investigate whether DDT-derived signatures extracted from RPE-1 samples are cell line specific or represent more common mutagenic processes across human cell lines. Analysis of DT40 lymphoblast cell lines of avian origin to investigate evolutionarily conserved role of DDT in mutagenesis.
4. Evaluation of the role of DDT in the bypass of DNA lesions caused by cisplatin treatment, by analyzing contribution of cisplatin-derived signatures in WGS data of cisplatin treated RPE-1 cell lines.

Contributions:

The workflow in section 4.1.8 to determine large-scale mutation events and detailed in Methods 3.2 was established by Dr. Ádám Póti. Dr. Németh Eszter contributed to the data collections for experiments in section 4.14. Furthermore, Dr. Szikriszt Bernadett contributed in cytoxicity assays in section 4.2.1 (plating of cells and drug treatment).

3 Methods

3.1 Cell line cultures

RPE-1 cell lines were grown in Dulbecco's Modified Eagle Medium F12 (DMEM/F12) medium (Thermo Fisher Scientific) supplemented with 10% fetal bovine serum (FBS) (Thermo Fisher Scientific), 1% PenStrep (Lonza) and 0.01 mg/ml Hygromycin B Gold solution (Invivogen), whereas hTERT-HMEC cells were grown in MEGM Mammary Epithelial Cell Growth Medium BulletKit (Lonza).

Cell lines were cultured for days after first single cell cloning. Where indicated, cell lines were treated with 2µm cisplatin for one hour in four rounds at weekly intervals.

3.2 Establishment of mutant cell lines

Knockout cell lines *REV1*$^{-/-}$, *REV3L*$^{-/-}$, *PRIMPOL*$^{-/-}$, *HLTF*$^{-/-}$ and point mutant *PCNA*^{K164R} cell line were generated in hTERT-RPE1 *TP53*$^{-/-}$ background using CRISPR knockout and ssDNA template-mediated mutagenesis, respectively. Double mutant *PCNA*^{K164R} *PRIMPOL*$^{-/-}$, *PCNA*^{K164R} *REV1*$^{-/-}$, *PCNA*^{K164R} *HLTF*$^{-/-}$ and *REV1*$^{-/-}$ *PRIMPOL*$^{-/-}$ cell lines were generated in *PCNA* ^{K164R} and *REV1-/-* single mutant backgrounds, respectively (Table 2).

Plasmids expressing components of CRISPR-system were constructed by cloning sgRNA-encoding oligonucleotides (Table 3) into pSpCas9(BB)-2A-GFP vector (Addgene #48138). Transfection of cell lines with corresponding CRISPR-constructs were conducted with 4D-Nucleofector with P3 Primary Cell transfection reagent (Lonza), supplemented with 1 µl of ssDNA template (100 µM) in case of site-specific mutagenesis of PCNA. To enhance probability of template integration, cells in PCNA^{K164R} were treated with 50uM NHEJ-inhibitor *scr7* (241). 24 hours following transfection, GFP+ single cell clones selected and plated using a BD FACSAria™ III High Sensitivity Flow Cytometer. Single cell clones were cultured in 96-well plates for approximately 3 weeks. As soon as cell numbers allowed, genomic DNA were isolated, followed by the amplification of corresponding genomic target site with Phire Tissue Direct PCR Master Mix (Thermo Fisher Scientific). In case of knockout experiments, genomic loci carrying mutations were detected using T7 Endonuclease I assays (New England BioLabs) and desired biallelic frameshift indels were found and confirmed by Sanger-sequencing

(Microsynth GmbH). Chromatograms were analysed with publicly available indel-analyser Indigo tool (GEAR-Genomics)(242). In case of site-specific mutagenesis of PCNA, an Esp3I-binding site was introduced simultaneously with the base modification, allowing detection of successful modification with an endonucleotic digestion. Again, existence of biallelic mutation was confirmed with Sanger-sequencing. When it was possible, modifications were further confirmed by western blotting.

Table 2 List of mutant RPE-1 cell lines.

Cell line	Parental cell line	Origin
hTERT RPE-1 *TP53$^{-/-}$*	hTERT RPE-1	Lim et al (169)
hTERT RPE-1 *TP53$^{-/-}$ REV1$^{-/-}$*	hTERT RPE-1 *TP53$^{-/-}$*	This thesis
hTERT RPE-1 *TP53$^{-/-}$ REV3L$^{-/-}$*	hTERT RPE-1 *TP53$^{-/-}$*	This thesis
hTERT RPE-1 *TP53$^{-/-}$ PRIMPOL$^{-/-}$*	hTERT RPE-1 *TP53$^{-/-}$*	This thesis
hTERT RPE-1 *TP53$^{-/-}$ PCNAK^{164R}*	hTERT RPE-1 *TP53$^{-/-}$*	This thesis
hTERT RPE-1 *TP53$^{-/-}$ HLTF$^{-/-}$*	hTERT RPE-1 *TP53$^{-/-}$*	This thesis
hTERT RPE-1 *TP53$^{-/-}$ BRCA1$^{-/-}$*	hTERT RPE-1 *TP53$^{-/-}$*	Lim et al (169)
hTERT RPE-1 *TP53$^{-/-}$ REV1$^{-/-}$ PRIMPOL$^{-/-}$*	hTERT RPE-1 *TP53$^{-/-}$ REV1$^{-/-}$*	This thesis
hTERT RPE-1 *TP53$^{-/-}$ PCNAK^{164R} PRIMPOL$^{-/-}$*	hTERT RPE-1 *TP53$^{-/-}$ PCNAK^{164R}*	This thesis
hTERT RPE-1 *TP53$^{-/-}$ PCNAK^{164R} REV1$^{-/-}$*	hTERT RPE-1 *TP53$^{-/-}$ PCNAK^{164R}*	This thesis
hTERT RPE-1 *TP53$^{-/-}$ PCNAK^{164R} HLTF$^{-/-}$*	hTERT RPE-1 *TP53$^{-/-}$ PCNAK^{164R}*	This thesis

Table 3 CRISRP target sites and sequencing primers, ssDNA template for PCNA modification

Gene	Target sequence	Forward primer	Reverse primer
REV1	GAAGGGCAGCAAATACCTCA(GGG)	TGGTCATGTGATAGTGGCTGG	GCTCTTAATGCAACAGCTTAGACT
REV3L	AGTACCAGATCTAATCCATG(AGG)	TAGCGGAACAGTCAAAGCACAG	CTGTGGGAGGCTAAGAAACACTTC
PRIMPOL	TTTAACAAACCTGCCAACCC(AGG)	TGCAATGTAAGATAGACTGCCATGA	TCCTTCCTTTTCACAGTTTACTCA
PCNA	GTAATTTCCTGTGCACGAGA(CGG)	AGTGATCCTCCTCCGTCAAGA	TCGCAGATTTCAACAGTATCTCAA
HLTF	CATTTATTGATAGAGAATGG(TGG)	TGCTGCTTGGGTTTGAATGC	CTACCCTTCCCCTGTTGTGG
ssDNA template for PCNA modification			
G*A*G*ATCTCAGCCATATTGGAGATGCTGTTGTAATTTCCTGTGCACGAGACGGAGTGAAATTTTCT GCAAGTGGAGAACTTGGAAATG*G*A*A			

3.3 Preparation of whole cell lysates

Cells were washed by 1x PBS and detached from culturing surface using TripLE Expresse Enzyme (#12604013, ThermoFisher Scientific). Collected cells were lysed in 4x Laemmli buffer (200 mM TRIS (pH 6.8), 400 mM DTT, 8% SDS, 40% glycerol, 0.08% (w/v) bromophenol blue), and incubated at boiling water bath for 5 minutes. Samples were stored at -80˚C.

3.4 Western Blotting

Lysates were resolved on Mini-PROTEAN TGX Precast Protein gels (Bio-Rad) and transferred onto PVDF membranes (Bio-Rad) using electrophoretic wet transfer system. After transfer, membranes were blocked with 5% non-fat milk in TBST (20 mM TRIS pH 7.6 and 150 mM NaCl, 0.1% Tween 20) and incubated with corresponding primary antibody (dilution 1:2000 in 5% milk/TBST) overnight at 4˚C. Membranes were washed with TBST before incubation with HRP-coupled secondary antibodies (dilution 1:20000 in 5% milk/TBST). Chemiluminescence HRP-signal was detected with ClarityTM Western ECL Substrate (Bio-Rad) and a ChemiDox MP Imaging System (Bio-Rad) according to manufacturer's instruction.

3.5 Sensitivity measurements

For cytotoxicity assays, 250 RPE-1 cells per well in 384-well plates were seeded and incubated with cisplatin at a range of concentrations using threefold dilution series from 10 µM to 4.5 nm. Cell viability was measured after 120 hours using PrestoBlue (Thermo Fisher) and an EnSpire plate reader (Perkin-Elmer). Three technical replicates were averaged per experiment. Data were normalised to untreated cells; curves were fitted *drm* stats function in R and IC50 values for each experiment per cell lines were calculated according to the formula:

$$IC50 = exp^{\frac{e^b}{b} log\left(\frac{d-1}{50-1}-1\right)}$$

Where ***c*** is the lowest point of the curve, ***d*** is the highest point of the curve, ***b*** is the slope of the curve. Individual IC50 values were divided by the mean of IC50 values of control cell line producing relative IC50 values.

3.6 Whole-genome sequencing, mutation calling and data analysis

Library preparation and DNA sequencing were done at Novogene, Beijing, China on Illumina NovaSeq instruments in 2x150 bp paired-end format. Besides ancestral sample, three independent clones were sequenced from each treatment per each cell line. After quality control of raw sequences with FastQC, low quality and adapter sequences were removed using Trimmomatic (243) as well as duplicated reads using Samblaster. Remaining reads were aligned against the GRCh38 reference genome with bwa-mem (244). In order to improve accuracy of variant calling and detection of sort indels, samples were realigned using dedicated tools from GATK (245). To detect unique mutation in each sample, I used modified version of mutation detector tool Isomut, which used samtools with the -E flag during pileup generation to improve sensitivity towards complex mutations (246). Resulting lists of unique mutations were analysed further using R programming language. First, mutations were filtered, based on S-score generated by Isomut, allowing no more than five SBS mutation and one indel in any ancestral clone. Detected unique mutations in these samples provide an internal control for false positives.

Data presented in this thesis came from three Isomut runs:

- Mock treated RPE-1 control cell line and TLS mutants (one ancestral and three descendent clones per cell line, in total 32 samples),
- "twin" runs including mock treated RPE-1 control, *BRCA1* and *HLTF* mutants, HMEC mock treated, and cisplatin treated RPE-1 samples (total 32 samples), excluding one semi-independent cisplatin-treated *BRCA1*$^{-/-}$ clone from each run

Preprocessing and analysis of mutation spectra, non-negative matrix factorization and deconstruction to COSMIC and *de novo* signatures were conducted using the MutationalPatterns R package (version 3.2.0) (247) and Python tool SigProfilerExtractor (248).

3.7 Structural variant calling

Structural variations in samples grouped by genotypes were detected with GRIDSS2 (249) using default parameters. After identification of somatic events with associated *gridss_somatic_filter* script, hits were filtered for confidence PASS variants. To enhance sensitivity for shorter (<200 bp) events, variants without soft-clipped

evidence were also included. Replication timing analysis was performed using the high-resolution HepG2 Repli-seq dataset.

3.8 Copy number variant calling

To visualize ploidity of starting clones, I used a list custom RPE-1 specific mutations distributed uniformly across the reference genome (GRCh38), with average intermutation distance of 10 kbp. Coverages and allele frequencies of selected positions were calculated using *pysam* Python library, followed by determination of coverage profiles of mock treated clones using mean coverage of each sample and the mean GC ratio across non-overlapping 10 kbp windows calculated using bedtools (250). Windows overlapping with either centromeres or ENCODE blacklisted regions (251) were omitted. The modelled coverage in each window was determined using linear regression with the formula:

$$Cov_{ji} = Cov_{SCi} + GC_i + \varepsilon_i,$$

- Cov_{ji} is the coverage of the i^{th} window in sample j,
- Cov_{SCi} is the coverage of the i^{th} window in the corresponding ancestral clone,
- GC_i is the GC content of the i^{th} window,
- ε_i is random error and systematic ploidy change-induced deviations from the expected coverage.

Copy number variant were quantified with ASCAT (252), using aforementioned custom mutation list and parameter *gamma* set to 1. Due to the absence of available germline data, dummy germline for each sample were created by setting LogR values at 0, and setting BAF values at 0, 0.5 and 1 for loci with allele frequencies between 0-0.1, 0.1-0.9 and 0.9-1, respectively. The custom GC-content and replication timing files for LogR correction were generated using the associated helper scripts. Segmented ploidy levels were subtracted from each starting clone using the ploidy levels of corresponding mock treated clones. The resulting profiles were filtered for significant change of ploidy. Finally, the identified ploidy change events were finally manually checked to obtain a high-confidence variant set.

3.9 Comparison of cancer cell line genomes

Mutational data of 19 WGS samples published by Petljak and colleagues (253) were downloaded and mutation numbers from isogenic clones were summarized. Triplet spectra were reconstructed using Spectra were deconstructed with Mutational Patterns (247) using strict mutational fitting with maximum delta set to 0.004. Reference set for deconstruction contained solely *de novo* signatures SBS-A and SBS-B obtained from NMF on TLS-mutant RPE-1 cell lines. Reconstructed samples reached 0.9 or higher cosine similarity with original spectra were selected for further analysis.

3.10 Analysis of DT40 genomes

Triplet spectra of DT40 cell lines are derived from a previous publication of our research group (166). DT40-specific *de novo* SBS signatures were retrieved using NMF with MutationalPattern R package (247).

3.11 Comparison of cisplatin-treated genomes

Published mutation data of cisplatin treated human and DT40 data (254-256) were downloaded and NMF was performed together with cisplatin-treated RPE-1 samples using MutationPatterns (247). Principal component analysis was performed on centered and scaled triplet spectra data using *prcomp* stats function in R, whereas UMAP and tSNE analysis were performed on scaled but uncentered data, using *umap* and *Rtsne* R packages, respectively.

3.12 Statistical analysis

Unpaired two-sided *t*-tests were used for statistical comparisons of mutation numbers, with no adjustments for multiple comparisons except where noted. Significant ploidy changes were filtered with Mann-Whitney test ($p < 0.001$, effect size > 0.1).

4 Results

4.1 Investigating the role of translesion synthesis in spontaneous mutagenesis.

4.1.1 Disruption of TLS by targeting major regulator and effector proteins

To determine how DNA damage tolerance shapes mutational landscape of human cells, I first investigated the role of TLS in spontaneous mutagenesis. My model RPE-1 is an hTERT-immortalized, untransformed cell line of retina pigment epithelial origin what is an emerging model for mutagenesis. *TP53*-knockout line (hTERT RPE-1 *TP53*$^{-/-}$) was selected as control as this background allows inactivation of HR genes like BRCA1 (169, 257). I utilized CRISPR-mutagenesis to establish homozygous *REV1*$^{-/-}$ (regulator of TLS), and *PRIMPOL*$^{-/-}$ (effector protein of repriming, thus separates possible replicative and post-replicative DDT pathways) knockout cell lines and to introduce K164R (lysine 164 to arginine) amino acid-changing mutation to *PCNA* (*PCNA*^{K164R} from now on), which results in the loss of PCNA-(mono)ubiquitination-dependent activation of TLS. Besides single mutants I established all possible double mutant combinations as well. Furthermore, I made a homozygous *REV3L*$^{-/-}$ line to investigate REV1/Polζ mutasome-independent role of both REV1 and universal extensor TLS-polymerase Polζ.

The *REV1*-specific sgRNA targeted UBM2-domain of gene near the C-terminus and resulted complete loss of protein, whereas *in situ* modification of PCNA prevents its DNA damaged-induced monoubiquitylation. Frameshift mutations are introduced immediately upstream the polymerase domain of *PRIMPOL*. Finally, *REV3L* were knocked out by targeting exon 12 which presented in functional splicing variant of the gene (258) (Fig. 4A).

4.1.2 Assessment of spontaneous mutagenesis in TLS-mutant line by whole-genome sequencing

To investigate patterns of spontaneous mutagenesis in TLS-mutants, single cell clones were isolated from each cell line. Expanding clonal cell populations were separated as soon as cell numbers allowed. Cells were further cultured under normal conditions for a total of 60 days, followed by a second single cell cloning step from each culture (Fig. 4B). Three

independent, isogenic cell clones and the ancestral clone for each cell line were whole genome sequenced at 30x mean coverage. Single base substitution and short indel events were detected utilizing IsoMut tool developed to find unique mutations in isogenic samples (259), making possible to identify the mutations arose between the two cloning steps. In control line hTERT RPE-1 *TP53-/-* I detected an average of 813 SBS-s, 17 insertions and 19 deletions per clone established in these 60 days. In mutants defective in either *REV1* or *REV3L* strong and significant reduction of SBS numbers ($p < 0.0001$, unpaired two-sided *t*-test) were observable, whereas *PRIMPOL* single mutant but not $PCNA^{K164R}PRIMPOL$ double mutant shows small decrease in SBS mutation rate (p = 0.015) (Fig. 4C). SBS rate in $PCNA^{K164R}$did not significantly differed from controls. Indel mutagenesis rates were broadly similar in every line with the exceptions of slightly decreased insertions rates in $PCNA^{K164R}$and *PRIMPOL* compared to control (p-value 0.022 and 0.031, respectively) and marked elevation of deletions in $PCNA^{K164R}REV1$ mutants (p= 0.013) (Fig. 4D,E).

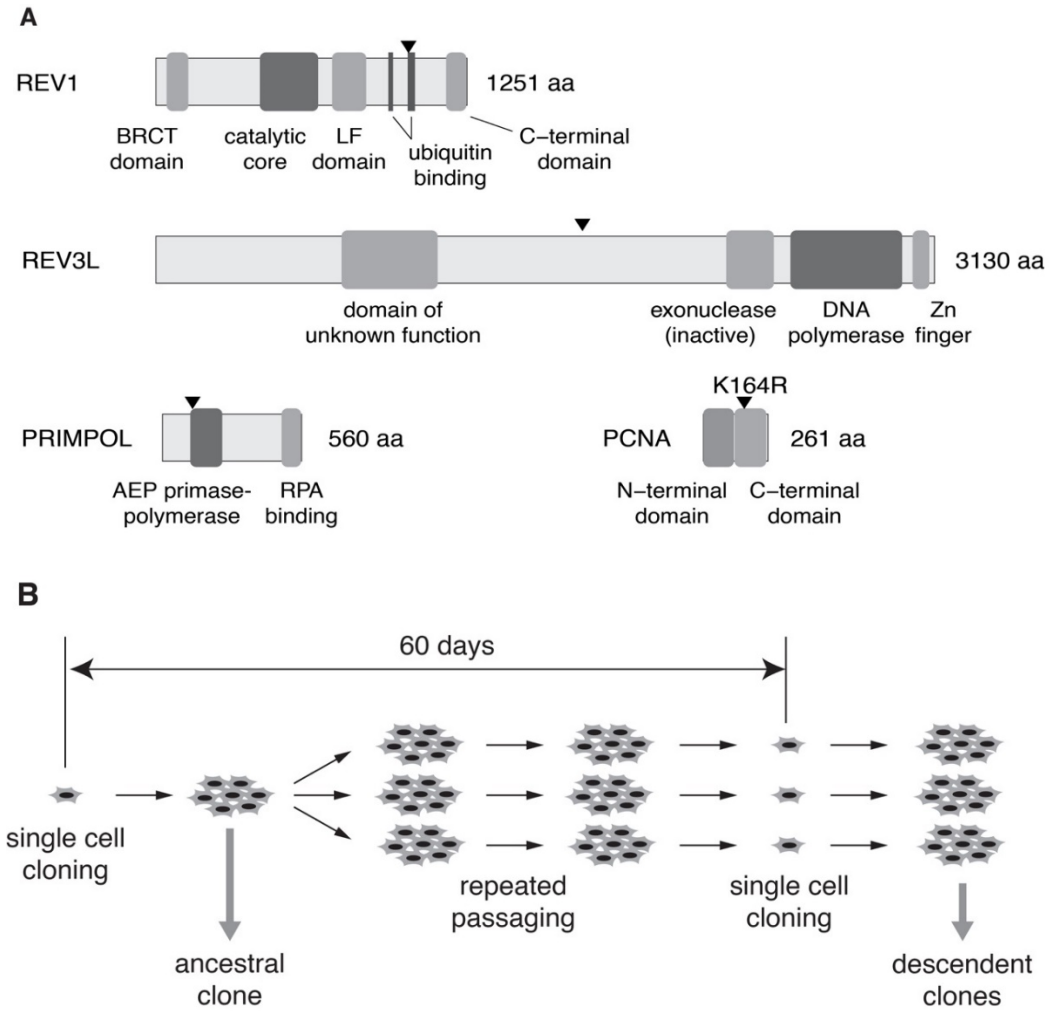

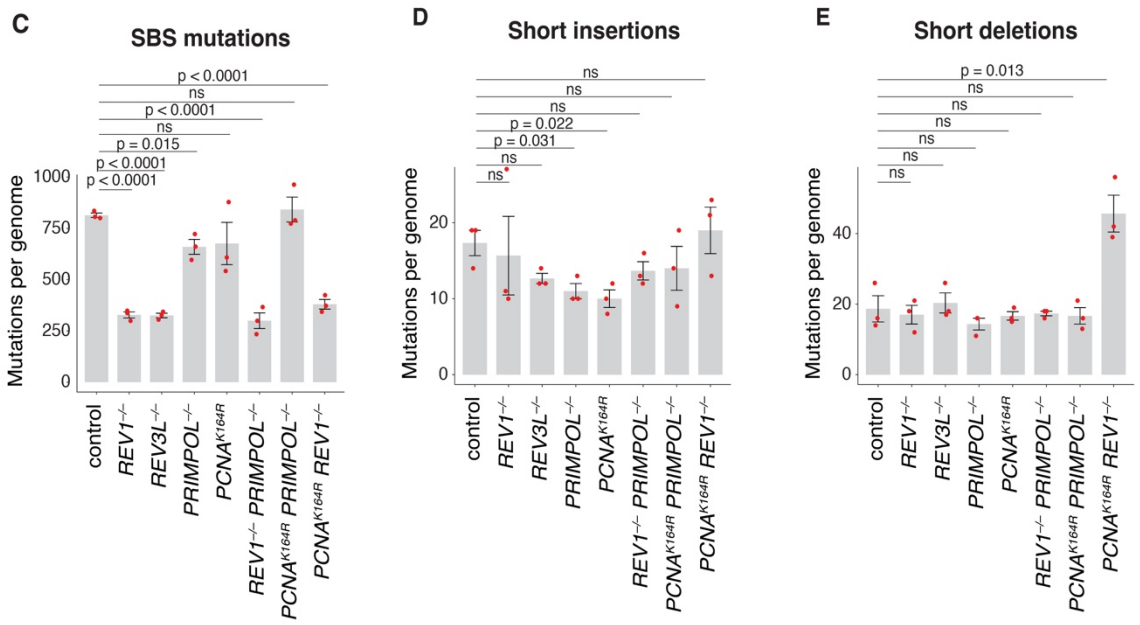

Figure 4 *Regulators of TLS affects spontaneous mutagenesis in human RPE-1 cells. (A) Schematic representation of REV1, REV3L, PRIMPOL and PCNA, with main domains highlighted according to InterPro database. CRISPR target sites are indicated with black triangles. (B) Experimental setup of long-term mutagenesis experiment. Between two single cell cloning steps, cells were separated into three parallel cultures and grew for 60 days. Genomic DNA were isolated and sequenced from the ancestral clone and three subclones from each cell line. (C-E) Number unique of SBS, short insertion and short deletion mutations found in descendent clones. Individual values indicated by red dots, bars show mean and SEM values. Significance of changes were compared to control using unpaired two-sided t-tests, p-value > 0.05 were considered non-significant (ns). No adjustment was made for multiple comparison. Modified version of a figure from Gyure et al (260)*

4.1.3 REV1, REV3L and PRIMPOL affect base substitution mutagenesis

During analysis of SBS signatures, mutations are categorized into six classes considering the pyrimidines: C>A, C>G, C>T, T>A, T>C, and T>G. Classes further expanded to subclasses considering the genomic context (upstream and downstream bases), resulting in a 96-channel representation, called triplet-spectra (218). Plotting SBS-spectra of control *TP53*$^{-/-}$ line showed high and specific C>A peaks especially in NCA and NCT triplet context (Fig. 5A). Based on triplet signatures of all cell lines revealed that SBS spectra of *PCNA*^{K164R} and *PCNA*^{K164R}*PRIMPOL*$^{-/-}$ were similar to the control, whereas all samples with either *REV1*- or *REV3L*-deficiency showed similar spectra with reduction in almost all mutation classes (Fig. 5B). In contrast, *PRIMPOL* mutant showed

unique spectrum (Fig. 5B). Mutational landscapes are usually shaped by distinct mutagenic effects with characteristic signatures (218). To identify these distinct patterns in my samples, I used non-negative matrix factorization (NMF) to derive two mutational signatures (Fig. 5C). Mixture of these two signatures (SBS-A and SBS-B) in varying proportion can reproduce original patterns of every sample with 0.91 to 0.98 cosine similarities. SBS-A showed strong similarity with COSMIC signatures SBS18 and SBS36 with cosine similarity 0.93 and 0.9, respectively, whereas SBS-B showed greatest similarity with COSMIC SBS3 and SBS40 (cosine similarity 0.87 and 0.93, respectively) (Fig. 5D). SBS18 and SBS36 show strong similarity (cosine similarity 0.91), and both considered to be result of impaired repair of 8-oxoG formed by reactive oxygen species (ROS), due to defect of DNA glycosylases OGG1 and MUTYH, respectively (261-263). Likewise, SBS40 and SBS3 show cosine similarity of 0.88. Whereas SBS3 was detected in tumour samples with deficiency in homologous recombination, like BRCA1/2-negative breast cancers (221, 264, 265), aetiology of SBS40 is unknown though its cosine similarity of 0.88 with SBS3 suggests similar underlying molecular mechanisms. Deconstruction of triplet spectra of samples to COSMIC signatures showed similar proportions of SBS18/36 and SBS3/40 mutagenesis, supporting results from *de novo* signatures (Fig. 5E,F). Robustness of deconstruction was further confirmed by repeating NMF with an alternative software. Recommended signatures of repeated analysis showed remarkable cosine similarity with SBS-A and SBS-B (1 and 0.978, respectively).

REV1, REV3L and PRIMPOL had strong influence on the ratio of SBS-A and SBS-B. Surprisingly, SBS-B almost completely vanished from samples with either REV1 or REV3L mutation, suggesting that the REV1/Polζ complex is responsible for this HRD-like mutagenic process (Fig. 5E). In contrast, $PRIMPOL^{-/-}$ samples showed increased contribution of SBS-B in expense of SBS-A. $PCNA^{K164R}$ and $PCNA^{K164R}$ $PRIMPOL^{-/-}$ did not differ from control samples (Fig. 5E). I concluded that REV1/Polζ is responsible for "flat" signature SBS-B, which resembles COSMIC SBS3 and SBS40, whereas PRIMPOL plays a role in an SBS18/36-like mutagenic process characterized by C>A transversions, and this role might depend on PCNA-ubiquitination (Fig. 5E).

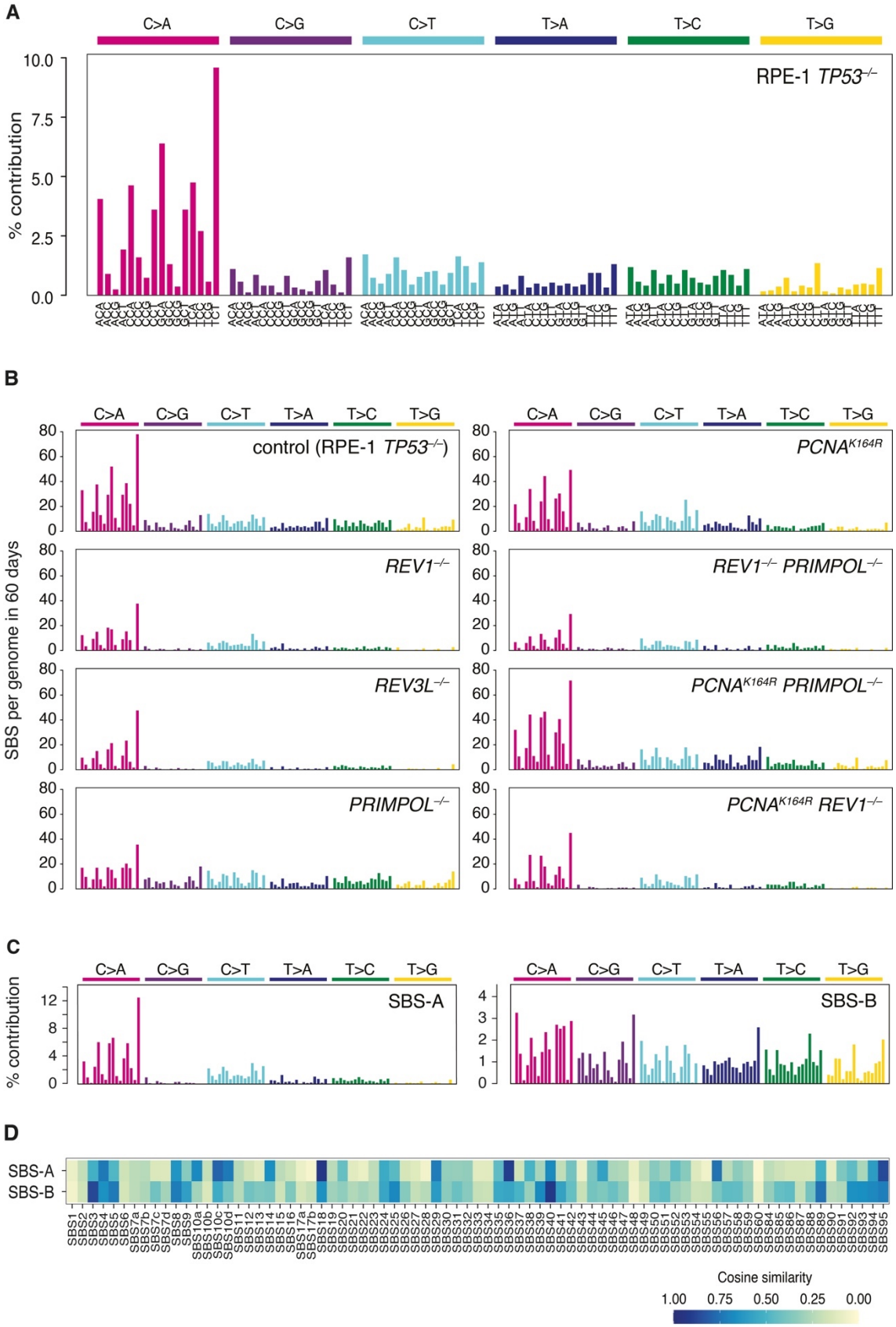
A
C>A
C>G
C>T
T>A
T>C
T>G
RPE-1 TP53−/−
% contribution
10.0
7.5
5.0
2.5
0.0
B
control (RPE-1 TP53−/−)
PCNAK164R
REV1−/−
REV1−/− PRIMPOL−/−
REV3L−/−
PCNAK164R PRIMPOL−/−
PRIMPOL−/−
PCNAK164R REV1−/−
SBS per genome in 60 days
C
SBS-A
SBS-B
% contribution
D
SBS-A
SBS-B
Cosine similarity
1.00
0.75
0.50
0.25
0.00

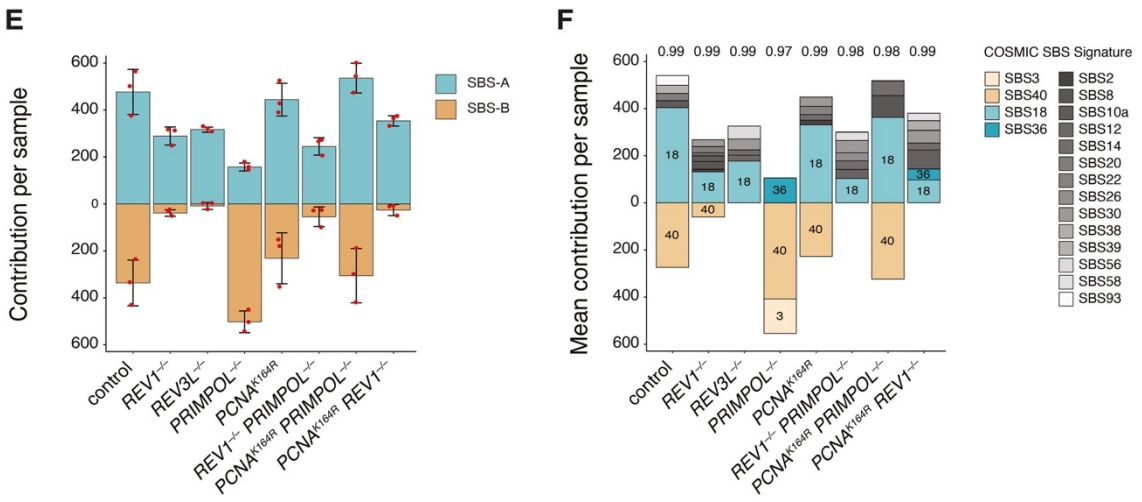

Figure 5 *SBS mutagenesis in consists of two components regulated by REV1/Polζ and PRIMPOL (A) Averaged SBS mutation spectra of control hTERT RPE-1 TP53$^{-/-}$ cell line (n=3). The main categories of 96-dimensional representation indicated above the panel whereas sequence context (preceding and following bases, forming 16 subcategories within is main categories) are shown below. (B) Average SBS spectra of DDT-mutant cell lines (n=3). (C) Triplet spectra of de novo mutagenesis signatures retrieved from all 24 samples using non-negative matrix factorization. (D) Heatmap of cosine similarities values between de novo signatures and all COSMIC v3.3 SBS signatures. (E) The contribution of SBS-A and SBS-B to the SBS spectrum of samples with the indicated genotypes. Mean and SEM are shown, individual values are indicated by red markers. (F) Deconstruction of the mean SBS spectrum of each genotype into COSMIC v3.3 SBS signatures. Cosine similarities of the original and reconstructed spectra are shown above each column. Figure from Gyure et al (260)*

4.1.4 SBS-A and SBS-B are generated by mutagenic processes common in human cultured cells

According to my results, spontaneous mutagenesis of RPE-1 *TP53*$^{-/-}$ cells are mainly shaped by processes attributed to HRD-deficiency and oxidative stress, though the cell line is HR-proficient and was not exposed to deliberate oxidative effects. To exclude the possibility that SBS-A and SBS-B are RPE-1 specific signatures, I validated results by investigating of another hTERT-immortalized normal human cell line. Triplet signature of HMEC was very similar to that of RPE-1 *TP53*$^{-/-}$ and could be reconstructed using SBS-A and SBS-B with high efficiency (cosine similarity of reconstructed signatures to originals were >0.94 in all clones) (Fig. 6A-B). I also reanalyzed spectra of 19 human cell lines published by Petljak and colleagues (266). Spontaneous mutation spectra of 12 out of 19 cell lines could be reconstructed using SBS-A and SBS-B with

cosine similarity 0.9 or greater, supporting that mutagenic signatures found in RPE-1 cells are results of common mutagenic processes of cultured cell lines (Fig. 6C-D). The remaining seven cell lines showed extensive APOBEC- or MMR-related mutagenesis, two hypermutator phenotype with characteristic triplet patterns. Three out of twelve cell lines spectra could be reconstructed using only SBS-B (Fig. 6D). MDA-MB-436 is a *BRCA1*-mutant triple negative breast cancer (TNBC) cell line, whereas HCC38 is another TNBC line with confirmed *BRCA1* promoter methylation (267). Similarly, NCI-H650 carries truncating *BRCA2* mutation. Furthermore, analysis of spontaneous mutational spectra of RPE-1 *TP53*$^{-/-}$*BRCA1*$^{-/-}$ lines showed that elevated SBS mutagenesis in this cell line could be wholly attributed to SBS-B (Fig. 6H). Taken together, these results prove a connection between REV1/Polζ-dependent SBS-B and defect of HR and show that the (TLS-dependent) mutagenic process responsible for elevated mutagenesis in HR-deficient cells operates in HR-proficient cells as well.

To cover all DDT pathways, I knocked out yeast Rad5 homolog *HLTF* in RPE-1 *TP53*$^{-/-}$ and RPE-1 *TP53*$^{-/-}$*PCNA*^{K164R} backgrounds, targeting its SNF2 domain. *HLTF*$^{-/-}$ showed increased SBS-mutagenesis but decreased number of indels, whereas all mutation types decreased in *PCNA*^{K164R}*HLTF*$^{-/-}$ (Fig. 6F,G). Deconstruction of triplet spectra with *de novo* signatures showed that lack of HLTF increased the proportion of SBS-B, which phenotype is PCNA-(mono)ubiquitination-dependent (Fig. 6E,H).

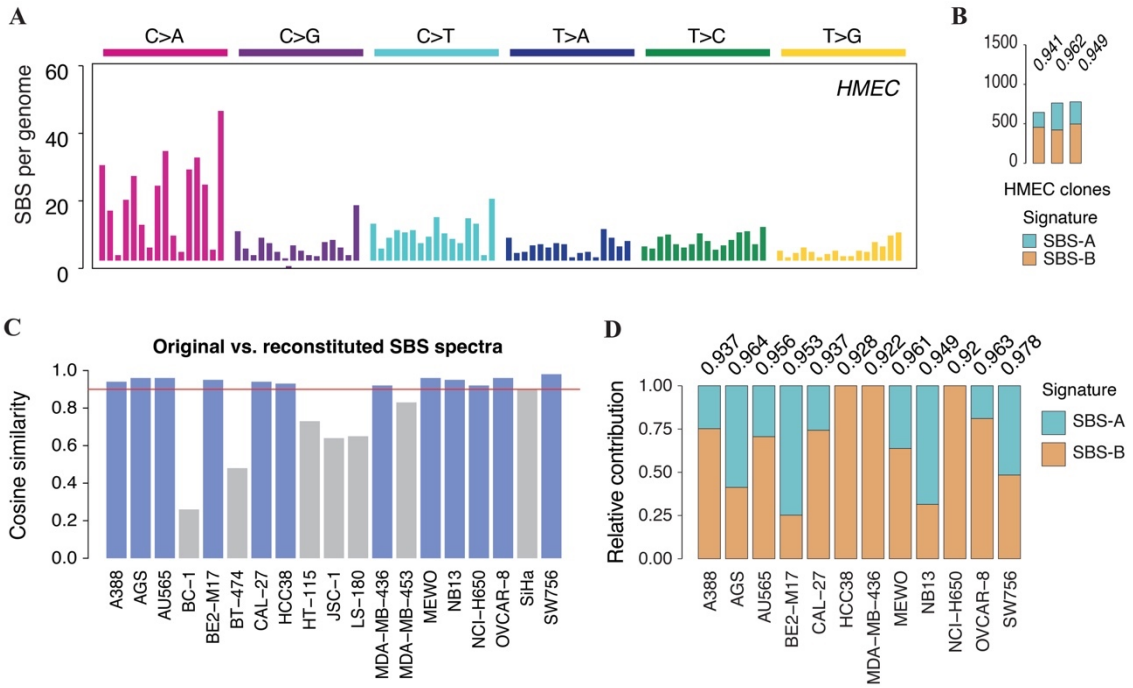

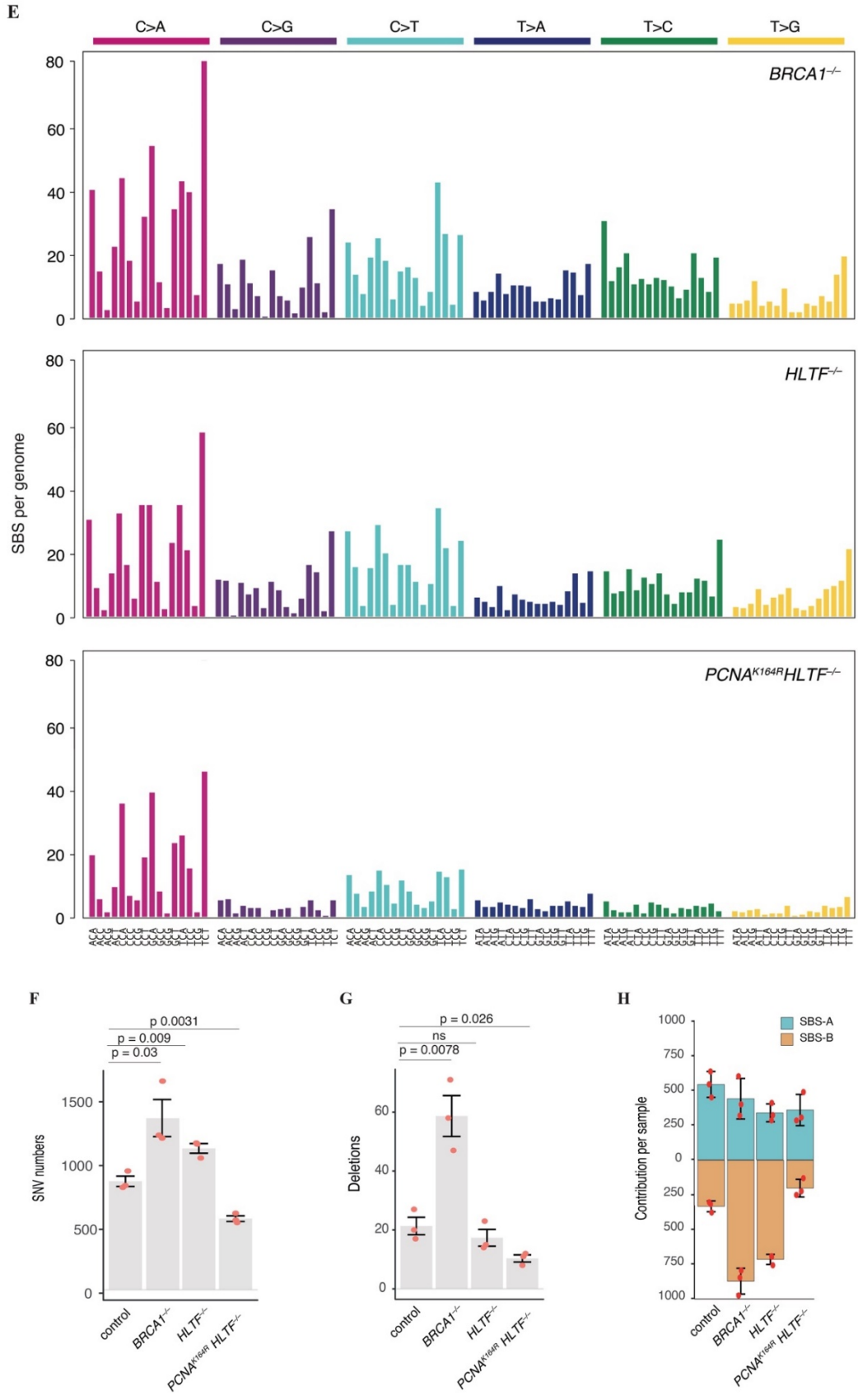
E
C>A
C>G
C>T
T>A
T>C
T>G
BRCA1-/-
HLTF-/-
PCNAK164RHLTF-/-
SBS per genome
F
p 0.0031
p = 0.009
p = 0.03
SNV numbers
control
BRCA1-/-
HLTF-/-
PCNAK164R HLTF-/-
G
p = 0.026
ns
p = 0.0078
Deletions
H
SBS-A
SBS-B
Contribution per sample

Figure 6 *SBS-A and SBS-B identify common mutagenesis processes in human cell lines (A) Averaged triplet SBS spectrum of spontaneous mutagenesis of three mock treated hTERT HMEC human cell line clones. (B) Deconstruction of each HMEC clones to de novo signatures SBS-A and SBS-B. Cosine similarity of each reconstructed spectra with original sample are shown on the top of each column. (C) Deconstruction efficiency of SBS of spectra of 19 human cell lines based on cosine similarity of original vs reconstructed spectra, threshold indicated at 0.9. (D) relative contribution of SBS-A and SBS-B in the SBS spectra of cell lines with reconstruction efficiency of 0.9 or above. (E) SBS spectra of BRCA1$^{-/-}$, HLTF$^{-/-}$ and PCNA^{K164R} HLTF$^{-/-}$* cell lines. (F-G) *Number unique of SBS and short deletion mutations arose cell lines from (E). Individual values indicated by red dots, bars show mean and SEM values. Significance of changes were compared to control using unpaired two-sided t-tests, p-value > 0.05 were considered non-significant (ns). No adjustment was made for multiple comparison. (H). The contribution of SBS-A and SBS-B to the SBS spectrum of samples with the indicated genotypes from (E). Mean and SEM are shown, individual values are indicated by red markers. Modified version of a figure from Gyure et al (260)*

4.1.5 TLS-dependent mutagenesis in HRD background is evolutionally conserved

To investigate whether TLS-dependent HRD-mutagenesis is an evolutionary conserved mechanism, I reanalysed TLS- and HR-deficient DT40 chicken lymphoblast cell samples from a previous publication of our lab (166). In accordance with RPE-1 mutants, *REV1*$^{-/-}$ and *BRCA1*$^{-/-}$ DT40 cell lines show decreased and markedly increased SBS numbers, respectively. Although triplet spectra of DT40 miss C>A peaks and have flatter pattern (Fig. 7A), signatures derived from NMF show similar behaviour that of in RPE-1: a REV1-dependent signature is wholly responsible for extensive SBS-mutagenesis in *BRCA1*$^{-/-}$ mutant (Fig. 7B-C). These similarities suggest evolutionary conserved role of TLS in HRD genotypes, even if signatures from an evolutionarily distinct species cannot be fully comparable to that of derived from human tumour samples.

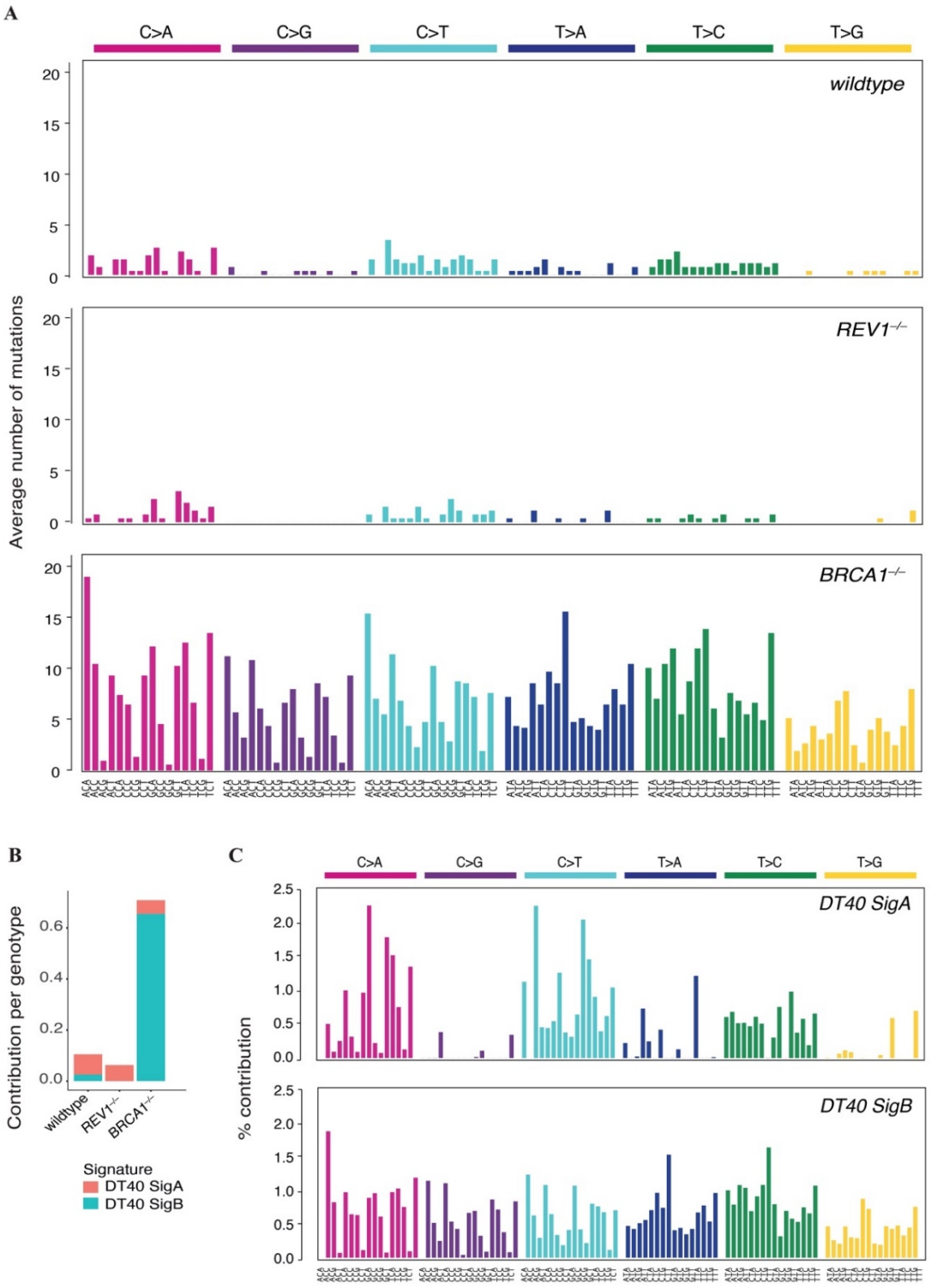

Figure 7 *SBS mutagenesis in DT40 cell lines shows analogues to that of human cell lines. (A)Averaged triplet spectra of DT40 cell lines. (B) The contribution of DT40 SigA and DT40 SigB to the SBS spectrum of indicated DT40 genotypes. Each column represents mutations of three clones. (C) De novo triplet spectra derived from DT40 wildtype control, REV1$^{-/-}$ POLH$^{-/-}$, BRCA1$^{-/-}$ REV1$^{-/-}$ and BRCA1$^{-/-}$POLH$^{-/-}$using NMF*

4.1.6 TLS regulates accurate replication of homopolymer repeats

Analysis of indels based on their sequence context revealed increase of short deletions no longer than 3 bp at repeat sequences in the *PCNA*^{K164R}*REV1*$^{-/-}$ cell line (Fig. 8A). Arising deletions were predominantly single A/T deletions at homopolymer repeats longer than 4 bp, 2 bp deletions at 2- or 3-unit repeats or 3 bp deletions at 2-unit repeats (Fig. 8A). Cell line also showed modest increase of 2 bp deletion at with microhomology, though these deletions are predominantly 2 bp long, thus single nucleotide microhomology could also happen by chance. *PCNA*^{K164R} decreased the single C deletion either on its own compared to control or in combination with any other mutations compared to the corresponding single mutants (Fig. 8A). *BRCA1*$^{-/-}$ showed unique pattern characterized predominantly by 5 bp or longer deletions with or without microhomology what is attributed to activation of non-homologous end joining repair of DSB-s in absence of HR (225) (Fig. 8A). Decomposition of indel patterns using COSMIC indel signatures showed large contribution of ID4 signatures *PCNA*^{K164R}*REV1*$^{-/-}$ (Fig. 8C). As REV1, which promotes error-prone TLS producing SBS-A, and PCNA-(mono)ubiquitination which seems to contribute in SBS-B, are the two primary regulators of TLS, this suggests the activation of a backup mechanism which might utilise 1-3 bp repeat sequences for translesion replication by template slippage. Interestingly, while PCNA-ubiquitination prevents from 2-3 bp deletions, *PCNA*^{K164R} mutation decreases the number of 1 bp deletions in all background as shown by the decreased proportion if ID9 signature in these cell lines. Furthermore, contribution of ID9 is increased in RPE-1 *REV1*$^{-/-}$ but completely disappeared in RPE-1 *PCNA*^{K164R}*REV1*$^{-/-}$(Fig. 8C). A possible explanation is that in the absence of REV1, overactivation of monoubiquitinated PCNA-mediated TLS produces 1 bp deletion at repeat sequences (Fig. 8B). The exact aetiology of ID9 has yet to be discovered, but it has been linked to AID-mediated formation abasic sites (268) and activation of Polθ (269) and has been shown to associate with genomic instability (270, 271).

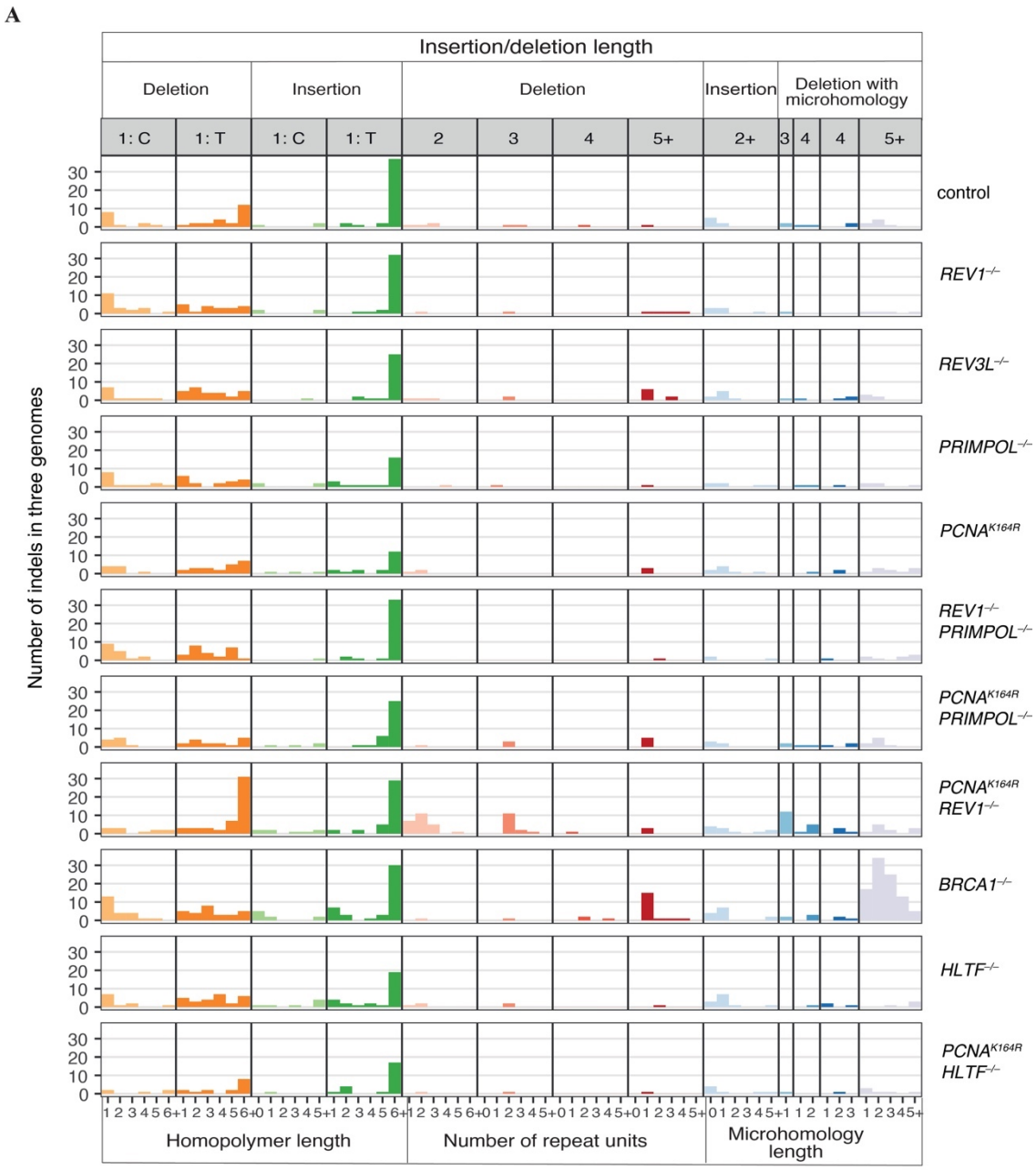
A
Insertion/deletion length
Deletion
Insertion
Deletion
Insertion
Deletion with microhomology
1: C
1: T
1: C
1: T
2
3
4
5+
2+
3
4
4
5+
Number of indels in three genomes
control
REV1−/−
REV3L−/−
PRIMPOL−/−
PCNAK164R
REV1−/− PRIMPOL−/−
PCNAK164R PRIMPOL−/−
PCNAK164R REV1−/−
BRCA1−/−
HLTF−/−
PCNAK164R HLTF−/−
Homopolymer length
Number of repeat units
Microhomology length

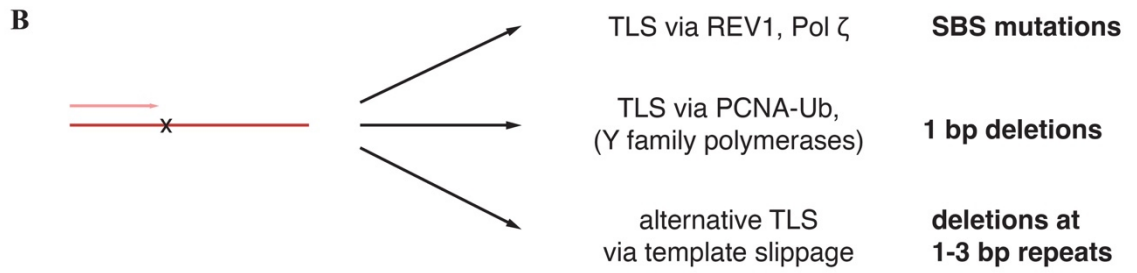
B
TLS via REV1, Pol ζ
SBS mutations
TLS via PCNA-Ub,
(Y family polymerases)
1 bp deletions
alternative TLS
via template slippage
deletions at
1-3 bp repeats

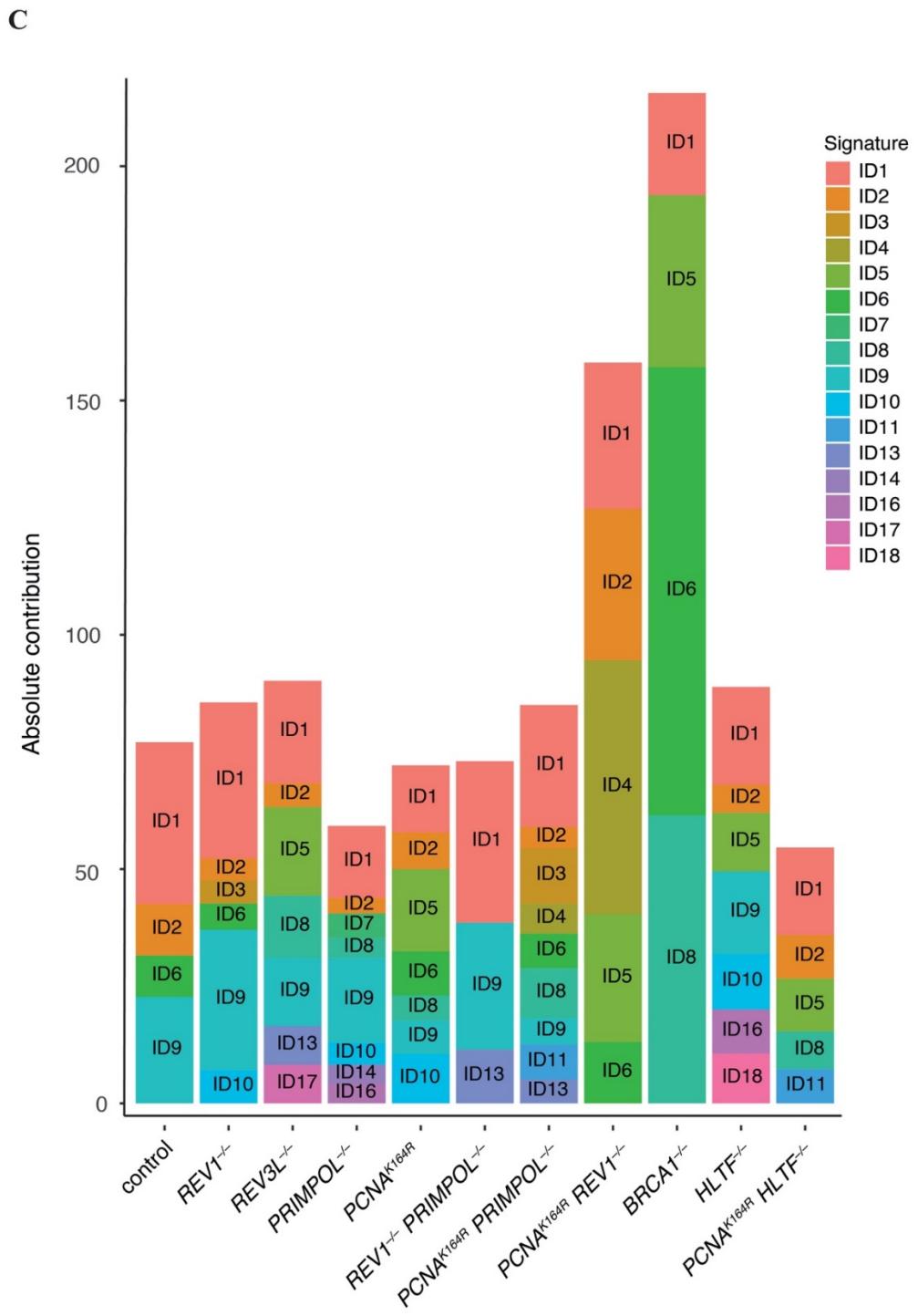

Figure 8 *TLS regulates accurate replication of homopolymer repeats (A) Indel spectra of all RPE-1cell lines, according to COSMIC indel classification, with insertion longer than 1 bp collapsed for clarity. (B) Simple model for role of TLS in formation of short indels: SBS mutagenesis is caused by bypassing genomic lesion by REV1/Polζ., whereas PCNA-(mono)ubiquitination driven TLS produces 1 bp deletion. In the absence of both processes, an alternative TLS pathway is activated which utilizes short deletions and produces short deletions due to template slipping. (C)Deconstruction of short indels per genotypes using COSMIC ID signatures.*

4.1.7 REV1/Polζ prevents long deletions of kilobase pair size

To detect deletions above the size range covered by IsoMut analysis, I used GRIDSS2 structural variant caller which can detect rearrangement breakpoint using de Bruijn graph breakend assembly algorithm (249). In *TP53*$^{-/-}$ control, *PRIMPOL*$^{-/-}$, *PCNA*^{K164R}*PRIMPOL*$^{-/-}$ and *HLTF*$^{-/-}$ cell lines, less than 2 long deletions (> 50 bp) per genome arose in the 60 days of the experiment (Fig. 9A-B). In contrast, cell lines with either *REV1* or *REV3L* mutations developed large number of deletions that fell mostly in the range of 500-5000 bp size (Fig. 9A-B). Although defect in REV1/Polζ appears to be the main mediator of enrichment of deletions in this size range, phenotypes varied as I found 2.4-fold more deletions in *REV3L*$^{-/-}$ cells compared to *REV1* mutants (an average of 29 vs 12 events per genome, p=0.002, unpaired two-sided *t*-test) (Fig. 9B). These deletions predominantly developed in late replicating regions in *REV1*$^{-/-}$ and *REV3L*$^{-/-}$ cells (Fig. 9C). Although REV3L has shown to have a role in the prevention of large scale chromosome instability (272), such narrow size range of deletions suggests distinct mutagenic process.

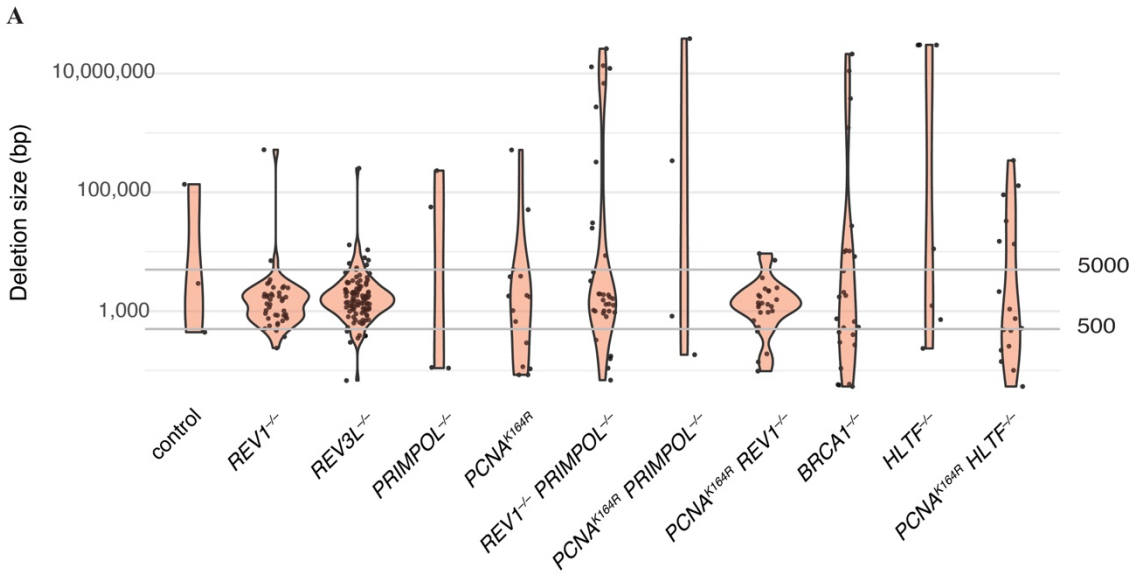

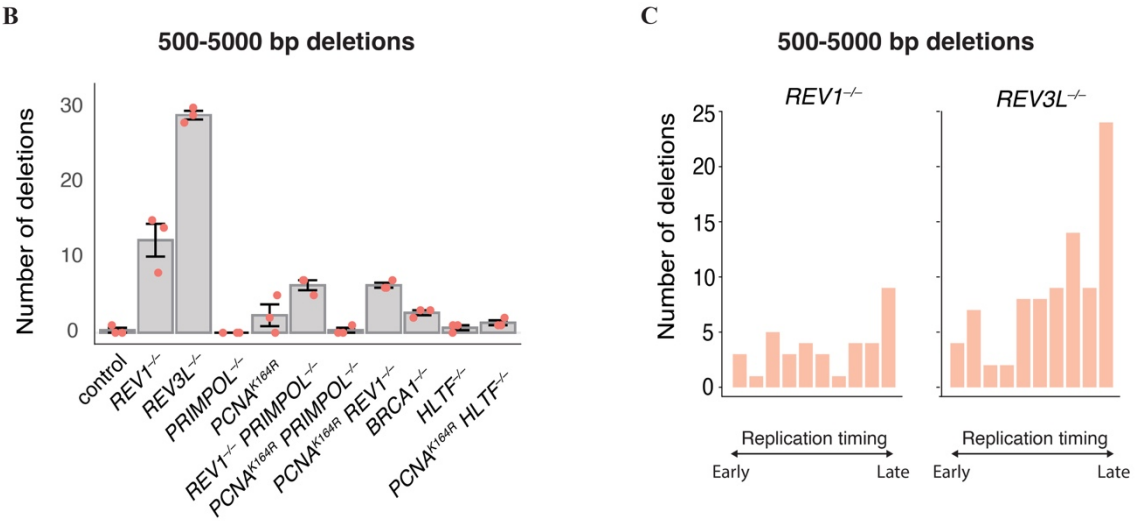

Figure 9 *REV1/Polζ prevents long deletions of kilobase pair size (A) Size distribution of >50 bp deletions identified with GRIDSS2. Event were pooled by genotypes; each marker represents one deletion. (B) Mean and SEM values of deletions numbers in the 500-5000 bp size range per genome. Markers represent values of individual clones. (C) Distribution of deletions in the 500-5000 bp size range by replication timing in REV1$^{-/-}$ and REV3L$^{-/-}$ cells.*

4.1.8 REV1 and PRIMPOL play redundant roles to prevent chromosome instability

To quantify chromosome-level changes arose during culturing time, I utilized an algorithm established by our lab (260), which detects copy number alterations (CNAs) in isogenic samples based on sequence coverage and allele frequency of heterozygous SNPs. I found copy number abnormalities in every ancestral clone. For instance, extra copy of chromosome 7 and 11, as well as even higher copy number of segments of chromosome were found in RPE-1 *TP53*$^{-/-}$ control ancestral (Fig. 10A). In contrast, these CNA-s were not found in other ancestral clones, though all single mutant cell lines were derived from RPE-1 *TP53*$^{-/-}$. Genomes of descendent clone were compared to corresponding ancestral clone to identify changes in copy number established during the 60 days of mock treatment. Mutants were defective in TLS-initialization but not in repriming (*REV1*$^{-/-}$, *PCNA*^{K164R} and *PCNA*^{K164R}*REV1*$^{-/-}$), showed low number of deletions and no duplications (Fig. 10B-C). Loss of PRIMPOL caused low number of both deletions at the 0.1-1 Mb range duplications of at least 10 Mb in size. Simultaneous depletion of REV1 and PRIMPOL resulted in the greatest number of CNAs compared to control (p=0.006, unpaired two-sided *t*-test), with both duplications and deletions longer than 1 Mb.

Increased numbers of deletions and duplications were found on *BRCA1*$^{-/-}$ as well (p=0.012) (Fig. 10B). Genomic instability caused BRCA1/2-deficiency has been previously observed (273-275) and may be attributed to the excessive accumulation of ssDNA gaps (276) or the defect in protection of stalled fork (277). I also found increased number of CNAs events in *REV3L*$^{-/-}$ and *PCNA*^{K164R}*HLTF*$^{-/-}$ cells, though these were not significant probably due to the small numbers (Fig. 10B).

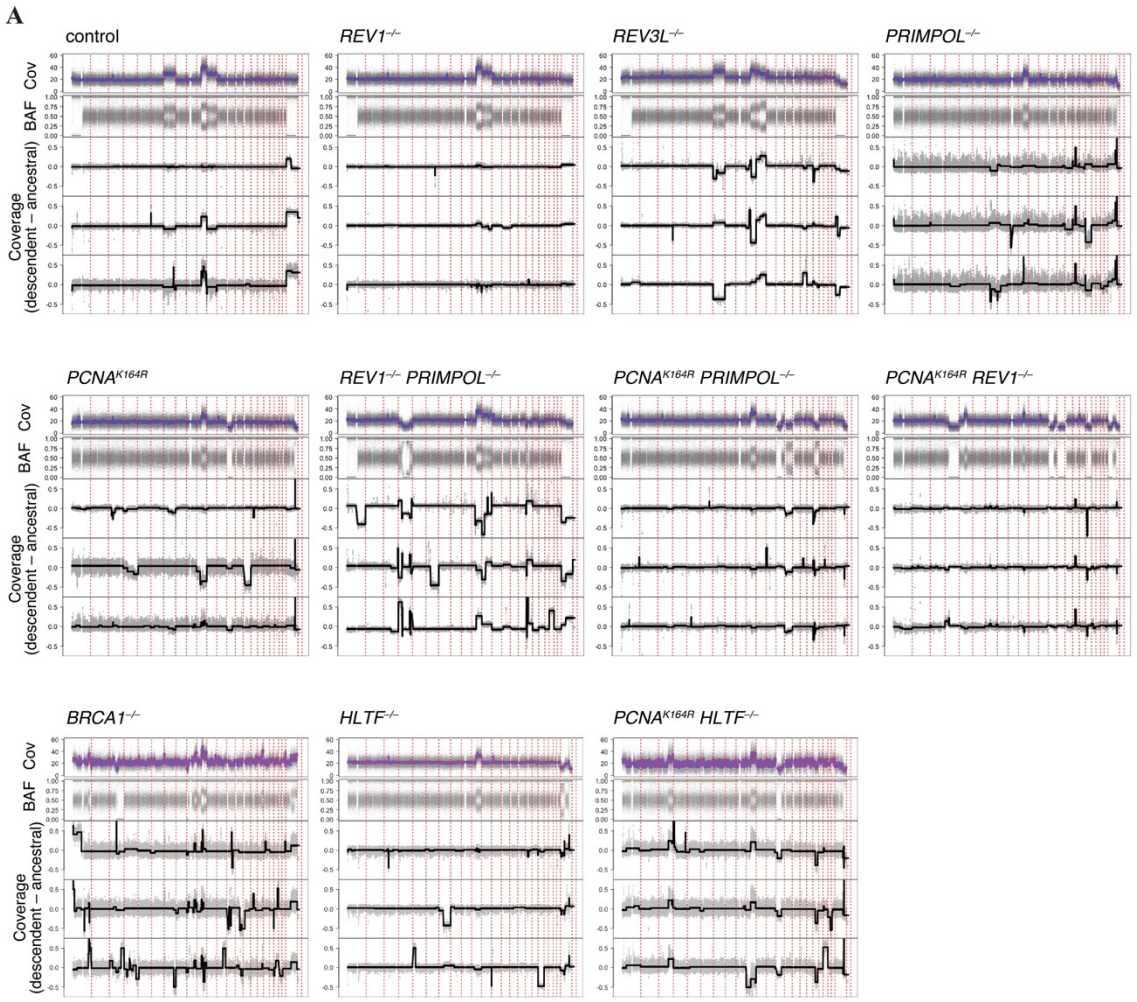

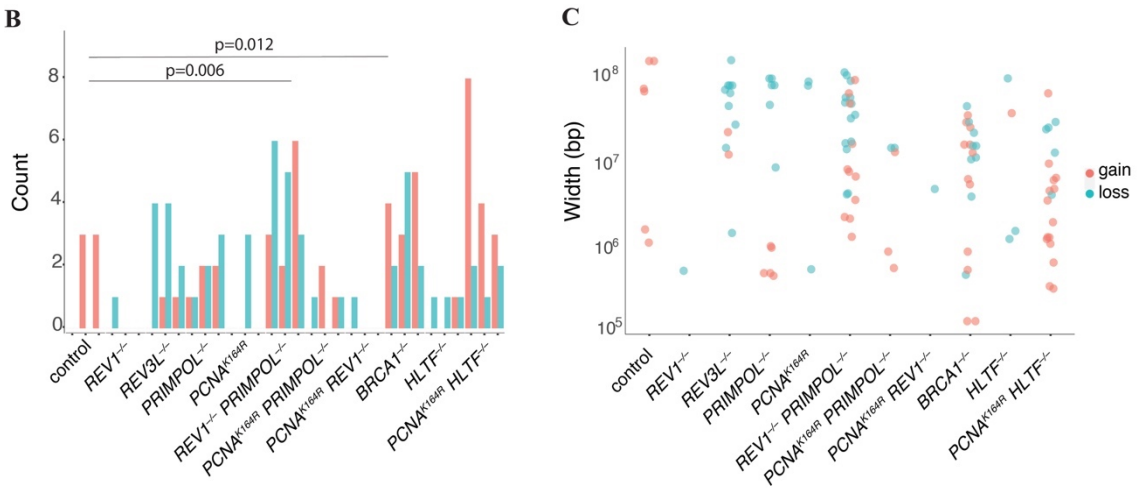

Figure 10 *REV1 and PRIMPOL play redundant role to prevent chromosome instability (A) top two tracks in each panel: Sequence coverage (COV) and B allele frequency (BAF) of selected human SNPs are shown along the human genome (dashed lines indicates chromosome boundaries). Three bottom tracks in each panel: Δcoverage of each descendent clones and corresponding ancestral clone. Visible alterations show changes affect partial or whole chromosomes. (B) Number of copy number alterations per samples grouped by genotypes, classified as gain or loss Total CNA numbers per clone in each genotype were compared to the control cell line using unpaired two-sided t-test. Only significant differences are indicated. (C) Size distribution of CAN events per genotypes: classified as gain and loss; each marker represents one event.*

4.2 Role of DDT pathways in cisplatin-induced mutagenesis

4.2.1 REV1 and PCNA-ubiquitination play redundant role in tolerance of genomic cisplatin adducts

To investigate the role of error-prone TLS in the bypass of cisplatin-induced lesions, I first determined the sensitivities of polymerase mutant cell lines to cisplatin, supplemented with the RPE-1 *TP53*$^{-/-}$ *BRCA1*$^{-/-}$ cell line in which excessive usage of REV1/Polζ has been observed. Cells were treated with decreasing concentration of cisplatin for 5 days followed by determination of the ratio of viable cells compared to corresponding untreated controls. All cell lines proved to be sensitive to cisplatin with relative IC50 concentration between 0.022 and 0.44 compared to the RPE-1 *TP53*$^{-/-}$ control (Fig. 11A). *PRIMPOL*$^{-/-}$ showed the lowest sensitivity, thus the highest relative IC50 concentration (0.44), though this did not significantly differ from *REV1*$^{-/-}$ due to the unexpectedly high standard error of latter (p=0.2, unpaired two-sided *t*-tests). Most

sensitive cell lines were *REV3L*$^{-/-}$ with mean relative IC50 0.022, though differences between *REV3L*$^{-/-}$ and double mutants *PCNA*^{K164R}*PRIMPOL*$^{-/-}$, *PCNA*^{K164R}*REV1* and *REV1*$^{-/-}$*PRIMPOL*$^{-/-}$ were not significant with p-values 0.17, 0.08 and 0.06, respectively (Fig. 11A). Undistinguishable phenotypes of *REV3L*$^{-/-}$ and complete abolishment of main TLS-inducer pathways implies that Polζ is the major extensor polymerase to bypass cisplatin-induced lesions. Furthermore, REV1 has PCNA-(mono)ubiquitination independent role as shown by the almost six-fold decrease of relative IC50 of *PCNA*^{K164R}*REV1* cell line compared to *PCNA*^{K164R} ($p=1.97\times10^{-6}$). *BRCA1*$^{-/-}$ and *PCNA*^{K164R} showed similar, almost nine-folds decreased mean relative IC50 value (0.12 and 0.11, respectively) (Fig. 11A).

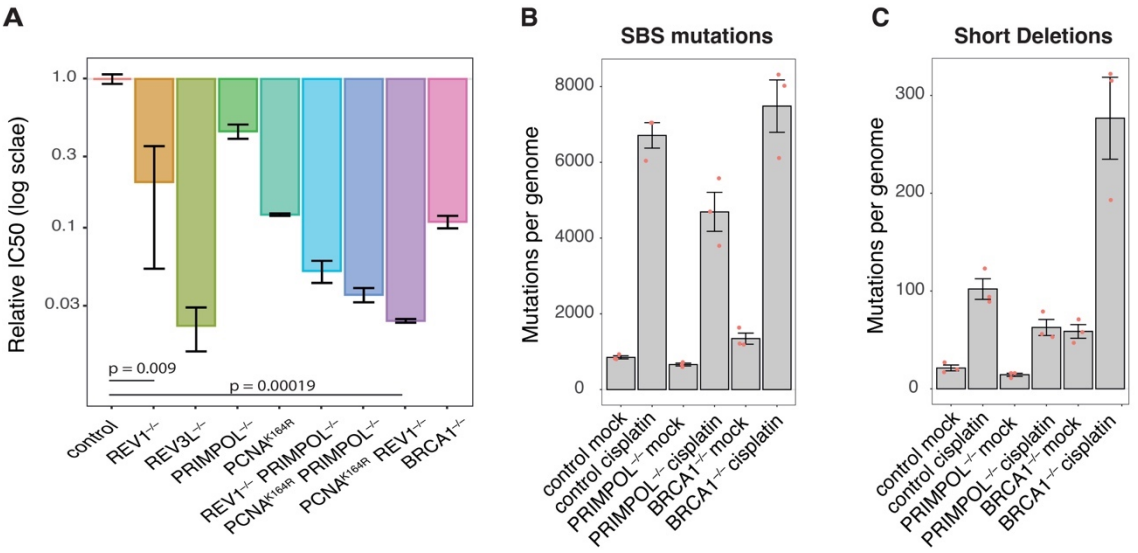

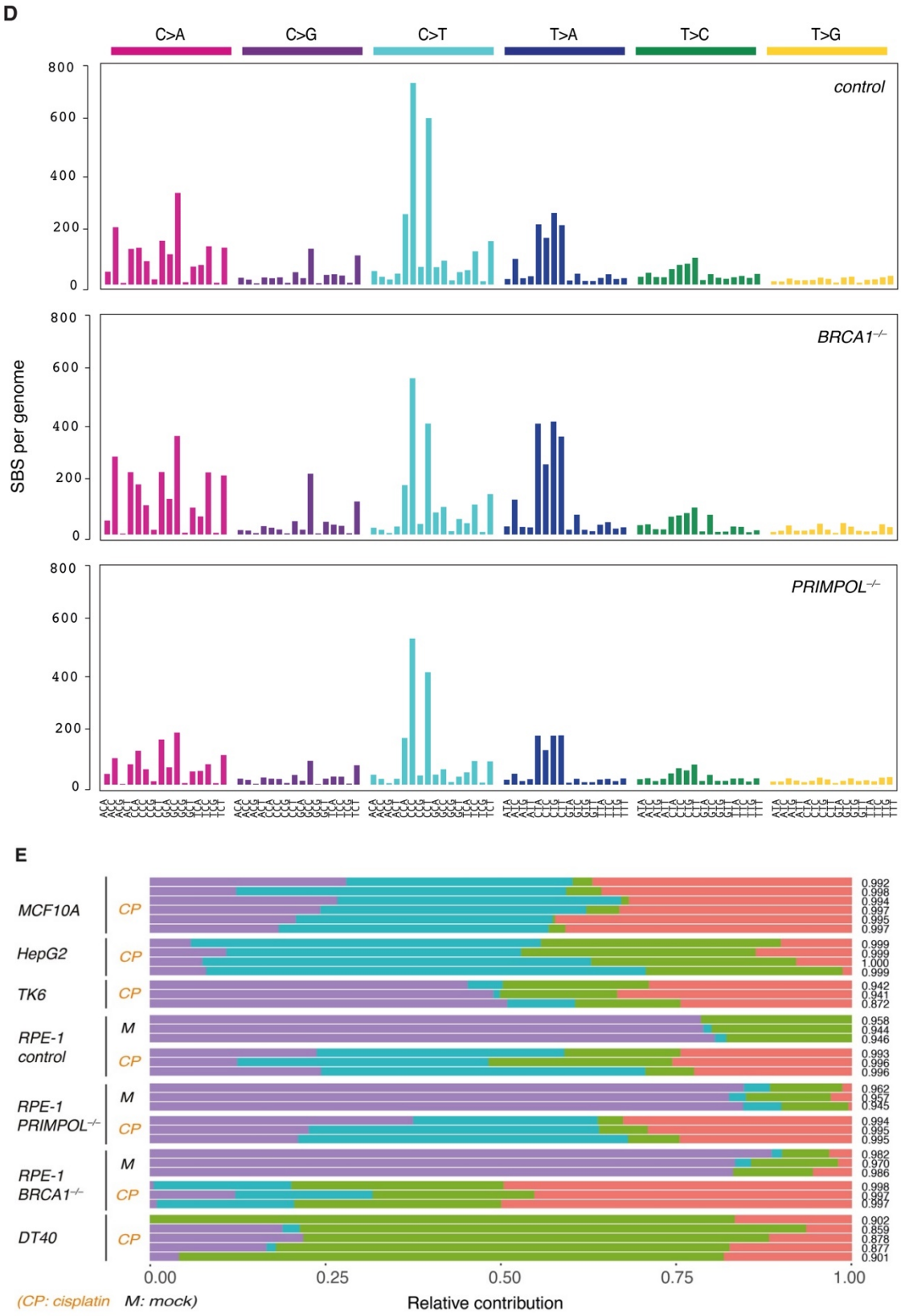
D
C>A
C>G
C>T
T>A
T>C
T>G
control
BRCA1−/−
PRIMPOL−/−
SBS per genome
800
600
400
200
0
E
MCF10A
HepG2
TK6
RPE-1 control
RPE-1 PRIMPOL−/−
RPE-1 BRCA1−/−
DT40
CP
M
0.992
0.998
0.994
0.997
0.995
0.997
0.999
0.999
1.000
0.999
0.942
0.941
0.872
0.958
0.944
0.946
0.993
0.996
0.996
0.962
0.957
0.945
0.994
0.995
0.995
0.982
0.970
0.986
0.998
0.997
0.997
0.902
0.859
0.878
0.877
0.901
0.00
0.25
0.50
0.75
1.00
Relative contribution
(CP: cisplatin M: mock)

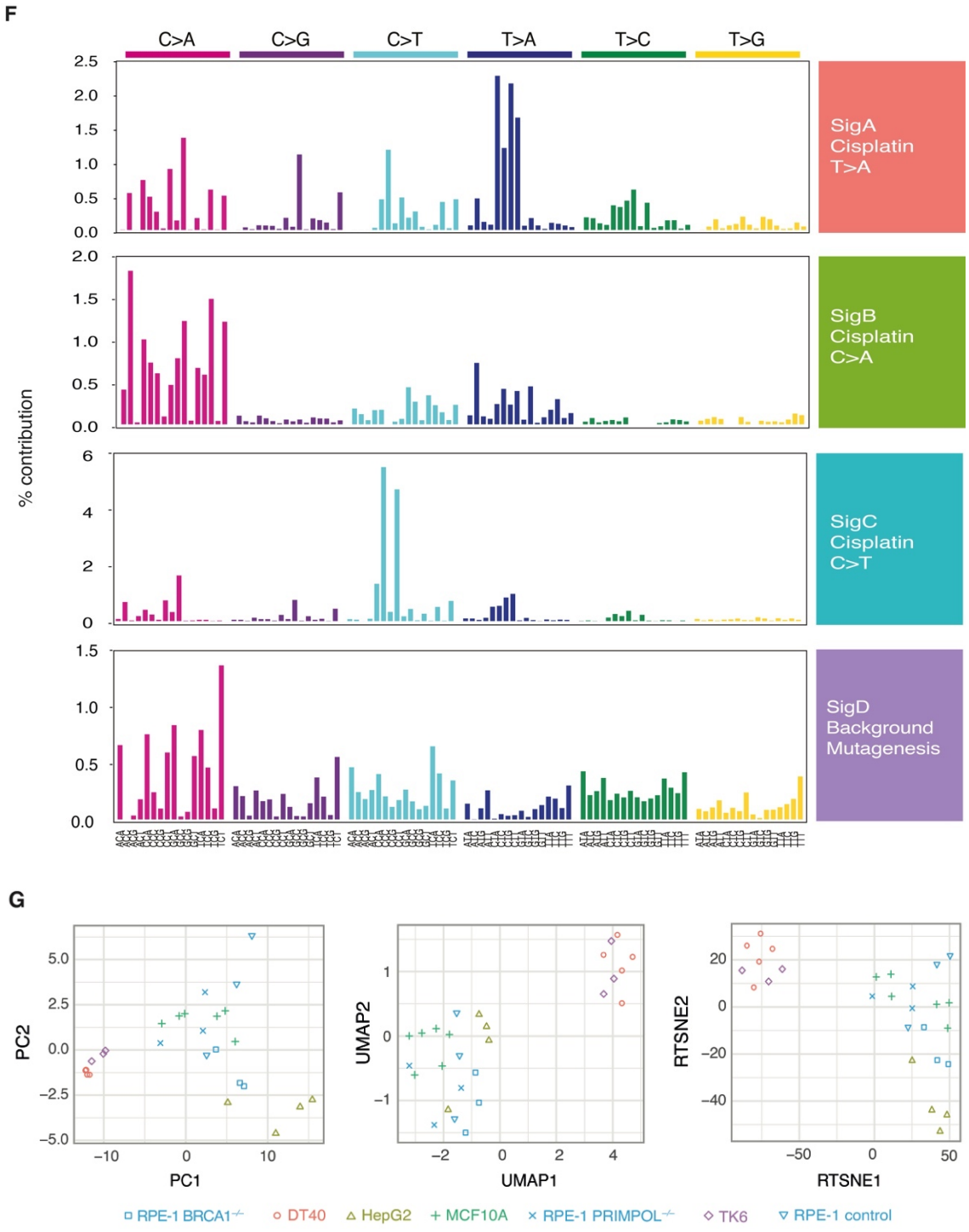

Figure 11 *DDT pathways affect both mutagenicity and cytotoxicity of cisplatin (A) Mean and SEM values of relative IC50 values per genotypes (n=3). IC50 values calculated per each experiment for each cell lines were normalized with mean IC50 value of control cell line RPE-1 TP53$^{-/-}$. Absolute IC50 values were compared to the control cell line using unpaired two-sided t-test, only least and most significant results are indicated. (B-C) Mean and SEM values of SBS and short deletions mutations per cell lines. Markers represent values of individual clones. (D) Averaged triplet spectra of cisplatin treated RPE-1 cell lines, each show averaged values of three*

descendent clones. (E-F) NMF analysis of cisplatin-treated RPE-1 cell lines; (E) shows relative distribution of de novo cisplatin signatures per samples, grouped by cell line or genotype; (F) Triplet spectra of de novo cisplatin signatures. (G) Analysis of SBS spectra of cisplatin treated cell lines using PCA, UMAP and tSNE algorithm. Data was centered and scaled for PCA and scaled without centering for UMAP and tSNE.

4.2.2 Cisplatin treatment increases both SNV and indel mutagenesis

To gain deeper insight into how DDT pathways influence cisplatin induced mutagenesis, I analysed triplet spectra of RPE-1 *TP53*$^{-/-}$, RPE-1 *TP53*$^{-/-}$*PRIMPOL*$^{-/-}$ and RPE-1 *TP53*$^{-/-}$*BRCA1*$^{-/-}$ cells treated with cisplatin. Cells were grown similarly to mock treated samples except for weekly one-hour long treatments with 2 µm cisplatin for four weeks before second single cell cloning step. One of the three RPE-1 *TP53*$^{-/-}$*BRCA1*$^{-/-}$ subcultures (#3) did not recover after the fourth cisplatin treatment. Instead, I sequenced two clones from subculture #2. Technically, unique mutations found in samples are being arose in samples between the last common ancestral and second cloning step and mutations collected between first cloning step and last common ancestral is shared, thus filtered out by IsoMut. Separation of subcultures as soon as cell number allows minimizes the shared mutations. To avoid loss of mutations shared in clones derived from the same subculture, I conducted two parallel IsoMut analysis excluding a semi-independent clones from each run.

SNV numbers drastically increased in all genotypes with average numbers of new SNVs 6710, 4691 and 7484 in RPE-1 *TP53*$^{-/-}$, RPE-1 *TP53*$^{-/-}$*PRIMPOL*$^{-/-}$ and RPE-1 *TP53*$^{-/-}$*BRCA1*$^{-/-}$, respectively, which means six to nine-fold increase of SBS mutagenesis. Similarly, the number of deletions and insertions showed four to eight-fold and five to seven-fold increase compared to mock treated samples, respectively (Fig. 11B-C).

4.2.3 Cisplatin induced mutation signatures are shaped by DDT-pathways

The most frequent mutations arising upon cisplatin-treatment can be grouped into three main categories: C>T mutation in CCY context, T>A mutations in CTN context and C>A mutations in YCN or NCY context. Additionally, C>G peaks at GCC or TCT triplets appeared in *BRCA1*$^{-/-}$ cells. It is important to highlight that all these mutation types arose at canonical cisplatin-target dinucleotides AG and GG (235). *TP53*$^{-/-}$ control and *PRIMPOL*$^{-/-}$ mutants showed similar C>T and T>A dominated spectra, whereas approximately same number of C>A, C>T and T>A mutations arose in *BRCA1*$^{-/-}$ cells

(Fig. 11D). These results are in line with previous observations in human tumours and cell lines (225, 254). To obtain more robust results, I added triplet spectra of previously published cisplatin-treated cell lines HepG2, MCF-10A (254), TK6 (255) and DT40 (256) to the NMF analysis, which produced four components to describe the triplet spectra most appropriately (Fig. 11E-F). Three out of four components were associated with cisplatin treatment, and each dominated by one of the major mutation types mentioned above, whereas fourth component resembled was enriched in mock treated samples and considered to be the background mutagenesis (Fig. 11F). Cisplatin-related signatures show cell line- or genotype-dependent contribution to SBS spectra (Fig. 11E).

I investigated the cosine similarity between SBS spectra of cisplatin-treated *BRCA1*$^{-/-}$ clones to estimate the effect of the aforementioned semi-independent clones. Although the clones from the same subcultures (clones #1 and #3) were proved to be almost identical (rounded cosine similarity was 1), the genuinely independent clone from the separated subculture showed high similarity as well (cosine similarity as high as 0.99), indicating that usage of semi-independent samples did not markedly decrease the reliability of observations.

In order to better understand what factors shape the cisplatin-induced mutagenesis I performed dimension reduction on scaled 96-channel SBS-spectra of samples, using both linear transformation algorithm principal component analysis (PCA) and non-linear transformation algorithms UMAP and tSNE for dimension reduction. All algorithms clearly separated DT40 and TK6 samples from rest of samples. In contrast, no clear clusters could be observed among neither RPE-1 genotypes nor cell lines of non-lymphoblastic origin (Fig. 11G).

4.2.4 Cisplatin induces single T insertions and C deletions in sequence-specific manner

Signature analysis of indels revealed that indels are predominantly 1 bp long insertions and deletions, especially C/G deletions and A/T insertions, in all genotypes. The majority of C/G deletions affects single- or dinucleotide C/G-s, whereas A/T insertions predominately happened at A/T units 1 bp or longer (Fig. 12A). Analysis of 1 bp insertions considering the preceding and following dinucleotides showed that T insertions are mostly GGTT > GGTTT mutations in every genotype, whereas C insertions

did not show similar sequence-dependence and difference between genotypes is more prominent (Fig. 12C). Distributions of sequence context of deletions are more diffuse, though C deletion were more likely to happened if next base was T or C in every genotype, whereas T deletions predominantly arose at T repeats, especially in *PRIMPOL*$^{-/-}$ (Fig. 12C). To sum up, T insertions and C deletions showed stronger sequences context- and weaker genotype-dependencies and could be attributed to cisplatin-induced intrastrand adducts at GG or GA dinucleotides, whereas T deletion predominantly happens at T-repeats. Decomposition of indel signatures revealed that indel spectra of all cell lines are predominately mixture of three COSMIC signatures ID3, ID9 (both characterized by 1 bp deletions) and ID11 (characterized by 1 bp A/T insertions) (Fig. 12B). ID3 is attributed to tobacco smoking (225) which causes 8-oxoG lesions (cisplatin predominately binds guanines as well), whereas ID11 (of unknown aetiology) has been linked to alcohol consumption (278) and HRD (279).

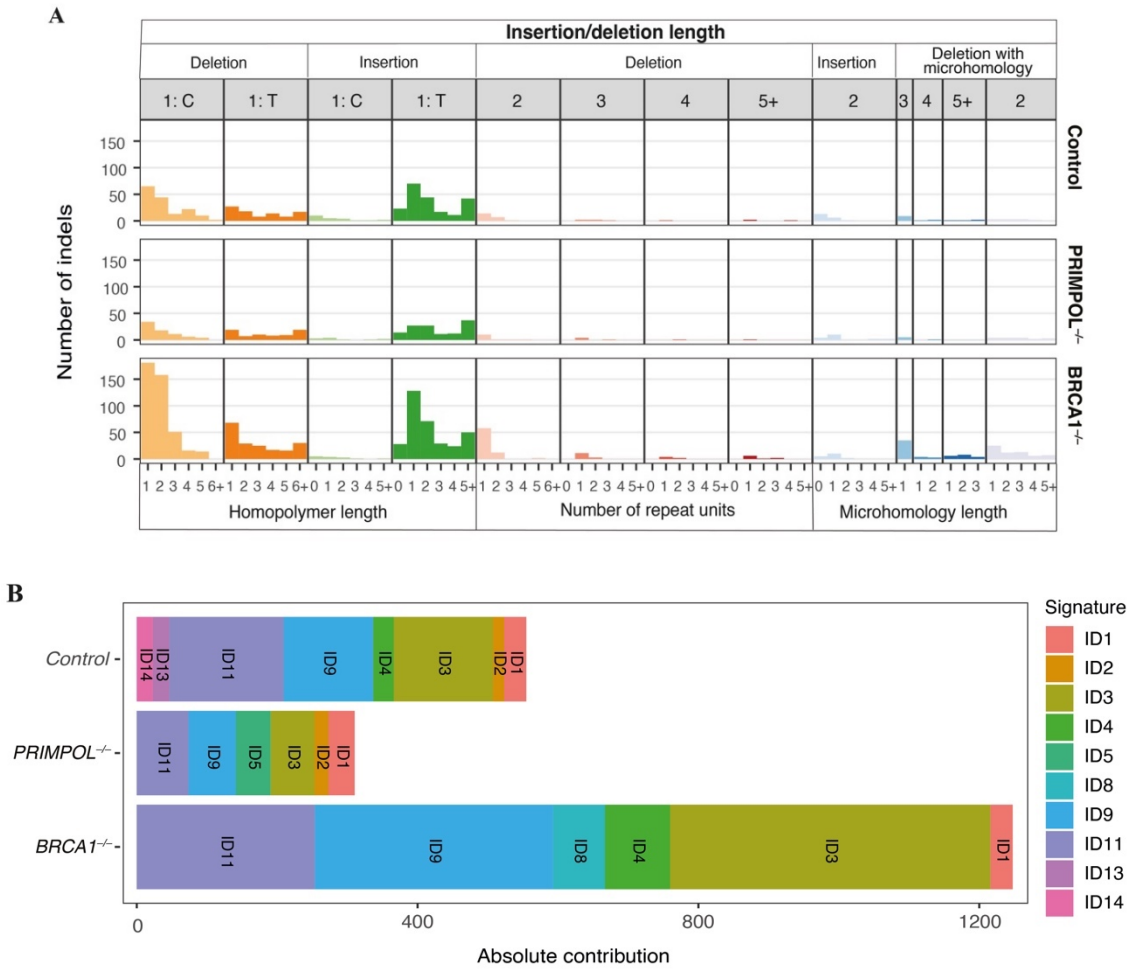

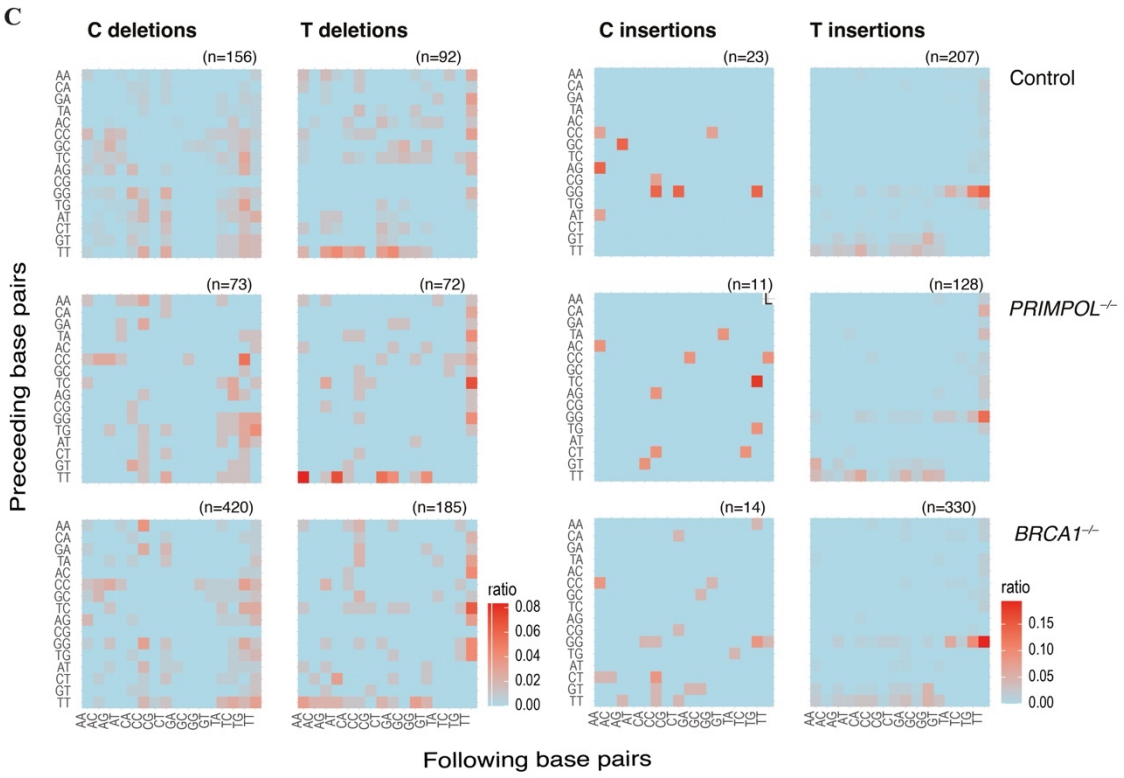

Figure 12 *Cisplatin predominantly induces single T insertions and C deletions in sequence-specific manner (A) Indel spectra of cisplatin-treated RPE-1cell lines, according to COSMIC indel classification, with insertion longer than 1 bp collapsed for clarity. (B)Deconstruction of short indels per genotypes using COSMIC ID signatures. (C) Heat map of the frequency of 1 bp indels, classified according to the preceding and the following dinucleotides as indicated. The deleted or inserted base is shown above panels. Number of events are shown above each individual panel.*

5 Discussion

In my thesis, I investigated the role of DNA damage tolerance pathways in spontaneous and cisplatin-induced mutagenesis in human cells using RPE-1 *TP53*$^{-/-}$ as model system. According to my results, spontaneous SBS mutagenesis is of two components: one which resemble HRD mutagenesis proved to be dependent on REV1 and Polζ TLS polymerases and promoted by PCNA-(mono)ubiquitination, whereas the second, similar to mutagenic effect of ROS, was influenced by both REV1/Polζ and PRIMPOL. Furthermore, PCNA-(mono)ubiquitination was found to promote 1 bp long deletions, which mechanism seemed to be REV1-dependent. In contrast, prevention of TLS polymerase recruitment via concurrent loss of major PCNA-(mono)ubiquitination and REV1 resulted in increased number of deletions at short repeats and arose of an ID signature not presented single mutants. Besides its role to prevents short deletions, REV1/Polζ prevents formation of deletions in a specific, several kilobase size range. Finally, simultaneous loss of REV1 and PRIMPOL caused chromosome-level instability. These results emphasized multifaceted roles of non-replicative DNA polymerases in spontaneous mutagenesis.

SBS signatures identified in RPE-1 (SBS-A and SBS-B) were successfully used to deconstruct SBS spectra of human somatic cell lines of various origin, proving that corresponding molecular mechanisms are common among cultured human cells. Furthermore, SBS signatures in evolutionarily distinct avian cell line DT40 showed analogous behavior, suggesting evolutionary conserved role of TLS in SBS mutagenesis. Similarly, a C>A dominated SBS signature closely resembles SBS-A was found in colon samples of a wide range of mammals (280). In the same study, a flat SBS signature resembles COSMIC signature SBS5 and the imprint of 5-methylcytosine deamination presenting as CG>TG mutations was also identified. Presence of a broad-spectrum component of SBS spectra may be related to the role of SBS-B in RPE-1. Possible explanation of differences between SBS-B and the SBS5-like signature in mammals is that 5-methylcytosine deamination have less prominent role in fast-growing cultured cells (281).

SBS-A resembled 8-oxoG-mediated mutagenesis (261) and have shown to be dependent on PRIMPOL. PRIMPOL can bypass 8-oxoG but its activity has only shown

in vitro (32, 282). Loss of PRIMPOL affected SBS-A mutagenesis only in PCNA-(mono)ubiquitination-proficient background, suggesting complex regulation of replicative lesion bypass and protection of stalled fork, in which PRIMPOL and PCNA-(mono)ubiquitination play concomitant role. Their involvement in an 8-oxoG-related pattern implies that replication is challenged by either oxidation of genomic guanines or incorporation of priori oxidised nucleotides. Furthermore, the decreased of its relative contribution in SBS spectra of *PRIMPOL*$^{-/-}$ cells raises the possibility that SBS-A is related to existence or filling of ssDNA gaps.

As I have clearly shown, SBS-B signature is fully dependent on REV1 and REV3L proving that REV1/Polζ makes a significant contribution to spontaneous mutagenesis in human cultured cells. Contribution of REV1 and Polζ in mutagenesis of HR-deficient cells has been shown in on various organisms (38, 166, 283). Furthermore, our group has previously shown that Pol η and Pol κ also contribute to SBS mutagenesis in *BRCA1*$^{-/-}$ chicken DT40 cells (166), in contrast to PCNA-(mono)ubiquitination which did not affect SBS mutagenesis (256), implicating that TLS polymerases of Y family are recruited by REV1. Taken together the similarity of SBS-B and HRD-mediated COSMIC signatures, the role of REV1 in both processes, the markedly increased contribution of SBS-B in SBS mutagenesis in BRCA1-deficient human cell lines and the presence of SBS-B in HR-proficient human cell lines, I draw the conclusion that "HRD-meditated" signature is the fingerprint of a common mutagenic mechanism which operates in human cells independent of their HR-status. Furthermore, *PCNA*^{K164R} mutation caused modest decrease of SBS-B in every genotype, suggesting that PCNA-(mono)ubiquitination promotes REV1-mediated TLS but not indispensable in its activation.

Loss of both BRCA1 and HLTF result in accumulation of ssDNA gaps due to PRIMPOL-mediated repriming (36, 38), whereas HR-factors make important contribution to postreplicative gap-filling via TSw (276, 284). In the absence of TSw, gaps can be filled by TLS (25). Increased contribution of SBS-B in both HLTF- and BRCA1-deficient cell lines suggests involvement of REV1/Polζ in postreplicative TLS, which appears to be constitutively active in HR-proficient cells as well, but BRCA1-deficient cells seem to be more dependent on this mechanism (38). Controversially, loss of PRIMPOL increases the contribution of SBS-B component as well, implying that *PRIMPOL*$^{-/-}$ cells are more dependent on REV1 upon replication fork stalling. As absence

of PRIMPOL prevents formation of ssDNA gaps (15, 38), it suggests that REV1/Polζ maintains the replication fork progression in absence of repriming. Possible explanation that REV1/Polζ perform "on-the-fly" TLS rescuing replication fork destabilized by loss of either BRCA1 (169), HLTF or PRIMPOL (36).

Phenotypes of *REV1*$^{-/-}$ and *REV3L*$^{-/-}$ showed high similarity in respect to SBS spectra and 500-5000 bp deletions, suggesting that chief role of REV1 is the recruitment of REV3L. It is in agreement with the formation of previously described REV1-REV7-REV3L complex called TLS-mutasome (122). Base substitutions can arise either during bypass of lesions through two-polymerase mechanism whereby one TLS polymerase inserts an incorrect base and Polζ acts as an obligate extensor polymerase utilizing mismatched primer (285) or downstream the lesions via mutagenesis process called collateral mutagenesis (256) due to low fidelity of Polζ (286). The mechanism behind the deletions of 500-5000 bp size is not yet clear, but may be attributed to one of the emerging TLS-independent roles of REV1 or Polζ such as replication through unusual DNA-structures (287), protection of stalled replication fork (288), replication of pericentromeric heterochromatin(289) or mitotic DNA synthesis (290). Furthermore, there is also a possible analogy with Polθ-dependent 50-500 bp deletions observed in the genomes of *rev-1* mutant C. elegans(291).

Both REV1 and PRIMPOL promote replication fork progression by bypassing lesions or repriming replication behind lesions, respectively. Simultaneous loss of both proteins may cause accumulation of unreplicated DNA, leading to mitotic segregation problems and chromosome instability. Alternatively, absence of both on-the-fly TLS and replication repriming may overactivates the third replicative DDT-pathway, the fork reversal. Prolonged regression eventually causes collapse of replication fork, leading to genome instability (13, 14). Furthermore, the fact that loss of PRIMPOL in combination with loss of REV1 but not with PCNA^{K164R}-modification causes excessive genome instability suggests that PCNA-(mono)ubiquitination plays a less important role during the replicative bypass of lesions than REV1.

Rise of ID4 indel signature in *PCNA*^{K164R}*REV1*$^{-/-}$ and its absence in both single mutant cell lines showed the joint role of REV1 and PCNA-(mono)ubiquitination in prevention of short deletions at short repeats. ID4 has been attributed to genomic

ribonucleotide-removing activity of topoisomerase 1 (TOP1) (292) and appeared in RNase-H2 knockout cell lines established in the same hTERT RPE-1 *TP53*$^{-/-}$ (292), suggesting that either REV1 or PCNA ubiquitylation could therefore have a hitherto undetected role in the repair of genomic ribonucleotides. However, ID4-like pattern in RNase-H2-KO RPE-1 cells show different frequency of 3 bp repeat deletions. This modest difference raises the possibility that not only one can produce ID4-like signature. Recently described "microhomology-mediated gap filling" activity of Polθ (293) and high frequency of indel mutagenesis and template slippage activity of PRIMPOL *in vitro* (34, 282) provide possible alternative mechanisms in the absence of TLS in *PCNA*^{K164R}*REV1*$^{-/-}$ cells.

Furthermore, I investigated cisplatin-induced mutagenesis in RPE-1 *TP53*$^{-/-}$, RPE-1 *TP53*$^{-/-}$*BRCA1*$^{-/-}$ and RPE-1 *TP53*$^{-/-}$*BRCA1*$^{-/-}$ cell lines. Cisplatin-treatment increased the numbers of point mutations and short indels compared to mock treated samples. Analysis of the sequence context of mutations revealed that DNA lesions of cisplatin origin are directly responsible for surplus mutations, though patterns varied across genotypes. As cisplatin-triggered SBS mutagenesis is attributed to TLS (294, 295), varying contribution of cisplatin-derived signatures may imply differential utilization of TLS polymerases. Importance of cisplatin-induced lesions bypass Polκ have been reported in human and chicken cell lines (45, 166). It is important to highlight that cisplatin induces almost exclusively C>A mutations in DT40 *BRCA1*$^{-/-}$ cell line what process is entirely Polκ-dependent. In contrast, triplet spectra of cisplatin-treated RPE-1 *TP53*$^{-/-}$*BRCA1*$^{-/-}$ showed more diverse landscape with C>T, T>A and C>G peaks, suggesting activation of more than one mutagenic process, which require further investigation. Identification of proteins involved in these molecular mechanisms would provide potential targets in combination therapies with cisplatin in treatment of BRCA1-deficient tumours. Finally, analysis of triplet spectra of cisplatin-treated human and DT40 cell lines revealed that the tissue of origin plays a more important role in cisplatin-induced mutagenesis than the BRCA1- or PRIMPOL-status of the cells.

6 Conclusions

- REV1 plays a central and a multifaceted role in spontaneous mutagenesis and protection of genome integrity, as being wholly responsible for HRD-like component of spontaneous SBS mutagenesis, prevents formation of kilobase-long deletions. REV1 probably exert these roles by recruiting Polζ an universal extender TLS-polymerase.
- Defective TLS in RPE-1 *PCNA^{K164R}REV1$^{-/-}$* cell line give rise to an unexpected mutagenic a process what was missing from single mutant cell lines and characterized by 1 bp deletions at longer A/T homopolymers, 2 bp deletions at 2- or 3-unit repeats and 3 bp deletions at 2-unit repeats. To conclude, REV1 prevents short deletions at repeat sequences in cooperation with PCNA-(mono)ubiquitination via a yet unknown molecular mechanism.
- REV1 guards large-scale genome integrity as well. Simultaneous loss of PRIMPOL and REV1 resulted in increased number of 1-100 Mb scale deletions in duplications of genome. As both PRIMPOL and REV1 promote replication fork progression, loss of both proteins may cause mitotic segregation problem due to the accumulation of unreplicated DNA or prolonged fork stalling.
- On the basis of SBS spectra and frequencies of CNA events in *PCNA^{K164R}PRIMPOL$^{-/-}$* and *REV1$^{-/-}$ PRIMPOL$^{-/-}$* cell lines, REV1 plays a more important role in the promotion of TLS than PCNA-(mono)ubiquitination in human cells.
- Cisplatin treatment induces single base substitution and 1 bp long indel mutations in sequence context specific manner. DDT pathways can affect both indel and SBS-signatures, maybe reflecting varying compositions of TLS-polymerases used for lesion-bypass.

7 Summary

Genomes of living organisms are continuously challenged by mutagenic agents, both extrinsic and intrinsic. Damaged genomic positions, called genomic lesions, interfere with replication as high-fidelity replicative polymerases cannot process template encodes ambiguous information. Various molecular pathways have evolved to maintain integrity of genetic information. Mechanisms which help replication machinery to cope with lesions and complete duplication of genome are jointly called DNA damage tolerance pathways or DDT for short. Fork reversal stabilizes stalled replication fork and restarts it when DNA repair fixed the damaged site. Replication repriming grants fork progression by starting replication machinery behind the lesion. Arising ssDNA gaps are eventually filled by either homologous recombination-based template switch or translesion synthesis. Translesion polymerases are special DNA polymerases of lower fidelity enabling them to bypass lesions postreplicatively or during replication.

I identified two components of spontaneous SBS mutagenesis in a human cell line RPE-1: an HRD-like component what is wholly depended on REV1 and Polζ, whereas the second component showed similarity with oxidative mutagenesis and was affected by PRIMPOL and PCNA-(mono)ubiquitination. Remarkably, *de novo* signatures were identified in DDT-mutant untransformed cells which were neither HR-deficient nor were exposed to deliberate oxidative damage. Investigation of RPE-1 *TP53*$^{-/-}$*BRCA1*$^{-/-}$ cell line showed that HRD-like signature was responsible for elevated mutation number in this cell line. I successfully reconstructed SBS spectra of 12 human cell lines with *de novo* signatures, proving that underlying molecular mechanisms are common in cultured human cells. Furthermore, the connection between REV1 and HRD was proved to be evolutionary conserved, as shown by the analysis DDT-mutant DT40 chicken cell lines. TLS and repriming prevent formation of deletions and insertions of as short 1 bp to as large as several Mb. REV1 plays central role in protection from deletions: simultaneous loss of PCNA-(mono)ubiquitination and REV1 give rise to short deletions, whereas REV1 and PRIMPOL redundantly prevents genomic instability. Finally, aberrant recruitment of REV3L due to loss of REV1 causes accumulation of kilobase long deletions. Furthermore, DDT pathways affect mutation signatures of cisplatin treatment, providing new diagnostic markers and therapeutic targets.

8 References

1. Hanahan D. Hallmarks of Cancer: New Dimensions. Cancer Discovery. 2022;12(1):31-46.

2. Hoeijmakers JHJ. DNA Damage, Aging, and Cancer. New England Journal of Medicine. 2009;361(15):1475-85.

3. Ward JF. DNA damage produced by ionizing radiation in mammalian cells: identities, mechanisms of formation, and reparability. Prog Nucleic Acid Res Mol Biol. 1988;35:95-125.

4. Collins AR. Oxidative DNA damage, antioxidants, and cancer. BioEssays. 1999;21(3):238-46.

5. Beroukhim R, Mermel CH, Porter D, Wei G, Raychaudhuri S, Donovan J, Barretina J, Boehm JS, Dobson J, Urashima M, Mc Henry KT, Pinchback RM, Ligon AH, Cho Y-J, Haery L, Greulich H, Reich M, Winckler W, Lawrence MS, Weir BA, Tanaka KE, Chiang DY, Bass AJ, Loo A, Hoffman C, Prensner J, Liefeld T, Gao Q, Yecies D, Signoretti S, Maher E, Kaye FJ, Sasaki H, Tepper JE, Fletcher JA, Tabernero J, Baselga J, Tsao M-S, Demichelis F, Rubin MA, Janne PA, Daly MJ, Nucera C, Levine RL, Ebert BL, Gabriel S, Rustgi AK, Antonescu CR, Ladanyi M, Letai A, Garraway LA, Loda M, Beer DG, True LD, Okamoto A, Pomeroy SL, Singer S, Golub TR, Lander ES, Getz G, Sellers WR, Meyerson M. The landscape of somatic copy-number alteration across human cancers. Nature. 2010;463(7283):899-905.

6. Masutani C, Kusumoto R, Yamada A, Dohmae N, Yokoi M, Yuasa M, Araki M, Iwai S, Takio K, Hanaoka F. The XPV (xeroderma pigmentosum variant) gene encodes human DNA polymerase η. Nature. 1999;399(6737):700-4.

7. McCulloch SD, Kunkel TA. The fidelity of DNA synthesis by eukaryotic replicative and translesion synthesis polymerases. Cell Research. 2008;18(1):148-61.

8. Pilzecker B, Buoninfante OA, Jacobs H. DNA damage tolerance in stem cells, ageing, mutagenesis, disease and cancer therapy. Nucleic Acids Res. 2019;47(14):7163-81.

9. Berti M, Vindigni A. Replication stress: getting back on track. Nature Structural & Molecular Biology. 2016;23(2):103-9.

10. Gaillard H, García-Muse T, Aguilera A. Replication stress and cancer. Nature Reviews Cancer. 2015;15(5):276-89.

11. Hills SA, Diffley JF. DNA replication and oncogene-induced replicative stress. Curr Biol. 2014;24(10):R435-44.

12. Casas-Delucchi CS, Daza-Martin M, Williams SL, Coster G. The mechanism of replication stalling and recovery within repetitive DNA. Nature Communications. 2022;13(1):3953.

13. Zeman MK, Cimprich KA. Causes and consequences of replication stress. Nature Cell Biology. 2014;16(1):2-9.

14. Kondratick CM, Washington MT, Spies M. Making Choices: DNA Replication Fork Recovery Mechanisms. Semin Cell Dev Biol. 2021;113:27-37.

15. Mourón S, Rodriguez-Acebes S, Martínez-Jiménez MI, García-Gómez S, Chocrón S, Blanco L, Méndez J. Repriming of DNA synthesis at stalled replication forks by human PrimPol. Nature Structural & Molecular Biology. 2013;20(12):1383-9.

16. Branzei D, Szakal B. DNA damage tolerance by recombination: Molecular pathways and DNA structures. DNA Repair (Amst). 2016;44:68-75.

17. Sale JE. Translesion DNA synthesis and mutagenesis in eukaryotes. Cold Spring Harb Perspect Biol. 2013;5(3):a012708.

18. Frick DN, Richardson CC. DNA Primases. Annual Review of Biochemistry. 2001;70(1):39-80.

19. Kuchta RD, Stengel G. Mechanism and evolution of DNA primases. Biochimica et Biophysica Acta (BBA) - Proteins and Proteomics. 2010;1804(5):1180-9.

20. Ogawa T, Okazaki T. Discontinuous DNA replication. Annual review of biochemistry. 1980;49(1):421-57.

21. Rupp WD, Howard-Flanders P. Discontinuities in the DNA synthesized in an excision-defective strain of Escherichia coli following ultraviolet irradiation. J Mol Biol. 1968;31(2):291-304.

22. Lopes M, Foiani M, Sogo JM. Multiple Mechanisms Control Chromosome Integrity after Replication Fork Uncoupling and Restart at Irreparable UV Lesions. Molecular Cell. 2006;21(1):15-27.

23. Lehmann AR, Kirk-Bell S. Post-Replication Repair of DNA in Ultraviolet-Irradiated Mammalian Cells. European Journal of Biochemistry. 1972;31(3):438-45.

24. Elvers I, Johansson F, Groth P, Erixon K, Helleday T. UV stalled replication forks restart by re-priming in human fibroblasts. Nucleic Acids Research. 2011;39(16):7049-57.

25. Tirman S, Quinet A, Wood M, Meroni A, Cybulla E, Jackson J, Pegoraro S, Simoneau A, Zou L, Vindigni A. Temporally distinct post-replicative repair mechanisms fill PRIMPOL-dependent ssDNA gaps in human cells. Molecular Cell. 2021;81(19):4026-40.e8.

26. Piberger AL, Bowry A, Kelly RDW, Walker AK, González-Acosta D, Bailey LJ, Doherty AJ, Méndez J, Morris JR, Bryant HE, Petermann E. PrimPol-dependent single-stranded gap formation mediates homologous recombination at bulky DNA adducts. Nature Communications. 2020;11(1):5863.

27. Iyer LM, Koonin EV, Leipe DD, Aravind L. Origin and evolution of the archaeo-eukaryotic primase superfamily and related palm-domain proteins: structural insights and new members. Nucleic acids research. 2005;33(12):3875-96.

28. Bianchi J, Rudd Sean G, Jozwiakowski Stanislaw K, Bailey Laura J, Soura V, Taylor E, Stevanovic I, Green Andrew J, Stracker Travis H, Lindsay Howard D, Doherty Aidan J. PrimPol Bypasses UV Photoproducts during Eukaryotic Chromosomal DNA Replication. Molecular Cell. 2013;52(4):566-73.

29. Keen BA, Jozwiakowski SK, Bailey LJ, Bianchi J, Doherty AJ. Molecular dissection of the domain architecture and catalytic activities of human PrimPol. Nucleic acids research. 2014;42(9):5830-45.

30. Rechkoblit O, Gupta YK, Malik R, Rajashankar KR, Johnson RE, Prakash L, Prakash S, Aggarwal AK. Structure and mechanism of human PrimPol, a DNA polymerase with primase activity. Sci Adv. 2016;2(10):e1601317.

31. Martínez-Jiménez MI, García-Gómez S, Bebenek K, Sastre-Moreno G, Calvo PA, Díaz-Talavera A, Kunkel TA, Blanco L. Alternative solutions and new scenarios for translesion DNA synthesis by human PrimPol. DNA Repair. 2015;29:127-38.

32. García-Gómez S, Reyes A, Martínez-Jiménez María I, Chocrón ES, Mourón S, Terrados G, Powell C, Salido E, Méndez J, Holt Ian J, Blanco L. PrimPol, an Archaic Primase/Polymerase Operating in Human Cells. Molecular Cell. 2013;52(4):541-53.

33. Helbock HJ, Beckman KB, Shigenaga MK, Walter PB, Woodall AA, Yeo HC, Ames BN. DNA oxidation matters: The HPLC–electrochemical detection assay of 8-oxo-deoxyguanosine and 8-oxo-guanine. Proceedings of the National Academy of Sciences. 1998;95(1):288-93.

34. Guilliam TA, Jozwiakowski SK, Ehlinger A, Barnes RP, Rudd SG, Bailey LJ, Skehel JM, Eckert KA, Chazin WJ, Doherty AJ. Human PrimPol is a highly error-prone polymerase regulated by single-stranded DNA binding proteins. Nucleic Acids Research. 2014;43(2):1056-68.

35. Tirman S, Cybulla E, Quinet A, Meroni A, Vindigni A. PRIMPOL ready, set, reprime! Crit Rev Biochem Mol Biol. 2021;56(1):17-30.

36. Bai G, Kermi C, Stoy H, Schiltz CJ, Bacal J, Zaino AM, Hadden MK, Eichman BF, Lopes M, Cimprich KA. HLTF Promotes Fork Reversal, Limiting Replication Stress Resistance and Preventing Multiple Mechanisms of Unrestrained DNA Synthesis. Molecular Cell. 2020;78(6):1237-51.e7.

37. Quinet A, Tirman S, Jackson J, Šviković S, Lemaçon D, Carvajal-Maldonado D, González-Acosta D, Vessoni AT, Cybulla E, Wood M, Tavis S, Batista LFZ, Méndez J, Sale JE, Vindigni A. PRIMPOL-Mediated Adaptive Response Suppresses Replication Fork Reversal in BRCA-Deficient Cells. Molecular Cell. 2020;77(3):461-74.e9.

38. Taglialatela A, Leuzzi G, Sannino V, Cuella-Martin R, Huang JW, Wu-Baer F, Baer R, Costanzo V, Ciccia A. REV1-Polζ maintains the viability of homologous recombination-deficient cancer cells through mutagenic repair of PRIMPOL-dependent ssDNA gaps. Mol Cell. 2021;81(19):4008-25.e7.

39. Wong RP, García-Rodríguez N, Zilio N, Hanulová M, Ulrich HD. Processing of DNA Polymerase-Blocking Lesions during Genome Replication Is Spatially and Temporally Segregated from Replication Forks. Molecular Cell. 2020;77(1):3-16.e4.

40. Waters LS, Minesinger BK, Wiltrout ME, D'Souza S, Woodruff RV, Walker GC. Eukaryotic translesion polymerases and their roles and regulation in DNA damage tolerance. Microbiol Mol Biol Rev. 2009;73(1):134-54.

41. Loeb LA, Monnat RJ. DNA polymerases and human disease. Nature Reviews Genetics. 2008;9(8):594-604.

42. Chang HH, Pannunzio NR, Adachi N, Lieber MR. Non-homologous DNA end joining and alternative pathways to double-strand break repair. Nature reviews Molecular cell biology. 2017;18(8):495-506.

43. Zietlow L, Smith LA, Bessho M, Bessho T. Evidence for the involvement of human DNA polymerase N in the repair of DNA interstrand cross-links. Biochemistry. 2009;48(49):11817-24.

44. Moldovan G-L, Madhavan MV, Mirchandani KD, McCaffrey RM, Vinciguerra P, D'Andrea AD. DNA polymerase POLN participates in cross-link repair and homologous recombination. Molecular and cellular biology. 2010;30(4):1088-96.

45. Shachar S, Ziv O, Avkin S, Adar S, Wittschieben J, Reissner T, Chaney S, Friedberg EC, Wang Z, Carell T, Geacintov N, Livneh Z. Two-polymerase mechanisms dictate error-free and error-prone translesion DNA synthesis in mammals. Embo j. 2009;28(4):383-93.

46. Bassett E, King NM, Bryant MF, Hector S, Pendyala L, Chaney SG, Cordeiro-Stone M. The role of DNA polymerase eta in translesion synthesis past platinum-DNA adducts in human fibroblasts. Cancer Res. 2004;64(18):6469-75.

47. Kirouac KN, Ling H. Unique active site promotes error-free replication opposite an 8-oxo-guanine lesion by human DNA polymerase iota. Proceedings of the National Academy of Sciences. 2011;108(8):3210-5.

48. Haracska L, Prakash S, Prakash L. Yeast Rev1 Protein Is a G Template-specific DNA Polymerase *. Journal of Biological Chemistry. 2002;277(18):15546-51.

49. Zhang Y, Wu X, Rechkoblit O, Geacintov NE, Taylor J-S, Wang Z. Response of human REV1 to different DNA damage: preferential dCMP insertion opposite the lesion. Nucleic Acids Research. 2002;30(7):1630-8.

50. Choi JY, Guengerich FP. Kinetic analysis of translesion synthesis opposite bulky N2- and O6-alkylguanine DNA adducts by human DNA polymerase REV1. J Biol Chem. 2008;283(35):23645-55.

51. Nair DT, Johnson RE, Prakash L, Prakash S, Aggarwal AK. Rev1 Employs a Novel Mechanism of DNA Synthesis Using a Protein Template. Science. 2005;309(5744):2219-22.

52. Haracska L, Yu SL, Johnson RE, Prakash L, Prakash S. Efficient and accurate replication in the presence of 7,8-dihydro-8-oxoguanine by DNA polymerase eta. Nat Genet. 2000;25(4):458-61.

53. Prakash S, Prakash L. Translesion DNA synthesis in eukaryotes: a one-or two-polymerase affair. Genes & development. 2002;16(15):1872-83.

54. Johnson RE, Washington MT, Haracska L, Prakash S, Prakash L. Eukaryotic polymerases ι and ζ act sequentially to bypass DNA lesions. Nature. 2000;406(6799):1015-9.

55. Haracska L, Unk I, Johnson RE, Johansson E, Burgers PM, Prakash S, Prakash L. Roles of yeast DNA polymerases δ and ζ and of Rev1 in the bypass of abasic sites. Genes & development. 2001;15(8):945-54.

56. Lee Y-S, Gregory MT, Yang W. Human Pol ζ purified with accessory subunits is active in translesion DNA synthesis and complements Pol η in cisplatin bypass. Proceedings of the National Academy of Sciences. 2014;111(8):2954-9.

57. Jansen JG, Tsaalbi-Shtylik A, Hendriks G, Verspuy J, Gali H, Haracska L, de Wind N. Mammalian polymerase ζ is essential for post-replication repair of UV-induced DNA lesions. DNA Repair. 2009;8(12):1444-51.

58. Bemark M, Khamlichi AA, Davies SL, Neuberger MS. Disruption of mouse polymerase zeta (Rev3) leads to embryonic lethality and impairs blastocyst development in vitro. Curr Biol. 2000;10(19):1213-6.

59. Esposito G, Godindagger I, Klein U, Yaspo ML, Cumano A, Rajewsky K. Disruption of the Rev3l-encoded catalytic subunit of polymerase zeta in mice results in early embryonic lethality. Curr Biol. 2000;10(19):1221-4.

60. Wittschieben J, Shivji MKK, Lalani E, Jacobs MA, Marini F, Gearhart PJ, Rosewell I, Stamp G, Wood RD. Disruption of the developmentally regulated Rev3l gene causes embryonic lethality. Current Biology. 2000;10(19):1217-20.

61. Zhang Y, Wu X, Guo D, Rechkoblit O, Geacintov NE, Wang Z. Two-step error-prone bypass of the (+)- and (−)-trans-anti-BPDE-N2-dG adducts by human DNA polymerases η and κ. Mutation Research/Fundamental and Molecular Mechanisms of Mutagenesis. 2002;510(1):23-35.

62. Jha V, Ling H. Structural Basis for Human DNA Polymerase Kappa to Bypass Cisplatin Intrastrand Cross-Link (Pt-GG) Lesion as an Efficient and Accurate Extender. Journal of Molecular Biology. 2018;430(11):1577-89.

63. Masutani C, Kusumoto R, Iwai S, Hanaoka F. Mechanisms of accurate translesion synthesis by human DNA polymerase η. The EMBO journal. 2000;19(12):3100-9.

64. Rupp WD, Wilde CE, Reno DL, Howard-Flanders P. Exchanges between DNA strands in ultraviolet-irradiated Escherichia coli. Journal of Molecular Biology. 1971;61(1):25-44.

65. Higgins NP, Kato K, Strauss B. A model for replication repair in mammalian cells. Journal of Molecular Biology. 1976;101(3):417-25.

66. Neecke H, Lucchini G, Longhese MP. Cell cycle progression in the presence of irreparable DNA damage is controlled by a Mec1-and Rad53-dependent checkpoint in budding yeast. The EMBO Journal. 1999;18(16):4485-97.

67. Karras GI, Fumasoni M, Sienski G, Vanoli F, Branzei D, Jentsch S. Noncanonical role of the 9-1-1 clamp in the error-free DNA damage tolerance pathway. Molecular cell. 2013;49(3):536-46.

68. Karras GI, Jentsch S. The RAD6 DNA damage tolerance pathway operates uncoupled from the replication fork and is functional beyond S phase. Cell. 2010;141(2):255-67.

69. Zhang H, Lawrence CW. The error-free component of the RAD6/RAD18 DNA damage tolerance pathway of budding yeast employs sister-strand recombination. Proc Natl Acad Sci U S A. 2005;102(44):15954-9.

70. Branzei D, Vanoli F, Foiani M. SUMOylation regulates Rad18-mediated template switch. Nature. 2008;456(7224):915-20.

71. Saberi A, Nakahara M, Sale JE, Kikuchi K, Arakawa H, Buerstedde JM, Yamamoto K, Takeda S, Sonoda E. The 9-1-1 DNA clamp is required for immunoglobulin gene conversion. Mol Cell Biol. 2008;28(19):6113-22.

72. Sale JE. Immunoglobulin diversification in DT40: a model for vertebrate DNA damage tolerance. DNA Repair (Amst). 2004;3(7):693-702.

73. García-Rodríguez N, Wong RP, Ulrich HD. The helicase Pif1 functions in the template switching pathway of DNA damage bypass. Nucleic Acids Research. 2018;46(16):8347-56.

74. Abe T, Ooka M, Kawasumi R, Miyata K, Takata M, Hirota K, Branzei D. Warsaw breakage syndrome DDX11 helicase acts jointly with RAD17 in the repair of bulky lesions and replication through abasic sites. Proceedings of the National Academy of Sciences. 2018;115(33):8412-7.

75. Sale JE, Calandrini DM, Takata M, Takeda S, Neuberger MS. Ablation of XRCC2/3 transforms immunoglobulin V gene conversion into somatic hypermutation. Nature. 2001;412(6850):921-6.

76. Hatanaka A, Yamazoe M, Sale JE, Takata M, Yamamoto K, Kitao H, Sonoda E, Kikuchi K, Yonetani Y, Takeda S. Similar effects of Brca2 truncation and Rad51 paralog deficiency on immunoglobulin V gene diversification in DT40 cells support an early role for Rad51 paralogs in homologous recombination. Mol Cell Biol. 2005;25(3):1124-34.

77. Longerich S, Orelli BJ, Martin RW, Bishop DK, Storb U. Brca1 in immunoglobulin gene conversion and somatic hypermutation. DNA repair. 2008;7(2):253-66.

78. Cota CD, García-García MJ. The ENU-induced cetus mutation reveals an essential role of the DNA helicase DDX11 for mesoderm development during early mouse embryogenesis. Developmental Dynamics. 2012;241(8):1249-59.

79. Suzuki A, de la Pompa JL, Hakem R, Elia A, Yoshida R, Mo R, Nishina H, Chuang T, Wakeham A, Itie A. Brca2 is required for embryonic cellular proliferation in the mouse. Genes & Development. 1997;11(10):1242-52.

80. Rantakari P, Nikkilä J, Jokela H, Ola R, Pylkäs K, Lagerbohm H, Sainio K, Poutanen M, Winqvist R. Inactivation of Palb2 gene leads to mesoderm differentiation defect and early embryonic lethality in mice. Human molecular genetics. 2010;19(15):3021-9.

81. Quinet A, Lemaçon D, Vindigni A. Replication Fork Reversal: Players and Guardians. Mol Cell. 2017;68(5):830-3.

82. Neelsen KJ, Lopes M. Replication fork reversal in eukaryotes: from dead end to dynamic response. Nature Reviews Molecular Cell Biology. 2015;16(4):207-20.

83. Bétous R, Mason AC, Rambo RP, Bansbach CE, Badu-Nkansah A, Sirbu BM, Eichman BF, Cortez D. SMARCAL1 catalyzes fork regression and Holliday junction migration to maintain genome stability during DNA replication. Genes & development. 2012;26(2):151-62.

84. Taglialatela A, Alvarez S, Leuzzi G, Sannino V, Ranjha L, Huang J-W, Madubata C, Anand R, Levy B, Rabadan R, Cejka P, Costanzo V, Ciccia A. Restoration of Replication Fork Stability in BRCA1- and BRCA2-Deficient Cells by Inactivation of SNF2-Family Fork Remodelers. Molecular Cell. 2017;68(2):414-30.e8.

85. Kolinjivadi AM, Sannino V, De Antoni A, Zadorozhny K, Kilkenny M, Técher H, Baldi G, Shen R, Ciccia A, Pellegrini L. Smarcal1-mediated fork reversal triggers Mre11-dependent degradation of nascent DNA in the absence of Brca2 and stable Rad51 nucleofilaments. Molecular cell. 2017;67(5):867-81. e7.

86. Vujanovic M, Krietsch J, Raso MC, Terraneo N, Zellweger R, Schmid JA, Taglialatela A, Huang J-W, Holland CL, Zwicky K. Replication fork slowing and reversal upon DNA damage require PCNA polyubiquitination and ZRANB3 DNA translocase activity. Molecular cell. 2017;67(5):882-90. e5.

87. Zellweger R, Dalcher D, Mutreja K, Berti M, Schmid JA, Herrador R, Vindigni A, Lopes M. Rad51-mediated replication fork reversal is a global response to genotoxic treatments in human cells. J Cell Biol. 2015;208(5):563-79.

88. Lemaçon D, Jackson J, Quinet A, Brickner JR, Li S, Yazinski S, You Z, Ira G, Zou L, Mosammaparast N, Vindigni A. MRE11 and EXO1 nucleases degrade reversed forks and elicit MUS81-dependent fork rescue in BRCA2-deficient cells. Nature Communications. 2017;8(1):860.

89. Taglialatela A, Alvarez S, Leuzzi G, Sannino V, Ranjha L, Huang J-W, Madubata C, Anand R, Levy B, Rabadan R. Restoration of replication fork stability in BRCA1-and BRCA2-deficient cells by inactivation of SNF2-family fork remodelers. Molecular cell. 2017;68(2):414-30. e8.

90. Hashimoto Y, Ray Chaudhuri A, Lopes M, Costanzo V. Rad51 protects nascent DNA from Mre11-dependent degradation and promotes continuous DNA synthesis. Nature structural & molecular biology. 2010;17(11):1305-11.

91. Berti M, Ray Chaudhuri A, Thangavel S, Gomathinayagam S, Kenig S, Vujanovic M, Odreman F, Glatter T, Graziano S, Mendoza-Maldonado R, Marino F, Lucic B, Biasin V, Gstaiger M, Aebersold R, Sidorova JM, Monnat RJ, Jr., Lopes M, Vindigni A. Human RECQ1 promotes restart of replication forks reversed by DNA topoisomerase I inhibition. Nat Struct Mol Biol. 2013;20(3):347-54.

92. Thangavel S, Berti M, Levikova M, Pinto C, Gomathinayagam S, Vujanovic M, Zellweger R, Moore H, Lee EH, Hendrickson EA, Cejka P, Stewart S, Lopes M, Vindigni A. DNA2 drives processing and restart of reversed replication forks in human cells. J Cell Biol. 2015;208(5):545-62.

93. Taylor MRG, Yeeles JTP. The Initial Response of a Eukaryotic Replisome to DNA Damage. Molecular Cell. 2018;70(6):1067-80.e12.

94. Davies AA, Huttner D, Daigaku Y, Chen S, Ulrich HD. Activation of ubiquitin-dependent DNA damage bypass is mediated by replication protein a. Mol Cell. 2008;29(5):625-36.

95. Huttner D, Ulrich HD. Cooperation of replication protein A with the ubiquitin ligase Rad18 in DNA damage bypass. Cell Cycle. 2008;7(23):3629-33.

96. Branzei D, Foiani M. The DNA damage response during DNA replication. Curr Opin Cell Biol. 2005;17(6):568-75.

97. Zou L, Liu D, Elledge SJ. Replication protein A-mediated recruitment and activation of Rad17 complexes. Proceedings of the National Academy of Sciences. 2003;100(24):13827-32.

98. Guilliam TA, Brissett NC, Ehlinger A, Keen BA, Kolesar P, Taylor EM, Bailey LJ, Lindsay HD, Chazin WJ, Doherty AJ. Molecular basis for PrimPol recruitment to replication forks by RPA. Nature Communications. 2017;8(1):15222.

99. Martínez-Jiménez MI, Lahera A, Blanco L. Human PrimPol activity is enhanced by RPA. Scientific Reports. 2017;7(1):783.

100. Kile AC, Chavez DA, Bacal J, Eldirany S, Korzhnev DM, Bezsonova I, Eichman BF, Cimprich KA. HLTF's ancient HIRAN domain binds 3′ DNA ends to drive replication fork reversal. Molecular cell. 2015;58(6):1090-100.

101. Hoege C, Pfander B, Moldovan G-L, Pyrowolakis G, Jentsch S. RAD6-dependent DNA repair is linked to modification of PCNA by ubiquitin and SUMO. Nature. 2002;419(6903):135-41.

102. Maga G, Hubscher U. Proliferating cell nuclear antigen (PCNA): a dancer with many partners. J Cell Sci. 2003;116(Pt 15):3051-60.

103. Moldovan G-L, Pfander B, Jentsch S. PCNA, the Maestro of the Replication Fork. Cell. 2007;129(4):665-79.

104. Celis JE, Madsen P. Increased nuclear cyclin/PCNA antigen staining of non S-phase transformed human amnion cells engaged in nucleotide excision DNA repair. FEBS letters. 1986;209(2):277-83.

105. Umar A, Buermeyer AB, Simon JA, Thomas DC, Clark AB, Liskay RM, Kunkel TA. Requirement for PCNA in DNA Mismatch Repair at a Step Preceding DNA Resynthesis. Cell. 1996;87(1):65-73.

106. Gary R, Kim K, Cornelius HL, Park MS, Matsumoto Y. Proliferating cell nuclear antigen facilitates excision in long-patch base excision repair. Journal of Biological Chemistry. 1999;274(7):4354-63.

107. Liberti SE, Andersen SD, Wang J, May A, Miron S, Perderiset M, Keijzers G, Nielsen FC, Charbonnier J-B, Bohr VA. Bi-directional routing of DNA mismatch repair protein human exonuclease 1 to replication foci and DNA double strand breaks. DNA repair. 2011;10(1):73-86.

108. Jónsson ZO, Hindges R, Hübscher U. Regulation of DNA replication and repair proteins through interaction with the front side of proliferating cell nuclear antigen. The EMBO journal. 1998;17(8):2412-25.

109. Montecucco A, Rossi R, Levin DS, Gary R, Park MS, Motycka TA, Ciarrocchi G, Villa A, Biamonti G, Tomkinson AE. DNA ligase I is recruited to sites of DNA replication by an interaction with proliferating cell nuclear antigen: identification of a common targeting mechanism for the assembly of replication factories. The EMBO journal. 1998;17(13):3786-95.

110. Bienko M, Green CM, Crosetto N, Rudolf F, Zapart G, Coull B, Kannouche P, Wider G, Peter M, Lehmann AR, Hofmann K, Dikic I. Ubiquitin-Binding Domains in Y-Family Polymerases Regulate Translesion Synthesis. Science. 2005;310(5755):1821-4.

111. Garg P, Burgers PM. Ubiquitinated proliferating cell nuclear antigen activates translesion DNA polymerases η and REV1. Proceedings of the National Academy of Sciences. 2005;102(51):18361-6.

112. Tellier-Lebegue C, Dizet E, Ma E, Veaute X, Coic E, Charbonnier J-B, Maloisel L. The translesion DNA polymerases Pol ζ and Rev1 are activated independently of PCNA ubiquitination upon UV radiation in mutants of DNA polymerase δ. PLoS genetics. 2017;13(12):e1007119.

113. Guilliam TA, Yeeles JTP. Reconstitution of translesion synthesis reveals a mechanism of eukaryotic DNA replication restart. Nature Structural & Molecular Biology. 2020;27(5):450-60.

114. Hendel A, Krijger PH, Diamant N, Goren Z, Langerak P, Kim J, Reissner T, Lee K-y, Geacintov NE, Carell T. PCNA ubiquitination is important, but not essential for translesion DNA synthesis in mammalian cells. PLoS genetics. 2011;7(9):e1002262.

115. Gervai JZ, Gálicza J, Szeltner Z, Zámborszky J, Szüts D. A genetic study based on PCNA-ubiquitin fusions reveals no requirement for PCNA polyubiquitylation in DNA damage tolerance. DNA Repair. 2017;54:46-54.

116. Boehm EM, Powers KT, Kondratick CM, Spies M, Houtman JCD, Washington MT. The Proliferating Cell Nuclear Antigen (PCNA)-interacting Protein (PIP) Motif of DNA Polymerase η Mediates Its Interaction with the C-terminal Domain of Rev1*. Journal of Biological Chemistry. 2016;291(16):8735-44.

117. Ohashi E, Murakumo Y, Kanjo N, Akagi J-i, Masutani C, Hanaoka F, Ohmori H. Interaction of hREV1 with three human Y-family DNA polymerases. Genes to Cells. 2004;9(6):523-31.

118. Guo C, Fischhaber PL, Luk-Paszyc MJ, Masuda Y, Zhou J, Kamiya K, Kisker C, Friedberg EC. Mouse Rev1 protein interacts with multiple DNA polymerases involved in translesion DNA synthesis. Embo j. 2003;22(24):6621-30.

119. Boehm EM, Spies M, Washington MT. PCNA tool belts and polymerase bridges form during translesion synthesis. Nucleic Acids Research. 2016;44(17):8250-60.

120. Wojtaszek J, Liu J, D'Souza S, Wang S, Xue Y, Walker GC, Zhou P. Multifaceted recognition of vertebrate Rev1 by translesion polymerases ζ and κ. J Biol Chem. 2012;287(31):26400-8.

121. Wojtaszek J, Lee C-J, D'Souza S, Minesinger B, Kim H, D'Andrea AD, Walker GC, Zhou P. Structural Basis of Rev1-mediated Assembly of a Quaternary Vertebrate Translesion Polymerase Complex Consisting of Rev1, Heterodimeric Polymerase (Pol) ζ, and Pol κ*. Journal of Biological Chemistry. 2012;287(40):33836-46.

122. Rizzo AA, Korzhnev DM. The Rev1-Polζ translesion synthesis mutasome: Structure, interactions and inhibition. Enzymes. 2019;45:139-81.

123. Ohashi E, Hanafusa T, Kamei K, Song I, Tomida J, Hashimoto H, Vaziri C, Ohmori H. Identification of a novel REV1-interacting motif necessary for DNA polymerase κ function. Genes to Cells. 2009;14(2):101-11.

124. Sale JE, Batters C, Edmunds CE, Phillips LG, Simpson LJ, Szüts D. Timing matters: error-prone gap filling and translesion synthesis in immunoglobulin gene hypermutation. Philosophical Transactions of the Royal Society B: Biological Sciences. 2009;364(1517):595-603.

125. Edmunds CE, Simpson LJ, Sale JE. PCNA Ubiquitination and REV1 Define Temporally Distinct Mechanisms for Controlling Translesion Synthesis in the Avian Cell Line DT40. Molecular Cell. 2008;30(4):519-29.

126. Jansen JG, Tsaalbi-Shtylik A, Hendriks G, Gali H, Hendel A, Johansson F, Erixon K, Livneh Z, Mullenders LHF, Haracska L, de Wind N. Separate Domains of Rev1 Mediate Two Modes of DNA Damage Bypass in Mammalian Cells. Molecular and Cellular Biology. 2009;29(11):3113-23.

127. Huang TT, Nijman SMB, Mirchandani KD, Galardy PJ, Cohn MA, Haas W, Gygi SP, Ploegh HL, Bernards R, D'Andrea AD. Regulation of monoubiquitinated PCNA by DUB autocleavage. Nature Cell Biology. 2006;8(4):341-7.

128. Kashiwaba S-i, Kanao R, Masuda Y, Kusumoto-Matsuo R, Hanaoka F, Masutani C. USP7 Is a Suppressor of PCNA Ubiquitination and Oxidative-Stress-Induced Mutagenesis in Human Cells. Cell Reports. 2015;13(10):2072-80.

129. Park JM, Yang SW, Yu KR, Ka SH, Lee SW, Seol JH, Jeon YJ, Chung CH. Modification of PCNA by ISG15 plays a crucial role in termination of error-prone translesion DNA synthesis. Mol Cell. 2014;54(4):626-38.

130. Cotto-Rios XM, Békés M, Chapman J, Ueberheide B, Huang TT. Deubiquitinases as a signaling target of oxidative stress. Cell Rep. 2012;2(6):1475-84.

131. Niimi A, Brown S, Sabbioneda S, Kannouche PL, Scott A, Yasui A, Green CM, Lehmann AR. Regulation of proliferating cell nuclear antigen ubiquitination in mammalian cells. Proceedings of the National Academy of Sciences. 2008;105(42):16125-30.

132. Davis EJ, Lachaud C, Appleton P, Macartney TJ, Näthke I, Rouse J. DVC1 (C1orf124) recruits the p97 protein segregase to sites of DNA damage. Nature structural & molecular biology. 2012;19(11):1093-100.

133. Mosbech A, Gibbs-Seymour I, Kagias K, Thorslund T, Beli P, Povlsen L, Nielsen SV, Smedegaard S, Sedgwick G, Lukas C, Hartmann-Petersen R, Lukas J, Choudhary C, Pocock R, Bekker-Jensen S, Mailand N. DVC1 (C1orf124) is a DNA damage-targeting p97 adaptor that promotes ubiquitin-dependent responses to replication blocks. Nat Struct Mol Biol. 2012;19(11):1084-92.

134. Toth A, Hegedus L, Juhasz S, Haracska L, Burkovics P. The DNA-binding box of human SPARTAN contributes to the targeting of Polη to DNA damage sites. DNA Repair. 2017;49:33-42.

135. Juhasz S, Balogh D, Hajdu I, Burkovics P, Villamil MA, Zhuang Z, Haracska L. Characterization of human Spartan/C1orf124, an ubiquitin-PCNA interacting regulator of DNA damage tolerance. Nucleic Acids Research. 2012;40(21):10795-808.

136. Nakazato A, Kajita K, Ooka M, Akagawa R, Abe T, Takeda S, Branzei D, Hirota K. SPARTAN promotes genetic diversification of the immunoglobulin-variable gene locus in avian DT40 cells. DNA repair. 2018;68:50-7.

137. De March M, Barrera-Vilarmau S, Crespan E, Mentegari E, Merino N, Gonzalez-Magana A, Romano-Moreno M, Maga G, Crehuet R, Onesti S. p15PAF binding to PCNA modulates the DNA sliding surface. Nucleic acids research. 2018;46(18):9816-28.

138. De Biasio A, De Opakua AI, Mortuza GB, Molina R, Cordeiro TN, Castillo F, Villate M, Merino N, Delgado S, Gil-Cartón D. Structure of p15PAF–PCNA complex and implications for clamp sliding during DNA replication and repair. Nature communications. 2015;6(1):6439.

139. Povlsen LK, Beli P, Wagner SA, Poulsen SL, Sylvestersen KB, Poulsen JW, Nielsen ML, Bekker-Jensen S, Mailand N, Choudhary C. Systems-wide analysis of ubiquitylation dynamics reveals a key role for PAF15 ubiquitylation in DNA-damage bypass. Nature cell biology. 2012;14(10):1089-98.

140. Gali H, Juhasz S, Morocz M, Hajdu I, Fatyol K, Szukacsov V, Burkovics P, Haracska L. Role of SUMO modification of human PCNA at stalled replication fork. Nucleic Acids Research. 2012;40(13):6049-59.

141. Mohiuddin M, Evans TJ, Rahman MM, Keka IS, Tsuda M, Sasanuma H, Takeda S. SUMOylation of PCNA by PIAS1 and PIAS4 promotes template switch in the chicken and human B cell lines. Proceedings of the National Academy of Sciences. 2018;115(50):12793-8.

142. Pfander B, Moldovan G-L, Sacher M, Hoege C, Jentsch S. SUMO-modified PCNA recruits Srs2 to prevent recombination during S phase. Nature. 2005;436(7049):428-33.

143. Coulon S, Ramasubramanyan S, Alies C, Philippin G, Lehmann A, Fuchs RP. Rad8Rad5/Mms2–Ubc13 ubiquitin ligase complex controls translesion synthesis in fission yeast. The EMBO Journal. 2010;29(12):2048-58.

144. Motegi A, Liaw H-J, Lee K-Y, Roest HP, Maas A, Wu X, Moinova H, Markowitz SD, Ding H, Hoeijmakers JH. Polyubiquitination of proliferating cell nuclear antigen by HLTF and SHPRH prevents genomic instability from stalled replication forks. Proceedings of the National Academy of Sciences. 2008;105(34):12411-6.

145. Lin J-R, Zeman Michelle K, Chen J-Y, Yee M-C, Cimprich Karlene A. SHPRH and HLTF Act in a Damage-Specific Manner to Coordinate Different Forms of Postreplication Repair and Prevent Mutagenesis. Molecular Cell. 2011;42(2):237-49.

146. Krijger PHL, Lee K-Y, Wit N, van den Berk PCM, Wu X, Roest HP, Maas A, Ding H, Hoeijmakers JHJ, Myung K, Jacobs H. HLTF and SHPRH are not essential for PCNA polyubiquitination, survival and somatic hypermutation: Existence of an alternative E3 ligase. DNA Repair. 2011;10(4):438-44.

147. Poole LA, Cortez D. Functions of SMARCAL1, ZRANB3, and HLTF in maintaining genome stability. Critical Reviews in Biochemistry and Molecular Biology. 2017;52(6):696-714.

148. Thakar T, Leung W, Nicolae CM, Clements KE, Shen B, Bielinsky A-K, Moldovan G-L. Ubiquitinated-PCNA protects replication forks from DNA2-mediated degradation by regulating Okazaki fragment maturation and chromatin assembly. Nature Communications. 2020;11(1):2147.

149. de la Torre-Ruiz M-A, Green CM, Lowndes NF. RAD9 and RAD24 define two additive, interacting branches of the DNA damage checkpoint pathway in budding yeast normally required for Rad53 modification and activation. The EMBO Journal. 1998;17(9):2687-98.

150. Caspari T, Dahlen M, Kanter-Smoler G, Lindsay HD, Hofmann K, Papadimitriou K, Sunnerhagen P, Carr AM. Characterization of Schizosaccharomyces pombe Hus1: a PCNA-related protein that associates with Rad1 and Rad9. Molecular and cellular biology. 2000;20(4):1254-62.

151. Kondo T, Matsumoto K, Sugimoto K. Role of a complex containing Rad17, Mec3, and Ddc1 in the yeast DNA damage checkpoint pathway. Molecular and cellular biology. 1999;19(2):1136-43.

152. Pandita RK, Sharma GG, Laszlo A, Hopkins KM, Davey S, Chakhparonian M, Gupta A, Wellinger RJ, Zhang J, Powell SN, Roti Roti JL, Lieberman HB, Pandita TK. Mammalian Rad9 Plays a Role in Telomere Stability, S- and G2-Phase-Specific Cell Survival, and Homologous Recombinational Repair. Molecular and Cellular Biology. 2006;26(5):1850-64.

153. Shinohara M, Sakai K, Ogawa T, Shinohara A. The mitotic DNA damage checkpoint proteins Rad17 and Rad24 are required for repair of double-strand breaks during meiosis in yeast. Genetics. 2003;164(3):855-65.

154. Budzowska M, Jaspers I, Essers J, de Waard H, van Drunen E, Hanada K, Beverloo B, Hendriks RW, de Klein A, Kanaar R. Mutation of the mouse Rad17 gene leads to embryonic lethality and reveals a role in DNA damage-dependent recombination. The EMBO journal. 2004;23(17):3548-58.

155. Waters LS, Walker GC. The critical mutagenic translesion DNA polymerase Rev1 is highly expressed during G(2)/M phase rather than S phase. Proc Natl Acad Sci U S A. 2006;103(24):8971-6.

156. Uchiyama M, Terunuma J, Hanaoka F. The Protein Level of Rev1, a TLS Polymerase in Fission Yeast, Is Strictly Regulated during the Cell Cycle and after DNA Damage. PLOS ONE. 2015;10(7):e0130000.

157. Sobolewska A, Halas A, Plachta M, McIntyre J, Sledziewska-Gojska E. Regulation of the abundance of Y-family polymerases in the cell cycle of budding yeast in response to DNA damage. Current Genetics. 2020;66(4):749-63.

158. Chun AC-S, Kok K-H, Jin D-Y. REV7 is required for anaphase-promoting complex-dependent ubiquitination and degradation of translesion DNA polymerase REV1. Cell Cycle. 2013;12(2):365-78.

159. Plachta M, Halas A, McIntyre J, Sledziewska-Gojska E. The steady-state level and stability of TLS polymerase eta are cell cycle dependent in the yeast S. cerevisiae. DNA Repair. 2015;29:147-53.

160. Skoneczna A, McIntyre J, Skoneczny M, Policinska Z, Sledziewska-Gojska E. Polymerase eta Is a Short-lived, Proteasomally Degraded Protein that Is Temporarily Stabilized Following UV Irradiation in Saccharomyces cerevisiae. Journal of Molecular Biology. 2007;366(4):1074-86.

161. Pillaire M-J, Betous R, Conti C, Czaplicki J, Pasero P, Bensimon A, Cazaux C, Hoffmann J-S. Upregulation of Error-Prone DNA Polymerases Beta and Kappa Slows Down Fork Progression Without Activating the Replication Checkpoint. Cell Cycle. 2007;6(4):471-7.

162. Weaver TM, Cortez LM, Khoang TH, Washington MT, Agarwal PK, Freudenthal BD. Visualizing Rev1 catalyze protein-template DNA synthesis. Proc Natl Acad Sci U S A. 2020;117(41):25494-504.

163. Haracska L, Johnson RE, Unk I, Phillips BB, Hurwitz J, Prakash L, Prakash S. Targeting of human DNA polymerase ι to the replication machinery via interaction with PCNA. Proceedings of the National Academy of Sciences. 2001;98(25):14256-61.

164. Ohashi E, Bebenek K, Matsuda T, Feaver WJ, Gerlach VL, Friedberg EC, Ohmori H, Kunkel TA. Fidelity and processivity of DNA synthesis by DNA polymerase κ, the product of the human DINB1 gene. Journal of Biological Chemistry. 2000;275(50):39678-84.

165. Gallo D, Kim T, Szakal B, Saayman X, Narula A, Park Y, Branzei D, Zhang Z, Brown GW. Rad5 recruits error-prone DNA polymerases for mutagenic repair of ssDNA gaps on undamaged templates. Molecular cell. 2019;73(5):900-14. e9.

166. Chen D, Gervai JZ, Póti Á, Németh E, Szeltner Z, Szikriszt B, Gyüre Z, Zámborszky J, Ceccon M, d'Adda di Fagagna F, Szallasi Z, Richardson AL, Szüts D. BRCA1 deficiency specific base substitution mutagenesis is dependent on translesion synthesis and regulated by 53BP1. Nature Communications. 2022;13(1):226.

167. Tian F, Sharma S, Zou J, Lin SY, Wang B, Rezvani K, Wang H, Parvin JD, Ludwig T, Canman CE, Zhang D. BRCA1 promotes the ubiquitination of PCNA and recruitment of translesion polymerases in response to replication blockade. Proc Natl Acad Sci U S A. 2013;110(33):13558-63.

168. Daniel S-L, Néstor G-R, Lisanne G, Arnoud de R, Peter AvV, Pablo H, Alfred COV, Román G-P. BRCA1/BARD1 ubiquitinates PCNA in unperturbed conditions to promote replication fork stability and continuous DNA synthesis. bioRxiv. 2023:2023.01.12.523782.

169. Lim KS, Li H, Roberts EA, Gaudiano EF, Clairmont C, Sambel LA, Ponnienselvan K, Liu JC, Yang C, Kozono D, Parmar K, Yusufzai T, Zheng N, D'Andrea AD. USP1 Is Required for Replication Fork Protection in BRCA1-Deficient Tumors. Molecular Cell. 2018;72(6):925-41.e4.

170. Arakawa H, Hauschild J, Buerstedde J-M. Requirement of the activation-induced deaminase (AID) gene for immunoglobulin gene conversion. Science. 2002;295(5558):1301-6.

171. Harris RS, Sale JE, Petersen-Mahrt SK, Neuberger MS. AID is essential for immunoglobulin V gene conversion in a cultured B cell line. Current Biology. 2002;12(5):435-8.

172. Muramatsu M, Kinoshita K, Fagarasan S, Yamada S, Shinkai Y, Honjo T. Class switch recombination and hypermutation require activation-induced cytidine deaminase (AID), a potential RNA editing enzyme. Cell. 2000;102(5):553-63.

173. Di Noia J, Neuberger MS. Altering the pathway of immunoglobulin hypermutation by inhibiting uracil-DNA glycosylase. Nature. 2002;419(6902):43-8.

174. Saribasak H, Saribasak NN, Ipek FM, Ellwart JW, Arakawa H, Buerstedde JM. Uracil DNA glycosylase disruption blocks Ig gene conversion and induces transition mutations. J Immunol. 2006;176(1):365-71.

175. Arakawa H, Moldovan G-L, Saribasak H, Saribasak NN, Jentsch S, Buerstedde J-M. A Role for PCNA Ubiquitination in Immunoglobulin Hypermutation. PLOS Biology. 2006;4(11):e366.

176. Langerak P, Nygren AO, Krijger PH, van den Berk PC, Jacobs H. A/T mutagenesis in hypermutated immunoglobulin genes strongly depends on PCNAK164 modification. The Journal of experimental medicine. 2007;204(8):1989-98.

177. Zeng X, Winter DB, Kasmer C, Kraemer KH, Lehmann AR, Gearhart PJ. DNA polymerase η is an AT mutator in somatic hypermutation of immunoglobulin variable genes. Nature immunology. 2001;2(6):537-41.

178. Jansen JG, Langerak P, Tsaalbi-Shtylik A, van den Berk P, Jacobs H, de Wind N. Strand-biased defect in C/G transversions in hypermutating immunoglobulin genes in Rev1-deficient mice. Journal of Experimental Medicine. 2006;203(2):319-23.

179. Kano C, Hanaoka F, Wang J-Y. Analysis of mice deficient in both REV1 catalytic activity and POLH reveals an unexpected role for POLH in the generation of C to G and G to C transversions during Ig gene hypermutation. International immunology. 2012;24(3):169-74.

180. Shimizu T, Shinkai Y, Ogi T, Ohmori H, Azuma T. The absence of DNA polymerase kappa does not affect somatic hypermutation of the mouse immunoglobulin heavy chain gene. Immunol Lett. 2003;86(3):265-70.

181. Kawamoto T, Araki K, Sonoda E, Yamashita YM, Harada K, Kikuchi K, Masutani C, Hanaoka F, Nozaki K, Hashimoto N. Dual roles for DNA polymerase η in homologous DNA recombination and translesion DNA synthesis. Molecular cell. 2005;20(5):793-9.

182. Bezzubova O, Silbergleit A, Yamaguchi-Iwai Y, Takeda S, Buerstedde J-M. Reduced X-ray resistance and homologous recombination frequencies in a RAD54−/− mutant of the chicken DT40 cell line. Cell. 1997;89(2):185-93.

183. Kasar S, Kim J, Improgo R, Tiao G, Polak P, Haradhvala N, Lawrence M, Kiezun A, Fernandes S, Bahl S. Whole-genome sequencing reveals activation-induced cytidine deaminase signatures during indolent chronic lymphocytic leukaemia evolution. Nature communications. 2015;6(1):8866.

184. Ziv O, Geacintov N, Nakajima S, Yasui A, Livneh Z. DNA polymerase ζ cooperates with polymerases κ and ι in translesion DNA synthesis across pyrimidine photodimers in cells from XPV patients. Proceedings of the National Academy of Sciences. 2009;106(28):11552-7.

185. Di Lucca J, Guedj M, Lacapère JJ, Fargnoli MC, Bourillon A, Dieudé P, Dupin N, Wolkenstein P, Aegerter P, Saiag P, Descamps V, Lebbe C, Basset-Seguin N, Peris K, Grandchamp B, Soufir N. Variants of the xeroderma pigmentosum variant gene (POLH) are associated with melanoma risk. Eur J Cancer. 2009;45(18):3228-36.

186. Sakiyama T, Kohno T, Mimaki S, Ohta T, Yanagitani N, Sobue T, Kunitoh H, Saito R, Shimizu K, Hirama C. Association of amino acid substitution polymorphisms in DNA repair genes TP53, POLI, REV1 and LIG4 with lung cancer risk. International journal of cancer. 2005;114(5):730-7.

187. Wittschieben JP, Patil V, Glushets V, Robinson LJ, Kusewitt DF, Wood RD. Loss of DNA polymerase ζ enhances spontaneous tumorigenesis. Cancer research. 2010;70(7):2770-8.

188. Valenti F, Ganci F, Fontemaggi G, Sacconi A, Strano S, Blandino G, Di Agostino S. Gain of function mutant p53 proteins cooperate with E2F4 to transcriptionally downregulate RAD17 and BRCA1 gene expression. Oncotarget. 2015;6(8):5547.

189. Moinova HR, Chen W-D, Shen L, Smiraglia D, Olechnowicz J, Ravi L, Kasturi L, Myeroff L, Plass C, Parsons R. HLTF gene silencing in human colon cancer. Proceedings of the National Academy of Sciences. 2002;99(7):4562-7.

190. Cheng CK, Chan NP, Wan TS, Lam LY, Cheung CH, Wong TH, Ip RK, Wong RS, Ng MH. Helicase-like transcription factor is a RUNX1 target whose downregulation promotes genomic instability and correlates with complex cytogenetic features in acute myeloid leukemia. haematologica. 2016;101(4):448.

191. Arcolia V, Paci P, Dhont L, Chantrain G, Sirtaine N, Decaestecker C, Remmelink M, Belayew A, Saussez S. Helicase-like transcription factor: a new marker of well-differentiated thyroid cancers. BMC cancer. 2014;14(1):1-12.

192. Das R, Kundu S, Laskar S, Choudhury Y, Ghosh SK. Assessment of DNA repair susceptibility genes identified by whole exome sequencing in head and neck cancer. DNA repair. 2018;66:50-63.

193. Lawrence MS, Stojanov P, Mermel CH, Robinson JT, Garraway LA, Golub TR, Meyerson M, Gabriel SB, Lander ES, Getz G. Discovery and saturation analysis of cancer genes across 21 tumour types. Nature. 2014;505(7484):495-501.

194. Russo M, Crisafulli G, Sogari A, Reilly NM, Arena S, Lamba S, Bartolini A, Amodio V, Magrì A, Novara L. Adaptive mutability of colorectal cancers in response to targeted therapies. Science. 2019;366(6472):1473-80.

195. Gao Y, Mutter-Rottmayer E, Greenwalt AM, Goldfarb D, Yan F, Yang Y, Martinez-Chacin RC, Pearce KH, Tateishi S, Major MB. A neomorphic cancer cell-specific role of MAGE-A4 in trans-lesion synthesis. Nature communications. 2016;7(1):12105.

196. Albertella MR, Green CM, Lehmann AR, O'Connor MJ. A role for polymerase η in the cellular tolerance to cisplatin-induced damage. Cancer research. 2005;65(21):9799-806.

197. Sun H, Zou S, Zhang S, Liu B, Meng X, Li X, Yu J, Wu J, Zhou J. Elevated DNA polymerase iota (Poli) is involved in the acquisition of aggressive phenotypes of human esophageal squamous cell cancer. International journal of clinical and experimental pathology. 2015;8(4):3591.

198. Peng C, Chen Z, Wang S, Wang H-W, Qiu W, Zhao L, Xu R, Luo H, Chen Y, Chen D. The error-prone DNA polymerase κ promotes temozolomide resistance in glioblastoma through Rad17-dependent activation of ATR-Chk1 signaling. Cancer Research. 2016;76(8):2340-53.

199. Albertella MR, Lau A, O'Connor MJ. The overexpression of specialized DNA polymerases in cancer. DNA repair. 2005;4(5):583-93.

200. Yang L, Shi T, Liu F, Ren C, Wang Z, Li Y, Tu X, Yang G, Cheng X. REV3L, a promising target in regulating the chemosensitivity of cervical cancer cells. PLoS One. 2015;10(3):e0120334.

201. Baatar S, Bai T, Yokobori T, Gombodorj N, Nakazawa N, Ubukata Y, Kimura A, Kogure N, Sano A, Sohda M. High RAD18 expression is associated with disease progression and poor prognosis in patients with gastric cancer. Annals of Surgical Oncology. 2020;27:4360-8.

202. Wu B, Wang H, Zhang L, Sun C, Li H, Jiang C, Liu X. High expression of RAD18 in glioma induces radiotherapy resistance via down-regulating P53 expression. Biomedicine & Pharmacotherapy. 2019;112:108555.

203. Cybulla E, Vindigni A. Leveraging the replication stress response to optimize cancer therapy. Nature Reviews Cancer. 2023;23(1):6-24.

204. Ketkar A, Maddukuri L, Penthala NR, Reed MR, Zafar MK, Crooks PA, Eoff RL. Inhibition of human DNA polymerases eta and kappa by indole-derived molecules occurs through distinct mechanisms. ACS chemical biology. 2019;14(6):1337-51.

205. Zafar MK, Maddukuri L, Ketkar A, Penthala NR, Reed MR, Eddy S, Crooks PA, Eoff RL. A small-molecule inhibitor of human DNA polymerase η potentiates the effects of cisplatin in tumor cells. Biochemistry. 2018;57(7):1262-73.

206. Pulvino M, Liang Y, Oleksyn D, DeRan M, Van Pelt E, Shapiro J, Sanz I, Chen L, Zhao J. Inhibition of proliferation and survival of diffuse large B-cell lymphoma cells by a small-molecule inhibitor of the ubiquitin-conjugating enzyme Ubc13-Uev1A. Blood, The Journal of the American Society of Hematology. 2012;120(8):1668-77.

207. Dikshit A, Jin YJ, Degan S, Hwang J, Foster MW, Li C-Y, Zhang JY. UBE2N promotes melanoma growth via MEK/FRA1/SOX10 signaling. Cancer research. 2018;78(22):6462-72.

208. Cheng J, Fan Y, Xu X, Zhang H, Dou J, Tang Y, Zhong X, Rojas Y, Yu Y, Zhao Y. A small-molecule inhibitor of UBE2N induces neuroblastoma cell death via activation of p53 and JNK pathways. Cell death & disease. 2014;5(2):e1079-e.

209. Fong PC, Boss DS, Yap TA, Tutt A, Wu P, Mergui-Roelvink M, Mortimer P, Swaisland H, Lau A, O'Connor MJ. Inhibition of poly (ADP-ribose) polymerase in tumors from BRCA mutation carriers. New England Journal of Medicine. 2009;361(2):123-34.

210. Farmer H, McCabe N, Lord CJ, Tutt AN, Johnson DA, Richardson TB, Santarosa M, Dillon KJ, Hickson I, Knights C. Targeting the DNA repair defect in BRCA mutant cells as a therapeutic strategy. Nature. 2005;434(7035):917-21.

211. Bryant HE, Schultz N, Thomas HD, Parker KM, Flower D, Lopez E, Kyle S, Meuth M, Curtin NJ, Helleday T. Specific killing of BRCA2-deficient tumours with inhibitors of poly (ADP-ribose) polymerase. Nature. 2005;434(7035):913-7.

212. Ray Chaudhuri A, Nussenzweig A. The multifaceted roles of PARP1 in DNA repair and chromatin remodelling. Nature Reviews Molecular Cell Biology. 2017;18(10):610-21.

213. Ying S, Hamdy FC, Helleday T. Mre11-Dependent Degradation of Stalled DNA Replication Forks Is Prevented by BRCA2 and PARP1BRCA2 and PARP Protect Stability of Stalled Forks. Cancer research. 2012;72(11):2814-21.

214. Pommier Y, O'Connor MJ, De Bono J. Laying a trap to kill cancer cells: PARP inhibitors and their mechanisms of action. Science translational medicine. 2016;8(362):362ps17-ps17.

215. Cong K, Kousholt AN, Peng M, Panzarino NJ, Lee WTC, Nayak S, Krais J, Calvo J, Bere M, Rothenberg E. PARPi synthetic lethality derives from replication-associated single-stranded DNA gaps. BioRxiv. 2019:781989.

216. D'Andrea AD. Mechanisms of PARP inhibitor sensitivity and resistance. DNA repair. 2018;71:172-6.

217. Ray Chaudhuri A, Callen E, Ding X, Gogola E, Duarte AA, Lee J-E, Wong N, Lafarga V, Calvo JA, Panzarino NJ. Replication fork stability confers chemoresistance in BRCA-deficient cells. Nature. 2016;535(7612):382-7.

218. Alexandrov LB, Stratton MR. Mutational signatures: the patterns of somatic mutations hidden in cancer genomes. Curr Opin Genet Dev. 2014;24(100):52-60.

219. Stratton MR, Campbell PJ, Futreal PA. The cancer genome. Nature. 2009;458(7239):719-24.

220. Li Y, Roberts ND, Wala JA, Shapira O, Schumacher SE, Kumar K, Khurana E, Waszak S, Korbel JO, Haber JE. Patterns of somatic structural variation in human cancer genomes. Nature. 2020;578(7793):112-21.

221. Nik-Zainal S, Alexandrov LB, Wedge DC, Van Loo P, Greenman CD, Raine K, Jones D, Hinton J, Marshall J, Stebbings LA. Mutational processes molding the genomes of 21 breast cancers. Cell. 2012;149(5):979-93.

222. Tate JG, Bamford S, Jubb HC, Sondka Z, Beare DM, Bindal N, Boutselakis H, Cole CG, Creatore C, Dawson E, Fish P, Harsha B, Hathaway C, Jupe SC, Kok CY, Noble K, Ponting L, Ramshaw CC, Rye CE, Speedy HE, Stefancsik R, Thompson SL, Wang S, Ward S, Campbell PJ, Forbes SA. COSMIC: the Catalogue Of Somatic Mutations In Cancer. Nucleic Acids Research. 2018;47(D1):D941-D7.

223. Degasperi A, Amarante TD, Czarnecki J, Shooter S, Zou X, Glodzik D, Morganella S, Nanda AS, Badja C, Koh G, Momen SE, Georgakopoulos-Soares I, Dias JML, Young J, Memari Y, Davies H, Nik-Zainal S. A practical framework and online tool for mutational signature analyses show inter-tissue variation and driver dependencies. Nat Cancer. 2020;1(2):249-63.

224. Koh G, Degasperi A, Zou X, Momen S, Nik-Zainal S. Mutational signatures: emerging concepts, caveats and clinical applications. Nature Reviews Cancer. 2021;21(10):619-37.

225. Alexandrov LB, Kim J, Haradhvala NJ, Huang MN, Tian Ng AW, Wu Y, Boot A, Covington KR, Gordenin DA, Bergstrom EN, Islam SMA, Lopez-Bigas N, Klimczak LJ, McPherson JR, Morganella S, Sabarinathan R, Wheeler DA, Mustonen V, Alexandrov LB, Bergstrom EN, Boot A, Boutros P, Chan K, Covington KR, Fujimoto A, Getz G, Gordenin DA, Haradhvala NJ, Huang MN, Islam SMA, Kazanov M, Kim J, Klimczak LJ, Lopez-Bigas N, Lawrence M, Martincorena I, McPherson JR, Morganella S, Mustonen V, Nakagawa H, Tian Ng AW, Polak P, Prokopec S, Roberts SA, Rozen SG, Sabarinathan R, Saini N, Shibata T, Shiraishi Y, Stratton MR, Teh BT, Vázquez-García I, Wheeler DA, Wu Y, Yousif F, Yu W, Getz G, Rozen SG, Stratton MR, Aaltonen LA, Abascal F, Abeshouse A, Aburatani H, Adams DJ, Agrawal N, Ahn KS, Ahn S-M, Aikata H, Akbani R, Akdemir KC, Al-Ahmadie H, Al-Sedairy ST, Al-Shahrour F, Alawi M, Albert M, Aldape K, Alexandrov LB, Ally A, Alsop K, Alvarez EG, Amary F, Amin SB, Aminou B, Ammerpohl O, Anderson MJ, Ang Y, Antonello D, Anur P, Aparicio S, Appelbaum EL, Arai Y, Aretz A, Arihiro K, Ariizumi S-i, Armenia J, Arnould L, Asa S, Assenov Y, Atwal G, Aukema S, Auman JT, Aure MRR, Awadalla P, Aymerich M, Bader GD, Baez-Ortega A, Bailey MH, Bailey PJ, Balasundaram M, Balu S, Bandopadhayay P, Banks RE, Barbi S, Barbour AP, Barenboim J, Barnholtz-Sloan J, Barr H, Barrera E, Bartlett J, Bartolome J, Bassi C, Bathe OF, Baumhoer D, Bavi P, Baylin SB, Bazant W, Beardsmore D, Beck TA, Behjati S, Behren A, Niu B, Bell C, Beltran S, Benz C, Berchuck A, Bergmann AK, Bergstrom EN, Berman BP, Berney DM, Bernhart SH, Beroukhim R, Berrios M, Bersani S, Bertl J, Betancourt M, Bhandari V, Bhosle SG, Biankin AV, Bieg M, Bigner D, Binder H, Birney E, Birrer M, Biswas NK, Bjerkehagen B, Bodenheimer T, Boice L, Bonizzato G, De Bono JS, Boot A, Bootwalla MS, Borg A, Borkhardt A, Boroevich KA, Borozan I, Borst C, Bosenberg M, Bosio M, Boultwood J, Bourque G, Boutros PC, Bova GS, Bowen DT, Bowlby R, Bowtell DDL, Boyault S, Boyce R, Boyd J, Brazma A, Brennan P, Brewer DS, Brinkman AB, Bristow RG, Broaddus RR, Brock JE, Brock M, Broeks A, Brooks AN, Brooks D, Brors B, Brunak S, Bruxner TJC, Bruzos AL, Buchanan A, Buchhalter I, Buchholz C, Bullman S, Burke H, Burkhardt B, Burns KH, Busanovich J, Bustamante CD, Butler AP, Butte AJ, Byrne NJ, Børresen-

Dale A-L, Caesar-Johnson SJ, Cafferkey A, Cahill D, Calabrese C, Caldas C, Calvo F, Camacho N, Campbell PJ, Campo E, Cantù C, Cao S, Carey TE, Carlevaro-Fita J, Carlsen R, Cataldo I, Cazzola M, Cebon J, Cerfolio R, Chadwick DE, Chakravarty D, Chalmers D, Chan CWY, Chan K, Chan-Seng-Yue M, Chandan VS, Chang DK, Chanock SJ, Chantrill LA, Chateigner A, Chatterjee N, Chayama K, Chen H-W, Chen J, Chen K, Chen Y, Chen Z, Cherniack AD, Chien J, Chiew Y-E, Chin S-F, Cho J, Cho S, Choi JK, Choi W, Chomienne C, Chong Z, Choo SP, Chou A, Christ AN, Christie EL, Chuah E, Cibulskis C, Cibulskis K, Cingarlini S, Clapham P, Claviez A, Cleary S, Cloonan N, Cmero M, Collins CC, Connor AA, Cooke SL, Cooper CS, Cope L, Corbo V, Cordes MG, Cordner SM, Cortés-Ciriano I, Covington K, Cowin PA, Craft B, Craft D, Creighton CJ, Cun Y, Curley E, Cutcutache I, Czajka K, Czerniak B, Dagg RA, Danilova L, Davi MV, Davidson NR, Davies H, Davis IJ, Davis-Dusenbery BN, Dawson KJ, De La Vega FM, De Paoli-Iseppi R, Defreitas T, Tos APD, Delaneau O, Demchok JA, Group PMSW, Consortium P. The repertoire of mutational signatures in human cancer. Nature. 2020;578(7793):94-101.

226. Németh E, Krzystanek M, Reiniger L, Ribli D, Pipek O, Sztupinszki Z, Glasz T, Csabai I, Moldvay J, Szallasi Z, Szüts D. The genomic imprint of cancer therapies helps timing the formation of metastases. Int J Cancer. 2019;145(3):694-704.

227. Angus L, Smid M, Wilting SM, van Riet J, Van Hoeck A, Nguyen L, Nik-Zainal S, Steenbruggen TG, Tjan-Heijnen VC, Labots M. The genomic landscape of metastatic breast cancer highlights changes in mutation and signature frequencies. Nature genetics. 2019;51(10):1450-8.

228. Szüts D. A fresh look at somatic mutations in cancer. Science. 2022;376(6591):351-2.

229. Piccart MJ, Bertelsen K, Stuart G, Cassidy J, Mangioni C, Simonsen E, James K, Kaye S, Vergote I, Blom R. Long-term follow-up confirms a survival advantage of the paclitaxel–cisplatin regimen over the cyclophosphamide–cisplatin combination in advanced ovarian cancer. International Journal of Gynecologic Cancer. 2003;13(Suppl 2).

230. Cheng L, Albers P, Berney DM, Feldman DR, Daugaard G, Gilligan T, Looijenga LH. Testicular cancer. Nature Reviews Disease Primers. 2018;4(1):29.

231. Yin M, Joshi M, Meijer RP, Glantz M, Holder S, Harvey HA, Kaag M, Fransen van de Putte EE, Horenblas S, Drabick JJ. Neoadjuvant chemotherapy for muscle-invasive bladder cancer: a systematic review and two-step meta-analysis. The oncologist. 2016;21(6):708-15.

232. Fennell D, Summers Y, Cadranel J, Benepal T, Christoph D, Lal R, Das M, Maxwell F, Visseren-Grul C, Ferry D. Cisplatin in the modern era: The backbone of first-line chemotherapy for non-small cell lung cancer. Cancer treatment reviews. 2016;44:42-50.

233. Ruggiero A, Trombatore G, Triarico S, Arena R, Ferrara P, Scalzone M, Pierri F, Riccardi R. Platinum compounds in children with cancer: toxicity and clinical management. Anti-cancer drugs. 2013;24(10):1007-19.

234. Kelland LR, Abel G, McKeage MJ, Jones M, Goddard PM, Valenti M, Murrer BA, Harrap KR. Preclinical antitumor evaluation of bis-acetato-ammine-dichloro-cyclohexylamine platinum (IV): an orally active platinum drug. Cancer research. 1993;53(11):2581-6.

235. Lemaire M-A, Schwartz A, Rahmouni AR, Leng M. Interstrand cross-links are preferentially formed at the d (GC) sites in the reaction between cis-diamminedichloroplatinum (II) and DNA. Proceedings of the National Academy of Sciences. 1991;88(5):1982-5.

236. Inoue A, Kikuchi S, Hishiki A, Shao Y, Heath R, Evison BJ, Actis M, Canman CE, Hashimoto H, Fujii N. A Small Molecule Inhibitor of Monoubiquitinated Proliferating Cell Nuclear Antigen (PCNA) Inhibits Repair of Interstrand DNA Cross-link, Enhances DNA Double Strand Break, and Sensitizes Cancer Cells to Cisplatin *. Journal of Biological Chemistry. 2014;289(10):7109-20.

237. Srivastava AK, Han C, Zhao R, Cui T, Dai Y, Mao C, Zhao W, Zhang X, Yu J, Wang Q-E. Enhanced expression of DNA polymerase eta contributes to cisplatin resistance of ovarian cancer stem cells. Proceedings of the National Academy of Sciences. 2015;112(14):4411-6.

238. Kermi C, Prieto S, van der Laan S, Tsanov N, Recolin B, Uro-Coste E, Delisle M-B, Maiorano D. RAD18 is a maternal limiting factor silencing the UV-dependent DNA damage checkpoint in Xenopus embryos. Developmental cell. 2015;34(3):364-72.

239. Xie K, Doles J, Hemann MT, Walker GC. Error-prone translesion synthesis mediates acquired chemoresistance. Proceedings of the National Academy of Sciences. 2010;107(48):20792-7.

240. Doles J, Oliver TG, Cameron ER, Hsu G, Jacks T, Walker GC, Hemann MT. Suppression of Rev3, the catalytic subunit of Polζ, sensitizes drug-resistant lung tumors to chemotherapy. Proceedings of the National Academy of Sciences. 2010;107(48):20786-91.

241. Maruyama T, Dougan SK, Truttmann MC, Bilate AM, Ingram JR, Ploegh HL. Increasing the efficiency of precise genome editing with CRISPR-Cas9 by inhibition of nonhomologous end joining. Nature biotechnology. 2015;33(5):538-42.

242. Rausch T, Fritz MH, Untergasser A, Benes V. Tracy: basecalling, alignment, assembly and deconvolution of sanger chromatogram trace files. BMC Genomics. 2020;21(1):230.

243. Bolger AM, Lohse M, Usadel B. Trimmomatic: a flexible trimmer for Illumina sequence data. Bioinformatics. 302014. p. 2114-20.

244. Li H, Durbin R. Fast and accurate short read alignment with Burrows-Wheeler transform. Bioinformatics. 2009;25(14):1754-60.

245. Van der Auwera GA, Carneiro MO, Hartl C, Poplin R, Del Angel G, Levy-Moonshine A, Jordan T, Shakir K, Roazen D, Thibault J, Banks E, Garimella KV, Altshuler D, Gabriel S, DePristo MA. From FastQ data to high confidence variant calls: the Genome Analysis Toolkit best practices pipeline. Curr Protoc Bioinformatics. 2013;11(1110):11.0.1-.0.33.

246. Pipek O, Ribli D, Molnar J, Poti A, Krzystanek M, Bodor A, Tusnady GE, Szallasi Z, Csabai I, Szuts D. Fast and accurate mutation detection in whole genome sequences of multiple isogenic samples with IsoMut. BMC Bioinformatics. 2017;18(1):73.

247. Manders F, Brandsma AM, de Kanter J, Verheul M, Oka R, van Roosmalen MJ, van der Roest B, van Hoeck A, Cuppen E, van Boxtel R. MutationalPatterns: the one stop shop for the analysis of mutational processes. BMC Genomics. 2022;23(1):134.

248. Islam SMA, Díaz-Gay M, Wu Y, Barnes M, Vangara R, Bergstrom EN, He Y, Vella M, Wang J, Teague JW, Clapham P, Moody S, Senkin S, Li YR, Riva L, Zhang T, Gruber AJ, Steele CD, Otlu B, Khandekar A, Abbasi A, Humphreys L, Syulyukina N, Brady SW, Alexandrov BS, Pillay N, Zhang J, Adams DJ, Martincorena I, Wedge DC, Landi MT, Brennan P, Stratton MR, Rozen SG, Alexandrov LB. Uncovering novel mutational signatures by. Cell Genom. 2022;2(11):None.

249. Cameron DL, Baber J, Shale C, Valle-Inclan JE, Besselink N, van Hoeck A, Janssen R, Cuppen E, Priestley P, Papenfuss AT. GRIDSS2: comprehensive characterisation of somatic structural variation using single breakend variants and structural variant phasing. Genome Biol. 2021;22(1):202.

250. Quinlan AR, Hall IM. BEDTools: a flexible suite of utilities for comparing genomic features. Bioinformatics. 2010;26(6):841-2.

251. Amemiya HM, Kundaje A, Boyle AP. The ENCODE Blacklist: Identification of Problematic Regions of the Genome. Sci Rep. 2019;9(1):9354.

252. Van Loo P, Nordgard SH, Lingjaerde OC, Russnes HG, Rye IH, Sun W, Weigman VJ, Marynen P, Zetterberg A, Naume B, Perou CM, Borresen-Dale AL, Kristensen VN. Allele-specific copy number analysis of tumors. Proc Natl Acad Sci U S A. 2010;107(39):16910-5.

253. Petljak M, Alexandrov LB, Brammeld JS, Price S, Wedge DC, Grossmann S, Dawson KJ, Ju YS, Iorio F, Tubio JMC, Koh CC, Georgakopoulos-Soares I, Rodriguez-Martin B, Otlu B, O'Meara S, Butler AP, Menzies A, Bhosle SG, Raine K, Jones DR, Teague JW, Beal K, Latimer C, O'Neill L, Zamora J, Anderson E, Patel N, Maddison M, Ng BL, Graham J, Garnett MJ, McDermott U, Nik-Zainal S, Campbell PJ, Stratton MR. Characterizing Mutational Signatures in Human Cancer Cell Lines Reveals Episodic APOBEC Mutagenesis. Cell. 2019;176(6):1282-94.e20.

254. Boot A, Huang MN, Ng AW, Ho S-C, Lim JQ, Kawakami Y, Chayama K, Teh BT, Nakagawa H, Rozen SG. In-depth characterization of the cisplatin mutational signature in human cell lines and in esophageal and liver tumors. Genome research. 2018;28(5):654-65.

255. Szikriszt B, Póti Á, Németh E, Kanu N, Swanton C, Szüts D. A comparative analysis of the mutagenicity of platinum-containing chemotherapeutic agents reveals direct and indirect mutagenic mechanisms. Mutagenesis. 2021;36(1):75-86.

256. Póti Á, Szikriszt B, Gervai JZ, Chen D, Szüts D. Characterisation of the spectrum and genetic dependence of collateral mutations induced by translesion DNA synthesis. PLoS Genet. 2022;18(2):e1010051.

257. Noordermeer SM, Adam S, Setiaputra D, Barazas M, Pettitt SJ, Ling AK, Olivieri M, Álvarez-Quilón A, Moatti N, Zimmermann M. The shieldin complex mediates 53BP1-dependent DNA repair. Nature. 2018;560(7716):117-21.

258. Lange SS, Tomida J, Boulware KS, Bhetawal S, Wood RD. The polymerase activity of mammalian DNA pol ζ is specifically required for cell and embryonic viability. PLoS genetics. 2016;12(1):e1005759.

259. Pipek O, Ribli D, Molnár J, Póti Á, Krzystanek M, Bodor A, Tusnády GE, Szallasi Z, Csabai I, Szüts D. Fast and accurate mutation detection in whole genome sequences of multiple isogenic samples with IsoMut. BMC Bioinformatics. 2017;18(1):73.

260. Gyüre Z, Póti Á, Németh E, Szikriszt B, Lózsa R, Krawczyk M, Richardson AL, Szüts D. Spontaneous mutagenesis in human cells is controlled by REV1-Polymerase ζ and PRIMPOL. Cell Reports. 2023;42(8).

261. Zou X, Koh GCC, Nanda AS, Degasperi A, Urgo K, Roumeliotis TI, Agu CA, Badja C, Momen S, Young J. A systematic CRISPR screen defines mutational mechanisms underpinning signatures caused by replication errors and endogenous DNA damage. Nature cancer. 2021;2(6):643-57.

262. Kucab JE, Zou X, Morganella S, Joel M, Nanda AS, Nagy E, Gomez C, Degasperi A, Harris R, Jackson SP. A compendium of mutational signatures of environmental agents. Cell. 2019;177(4):821-36. e16.

263. Viel A, Bruselles A, Meccia E, Fornasarig M, Quaia M, Canzonieri V, Policicchio E, Urso ED, Agostini M, Genuardi M. A specific mutational signature associated with DNA 8-oxoguanine persistence in MUTYH-defective colorectal cancer. EBioMedicine. 2017;20:39-49.

264. Póti Á, Gyergyák H, Németh E, Rusz O, Tóth S, Kovácsházi C, Chen D, Szikriszt B, Spisák S, Takeda S. Correlation of homologous recombination deficiency induced mutational signatures with sensitivity to PARP inhibitors and cytotoxic agents. Genome biology. 2019;20:1-13.

265. Zámborszky J, Szikriszt B, Gervai JZ, Pipek O, Póti Á, Krzystanek M, Ribli D, Szalai-Gindl JM, Csabai I, Szallasi Z. Loss of BRCA1 or BRCA2 markedly increases the rate of base substitution mutagenesis and has distinct effects on genomic deletions. Oncogene. 2017;36(6):746-55.

266. Petljak M, Alexandrov LB, Brammeld JS, Price S, Wedge DC, Grossmann S, Dawson KJ, Ju YS, Iorio F, Tubio JM. Characterizing mutational signatures in human cancer cell lines reveals episodic APOBEC mutagenesis. Cell. 2019;176(6):1282-94. e20.

267. Xu J, Huo D, Chen Y, Nwachukwu C, Collins C, Rowell J, Slamon DJ, Olopade OI. CpG island methylation affects accessibility of the proximal BRCA1 promoter to transcription factors. Breast cancer research and treatment. 2010;120:593-601.

268. DeWeerd RA, Németh E, Póti Á, Petryk N, Chen C-L, Hyrien O, Szüts D, Green AM. Prospectively defined patterns of APOBEC3A mutagenesis are prevalent in human cancers. Cell reports. 2022;38(12).

269. Hwang T, Reh S, Dunbayev Y, Zhong Y, Takata Y, Shen J, McBride KM, Murnane JP, Bhak J, Lee S. Defining the mutation signatures of DNA polymerase θ in cancer genomes. NAR cancer. 2020;2(3):zcaa017.

270. Thatikonda V, Islam SA, Jones BC, Gröbner SN, Warsow G, Hutter B, Huebschmann D, Fröhling S, Blattner-Johnson M, Jones DT. Comprehensive analysis of mutational signatures in pediatric cancers. bioRxiv. 2021:2021.09. 28.462210.

271. Bolkestein M, Wong JK, Thewes V, Körber V, Hlevnjak M, Elgaafary S, Schulze M, Kommoss FK, Sinn H-P, Anzeneder T. Chromothripsis in human breast cancer. Cancer research. 2020;80(22):4918-31.

272. Wittschieben JP, Reshmi SC, Gollin SM, Wood RD. Loss of DNA polymerase zeta causes chromosomal instability in mammalian cells. Cancer Res. 2006;66(1):134-42.

273. Xu X, Weaver Z, Linke SP, Li C, Gotay J, Wang X-W, Harris CC, Ried T, Deng C-X. Centrosome amplification and a defective G2–M cell cycle checkpoint induce genetic instability in BRCA1 exon 11 isoform–deficient cells. Molecular cell. 1999;3(3):389-95.

274. Sedic M, Skibinski A, Brown N, Gallardo M, Mulligan P, Martinez P, Keller PJ, Glover E, Richardson AL, Cowan J, Toland AE, Ravichandran K, Riethman H, Naber SP, Näär AM, Blasco MA, Hinds PW, Kuperwasser C. Haploinsufficiency for BRCA1 leads to cell-type-specific genomic instability and premature senescence. Nature Communications. 2015;6(1):7505.

275. Kraakman-Van Der Zwet M, Overkamp WJ, van Lange RE, Essers J, van Duijn-Goedhart A, Wiggers I, Swaminathan S, van Buul PP, Errami A, Tan RT. Brca2 (XRCC11) deficiency results in radioresistant DNA synthesis and a higher frequency of spontaneous deletions. Molecular and cellular biology. 2002.

276. Cong K, Peng M, Kousholt AN, Lee WTC, Lee S, Nayak S, Krais J, VanderVere-Carozza PS, Pawelczak KS, Calvo J, Panzarino NJ, Turchi JJ, Johnson N, Jonkers J, Rothenberg E, Cantor SB. Replication gaps are a key determinant of PARP inhibitor synthetic lethality with BRCA deficiency. Mol Cell. 2021;81(15):3128-44.e7.

277. Schlacher K, Wu H, Jasin M. A distinct replication fork protection pathway connects Fanconi anemia tumor suppressors to RAD51-BRCA1/2. Cancer cell. 2012;22(1):106-16.

278. Moody S, Senkin S, Islam SA, Wang J, Nasrollahzadeh D, Cortez Cardoso Penha R, Fitzgerald S, Bergstrom EN, Atkins J, He Y. Mutational signatures in esophageal squamous cell carcinoma from eight countries with varying incidence. Nature Genetics. 2021;53(11):1553-63.

279. Farmanbar A, Kneller R, Firouzi S. Mutational signatures reveal mutual exclusivity of homologous recombination and mismatch repair deficiencies in colorectal and stomach tumors. Scientific Data. 2023;10(1):423.

280. Cagan A, Baez-Ortega A, Brzozowska N, Abascal F, Coorens TH, Sanders MA, Lawson AR, Harvey LM, Bhosle S, Jones D. Somatic mutation rates scale with lifespan across mammals. Nature. 2022;604(7906):517-24.

281. Németh E, Lovrics A, Gervai JZ, Seki M, Rospo G, Bardelli A, Szüts D. Two main mutational processes operate in the absence of DNA mismatch repair. DNA repair. 2020;89:102827.

282. Makarova AV, Boldinova EO, Belousova EA, Lavrik OI. In vitro lesion bypass by human PrimPol. DNA repair. 2018;70:18-24.

283. Loeillet S, Herzog M, Puddu F, Legoix P, Baulande S, Jackson SP, Nicolas AG. Trajectory and uniqueness of mutational signatures in yeast mutators. Proc Natl Acad Sci U S A. 2020;117(40):24947-56.

284. Giannattasio M, Zwicky K, Follonier C, Foiani M, Lopes M, Branzei D. Visualization of recombination-mediated damage bypass by template switching. Nat Struct Mol Biol. 2014;21(10):884-92.

285. Hirota K, Sonoda E, Kawamoto T, Motegi A, Masutani C, Hanaoka F, Szuts D, Iwai S, Sale JE, Lehmann A, Takeda S. Simultaneous disruption of two DNA polymerases, Poleta and Polzeta, in Avian DT40 cells unmasks the role of Poleta in cellular response to various DNA lesions. PLoS Genet. 2010;6(10).

286. Kochenova OV, Daee DL, Mertz TM, Shcherbakova PV. DNA polymerase ζ-dependent lesion bypass in Saccharomyces cerevisiae is accompanied by error-prone copying of long stretches of adjacent DNA. PLoS Genet. 2015;11(3):e1005110.

287. Northam MR, Moore EA, Mertz TM, Binz SK, Stith CM, Stepchenkova EI, Wendt KL, Burgers PM, Shcherbakova PV. DNA polymerases ζ and Rev1 mediate error-prone bypass of non-B DNA structures. Nucleic Acids Res. 2014;42(1):290-306.

288. Yang Y, Liu Z, Wang F, Temviriyanukul P, Ma X, Tu Y, Lv L, Lin YF, Huang M, Zhang T, Pei H, Chen BP, Jansen JG, de Wind N, Fischhaber PL, Friedberg EC, Tang TS, Guo C. FANCD2 and REV1 cooperate in the protection of nascent DNA strands in response to replication stress. Nucleic Acids Res. 2015;43(17):8325-39.

289. Ben Yamin B, Ahmed-Seghir S, Tomida J, Despras E, Pouvelle C, Yurchenko A, Goulas J, Corre R, Delacour Q, Droin N, Dessen P, Goidin D, Lange SS, Bhetawal S, Mitjavila-Garcia MT, Baldacci G, Nikolaev S, Cadoret JC, Wood RD, Kannouche PL. DNA polymerase zeta contributes to heterochromatin replication to prevent genome instability. EMBO J. 2021;40(21):e104543.

290. Wu W, Barwacz SA, Bhowmick R, Lundgaard K, Gonçalves Dinis MM, Clausen M, Kanemaki MT, Liu Y. Mitotic DNA synthesis in response to replication stress requires the sequential action of DNA polymerases zeta and delta in human cells. Nat Commun. 2023;14(1):706.

291. van Bostelen I, van Schendel R, Romeijn R, Tijsterman M. Translesion synthesis polymerases are dispensable for C. elegans reproduction but suppress genome scarring by polymerase theta-mediated end joining. PLoS Genet. 2020;16(4):e1008759.

292. Reijns MAM, Parry DA, Williams TC, Nadeu F, Hindshaw RL, Rios Szwed DO, Nicholson MD, Carroll P, Boyle S, Royo R, Cornish AJ, Xiang H, Ridout K, Schuh A, Aden K, Palles C, Campo E, Stankovic T, Taylor MS, Jackson AP, Consortium GER, Colorectal Cancer Domain UK 100 GP. Signatures of TOP1 transcription-associated mutagenesis in cancer and germline. Nature. 2022;602(7898):623-31.

293. Belan O, Sebald M, Adamowicz M, Anand R, Vancevska A, Neves J, Grinkevich V, Hewitt G, Segura-Bayona S, Bellelli R, Robinson HMR, Higgins GS, Smith GCM, West SC, Rueda DS, Boulton SJ. POLQ seals post-replicative ssDNA gaps to maintain genome stability in BRCA-deficient cancer cells. Mol Cell. 2022;82(24):4664-80.e9.

294. Chaney SG, Campbell SL, Bassett E, Wu Y. Recognition and processing of cisplatin-and oxaliplatin-DNA adducts. Critical reviews in oncology/hematology. 2005;53(1):3-11.

295. Hicks JK, Chute CL, Paulsen MT, Ragland RL, Howlett NG, Guéranger Q, Glover TW, Canman CE. Differential roles for DNA polymerases eta, zeta, and REV1 in lesion bypass of intrastrand versus interstrand DNA cross-links. Molecular and cellular biology. 2010;30(5):1217-30.

9 Bibliography of candidate's publications

9.1 Publications related to the Ph.D. dissertation

1. Zsolt Gyüre, Ádám, Póti, Eszter Németh, Bernadett Szikriszt, Rita, Lózsa R, Michal Krawczyk, Andrea L Richardson and Dávid Szüts. Spontaneous mutagenesis in human cells is controlled by REV1-Polymerase ζ and PRIMPOL. Cell Reports. 2023;42(8).
2. Dan Chen, Judit Z. Gervai, Ádám Póti, Eszter Németh, Zoltán Szeltner, Bernadett Szikriszt, Zsolt Gyüre, Judit Zámborszky, Marta Ceccon, Fabrizio d'Adda di Fagagna, Zoltan Szallasi, Andrea L. Richardson and Dávid Szüts. BRCA1 deficiency specific base substitution mutagenesis is dependent on translesion synthesis and regulated by 53BP1. Nature Communications. 2022;13(1):226.

9.2 Other publications

1. Dávid Czimer, Klaudia Porok, Dániel Csete, Zsolt Gyüre, Viktória Lavró, Krisztina Fülöp, Zelin Chen, Hella Gyergyák, Gábor E. Tusnády, Shawn M. Burgess, Attila Mócsai, András Váradi and Máté Varga. A new zebrafish model for pseudoxanthoma elasticum. Frontiers in Cell and Developmental Biology. 2021;9:628699.

10 Acknowledgements

First of all, I would like to thank to Dávid Szüts for the support and mentorship he provided and the opportunity to work in his research group. I would also like to thank to Eszter Németh and Ádám Póti for their contribution in the analysis of sequencing data and to Bernadett Szikriszt for her contribution in cytotoxicity assays. I would also like to thank to the remainder of the Genome Stability Research Group for all the support, advice and help I got.

I am thankful to Sándor Spisák, Tamás Arányi and Péter Burkovics for being in-house and official reviewers of my thesis, Miklós Geiszt, Ildikó Unk and Bence Szalai for their work in the complex examination committee and Tamás Hegedűs, Krisztina Takács and Gergely Keszler for accepting my invitation as members of the reviewing committee.

I also would like to thank to my father, mother and brother for their help.

I cannot be grateful enough to my wife and son for supporting and tolerating me during all these hard times. I am sure it was not easy at all.